



Nanoskopowe układy logiczne na powierzchni półprzewodników

Marek Kolmer

*Praca doktorska napisana pod opieką profesora doktora habilitowanego Marka Szymońskiego
oraz doktora Szymona Godlewskiego w Zakładzie Fizyki Nanostruktur i Nanotechnologii
na Wydziale Fizyki, Astronomii i Informatyki Stosowanej
Uniwersytetu Jagiellońskiego*

Kraków 2014

*Chciałbym serdecznie podziękować mojemu Promotorowi,
profesorowi doktorowi habilitowanemu Markowi Szymońskiemu
za nieustanną, wieloletnią opiekę naukową.*

*Chciałbym także podziękować wszystkim pracownikom
Zakładu Fizyki Nanostruktur i Nanotechnologii,
z którymi miałem przyjemność pracować w ciągu ostatnich czterech lat,
za niezwykle serdeczną atmosferę i życzliwość.*

*Szczególne podziękowania chciałbym skierować do
doktora Szymona Godlewskiego
za wiele wspólnie wykonanych eksperymentów,
cenne uwagi oraz długie dyskusje nad materiałem
zawartym w niniejszej pracy.*

Spis treści.

1. Forma pracy doktorskiej oraz opis indywidualnego wkładu kandydata.....	4
2. Problem badawczy podejmowany w pracy doktorskiej.....	6
3. Zarys kontekstu naukowego pracy doktorskiej.....	10
4. Krótki opis badań składających się na pracę doktorską.....	16
5. Podsumowanie oraz wnioski z pracy doktorskiej.....	21
Bibliografia.....	26
Przedruki artykułów składających się na pracę doktorską.....	28

1. Forma pracy doktorskiej oraz opis indywidualnego wkładu kandydata.

Na pracę doktorską „*Nanoskopowe układy logiczne na powierzchni półprzewodników*” składają się cztery oryginalne artykuły opublikowane w recenzowanych czasopismach naukowych oraz jeden rozdział w książce będący materiałem pokonferencyjnym:

1. **[Kolmer, PRB 2012]** M. Kolmer, S. Godlewski, H. Kawai, B. Such, F. Krok, M. Saeys, C. Joachim, M. Szymonski, *Electronic properties of STM-constructed dangling-bond dimer lines on a Ge(001)-(2×1):H surface*, Physical Review B, **86**, 125307 (2012);
2. **[Kolmer, ME 2013]** M. Kolmer, S. Godlewski, J. Lis, B. Such, L. Kantorovich, M. Szymonski, *Construction of atomic-scale logic gates on a surface of hydrogen passivated germanium*, Microelectronic Engineering, **109**, 262–265 (2013);
3. **[Kolmer, ASS 2014]** M. Kolmer, S. Godlewski, R. Zuzak, M. Wojtaszek, C. Rauer, A. Thuairé, J.M. Hartmann, H. Moriceau, C. Joachim, M. Szymonski, *Atomic scale fabrication of dangling bond structures on hydrogen passivated Si(001) wafers processed and nanopackaged in a clean room environment*, Applied Surface Science, **288** 83– 89 (2014);
4. **[Kolmer, Springer 2013]** M. Kolmer, S. Godlewski, B. Such, P. De Mendoza, C. De Leon, A. M. Echavarren, H. Kawai, M. Saeys, C. Joachim, M. Szymonski, *SPM imaging of trinaphthylene molecular states on a hydrogen passivated Ge(001) surface*, Springer series “Advances in Atom and Single Molecule Machines”, vol.3, ISBN 978-3-642-38808-8, 105-114 (2013);
5. **[Godlewski, ACS Nano 2013]** S. Godlewski, M. Kolmer, H. Kawai, B. Such, R. Zuzak, M. Saeys, P. De Mendoza, A.M. Echavarren, C. Joachim, M. Szymonski, *Contacting a conjugated molecule with a surface dangling bond dimer on a Ge(001):H surface allows imaging of the hidden ground electronic state*, ACS Nano, **7 (11)**, 10105-10111 (2013).

Zgodnie z załączonymi oświadczeniami współautorów wkład kandydata w powstanie publikacji z pozycji 1-4 był wiodący. W przypadku artykułu [Godlewski, ACS Nano 2013] wkład trzech pierwszych autorów (w tym kandydata) był porównywalny oraz wiodący.

W publikacjach [Kolmer, PRB 2012] oraz [Kolmer, ME 2013] wkład kandydata polegał na przygotowaniu uwodornionej powierzchni Ge(001):H, opracowaniu metodologii przeprowadzania eksperymentów z użyciem skaningowej mikroskopii i spektroskopii tunelowej (*Scanning Tunneling Microscopy/Spectroscopy*, STM/STS), a w szczególności na opracowaniu protokołu kontrolowanej desorpcji atomów wodoru z powierzchni Ge(001):H. Kandydat wykonał większość pracy doświadczalnej, opracował dane eksperymentalne oraz uczestniczył w analizie wyników. Kandydat wspólnie z doktorem Szymonem Godlewskim napisał manuskrypt [Kolmer, PRB 2012]. Kandydat napisał manuskrypt [Kolmer, ME 2013].

W publikacji [Kolmer, ASS 2014] wkład kandydata polegał na charakteryzacji powierzchni Si(001):H za pomocą techniki STM. Kandydat opracował także metodologię tworzenia zadanych struktur z niewysyconych wiązań na powierzchni Si(001):H. Kandydat miał istotny wkład w wykonane eksperymenty STM/STS dla nanostruktur z niewysyconych wiązań na Si(001):H, opracował dane eksperymentalne, przeprowadził analizę wyników STM/STS oraz wspólnie z profesorem Markiem Szymońskim napisał manuskrypt.

W publikacjach [Kolmer, Springer 2013] oraz [Godlewski, ACS Nano 2013] wkład kandydata polegał na przygotowaniu uwodornionej powierzchni Ge(001):H oraz opracowaniu metodologii przeprowadzania eksperymentów STM/STS dla molekuł *trinaphthylene* na powierzchni Ge(001):H. Kandydat miał istotny wkład w wykonane eksperymenty STM/AFM oraz opracował część danych eksperymentalnych. Kandydat uczestniczył także w analizie uzyskanych wyników. Kandydat wraz z doktorem Szymonem Godlewskim napisał manuskrypt [Kolmer, Springer 2013].

2. Problem badawczy podejmowany w pracy doktorskiej.

Tematem pracy doktorskiej „*Nanoskopowe układy logiczne na powierzchni półprzewodników*” jest opracowanie protokołu wytwarzania oraz charakteryzacja właściwości nanostruktur uformowanych ze swobodnych wiązań na pasywowanych wodorem powierzchniach Ge(001):H oraz Si(001):H przy pomocy kriogenicznego skaningowego mikroskopu tunelowego (*Low Temperature-Scanning Tunneling Microscopy*, LT-STM). Głównym celem pracy jest weryfikacja potencjalnego zastosowania tych struktur w molekularnych oraz atomowych obwodach logicznych projektowanych w oparciu o koncepcję elektroniki monomolekularnej.

Praca doktorska dotyczy podstawowych zagadnień naukowych, które są związane w szerokim kontekście z dalszym rozwojem elektroniki. Postępująca miniaturyzacja elementów układów scalonych wytwarzanych w powszechnie stosowanej technologii CMOS (*Complementary Metal–Oxide–Semiconductor*) napotyka w tej chwili na fundamentalne ograniczenia związane między innymi z kwantowymi właściwościami materii w skali nanometrycznej. Kontynuacja trendu wyznaczonego od początku istnienia przemysłu elektronicznego przez empiryczne prawo Moore’a, które przewiduje podwajanie się liczby elementów układu scalonego (np. tranzystorów) co około 24 miesiące, niedługo wymagać będzie alternatywnych koncepcji realizacji obwodów logicznych. W tym aspekcie rozważa się szereg możliwych rozwiązań. Wśród nich jednym z najbardziej obiecujących jest elektronika molekularna.

Koncepcja elektroniki molekularnej, w której elementy elektronicznych układów scalonych zostają zastąpione przez odpowiednio zaprojektowane duże molekuly organiczne, nie jest ideą nową. Została ona zaproponowana przez Avirama i Ratnera w 1974 roku [1]. W swojej pracy wykazali oni, że molekula organiczna może zachowywać się jak prostownik, jeden z najprostszych elementów elektronicznych. Teoretyczna koncepcja elektroniki molekularnej rozwijała się i w kolejnych latach zaprojektowano szereg molekuł mogących zastąpić wszystkie podstawowe elementy układu scalonego [2]. Nastąpił także podział na tak zwaną hybrydową elektronikę molekularną, w ramach której aktywnymi elementami są układy złożone z wielu molekuł oraz elektronikę monomolekularną, gdzie pojedyncza molekula wykonuje zadane operacje logiczne [2]. W obrębie elektroniki monomolekularnej zaczęto ostatnio rozważać także

zastąpienie klasycznych elementów logicznych obwodu elektronicznego przez odpowiednie układy kwantowe złożone z pojedynczych atomów [3].

Obecnie poszukuje się prototypowych systemów realizujących ideę elektroniki monomolekularnej doświadczalnie, w warunkach laboratoryjnych. Zbadano do tej pory wiele systemów o potencjalnym zastosowaniu jako przełączniki, tranzystory czy klasyczne bramki logiczne. Zazwyczaj są to układy złożone z pojedynczych molekuł zaadsorbowanych na powierzchniach zapewniających stosunkowo prostą charakteryzację oraz manipulację w skali atomowej przy użyciu technik mikroskopii sond skanujących (*Scanning Probe Microscopy*, SPM). Pomimo niekwestionowanego wkładu badań nad tego typu układami w zrozumienie fundamentalnych zjawisk, większość układów molekularnych na takich metalicznych bądź półprzewodnikowych podłożach nie zostanie nigdy praktycznie wykorzystana. Jednym z niewielu wyjątków mogą być układy budowane na pasywowanych wodorem półprzewodnikach: germanie i krzemie o terminacji (001), które wydają się być najbardziej obiecującymi podłożami dla przyszłości elektroniki monomolekularnej. Dzieje się tak z co najmniej trzech powodów. Pierwszym z nich jest komplementarność tych materiałów z obecnie wykorzystywaną w przemyśle elektronicznym technologią CMOS. Co więcej uwodornione powierzchnie Ge(001):H i Si(001):H stanowią znakomite układy do mikro- i nano-litografii. Przykładowo Hallam i inni pokazali, że używając zogniskowanej wiązki elektronów o energii 25 keV można w kontrolowany sposób z precyzją dziesiątek nanometrów usuwać atomy wodoru z powierzchni [4]. Proces ten umożliwia tworzenie obszarów posiadających niewysyczone wiązania (*Dangling-Bonds*, DBs) powierzchniowych atomów Si bądź Ge. Dla obszarów tego typu pojawiają się dodatkowe lokalne powierzchniowe stany elektronowe, które zarówno zwiększają lokalnie aktywność chemiczną jak i umożliwiają lateralny transport ładunku. Ponadto można znacznie poprawić zdolność rozdzielczą litografii stosując techniki SPM. Za pomocą mikroskopu STM można kontrolować desorpcję z powierzchni nawet na poziomie pojedynczych atomów wodoru [5]. Daje to hipotetycznie możliwość tworzenia zadanych struktur z niewysyczonych wiązań z atomową precyzją. Powstaje pytanie, jakie właściwości elektronowe będą miały wytworzone w ten sposób nanostruktury, a w szczególności jakie będą ich właściwości transportowe. Dodatkowo rzędy dimerów atomów Si lub Ge tworzących rekonstrukcje obu omawianych powierzchni powodują, że na poziomie pojedynczego tarasu atomowego można wyróżnić dwa kierunki: równoległy oraz prostopadły do wspomnianych

rzędów rekonstrukcji. Odległości oraz wiązania między sąsiednimi atomami powierzchniowymi Ge bądź Si w obu tych kierunkach są inne. Powoduje to oczywiście różnicę w elektronowych sprzężeniach pomiędzy niewysyconymi wiązaniami w strukturze ułożonej wzdłuż bądź w poprzek kierunku wyznaczonego przez rzędy rekonstrukcji. Ten fakt został wykorzystany w badaniach teoretycznych poświęconych właściwościom transportowym różnych nanostruktur z niewysyconych wiązań na powierzchni Si(001):H [6]. Ich rezultatem są propozycje geometrii nanostruktur z niewysyconych wiązań odpowiadające poszczególnym klasycznym bramkom logicznym, które czekają na doświadczalną weryfikację. Trzecim, nie mniej istotnym niż poprzednie, argumentem na rzecz uwodornionych powierzchni Ge(001):H i Si(001):H jest fakt, iż monowarstwa wodoru odprzęga elektronowo od powierzchni tych półprzewodników zaadsorbowane na nich pojedyncze molekuly organiczne [7, 8]. Możliwość odizolowania stanów elektronowych molekuł od wpływu podłoża to jeden z najistotniejszych aspektów architektury układów monomolekularnych. Dodatkowo w przypadku powierzchni Ge(001):H i Si(001):H ze względu na opisaną procedurę w pełni kontrolowanego wytwarzania nanostruktur z pojedynczych niewysyconych wiązań, można także wysunąć koncepcje adresowania molekuł organicznych poprzez ich oddziaływanie z niewysyconymi wiązaniami tworzonymi na powierzchni. W takiej sytuacji struktury z niewysyconych wiązań oraz organiczne molekuly tworzyłyby układy hybrydowe. Słabe oddziaływanie zaadsorbowanych molekuł z pasywowanymi wodorem podłożami powoduje jednak, że są one na nich bardzo mobilne. W związku z tym zarówno charakteryzacja właściwości elektronowych układów monomolekularnych jak i możliwość precyzyjnej manipulacji nimi za pomocą technik SPM są w tym wypadku niezwykle trudnymi zadaniami doświadczalnymi. W tym momencie otwartym pozostaje pytanie, czy układy monomolekularne lub atomowe na powierzchniach Ge(001):H oraz Si(001):H mogą mieć praktyczne zastosowanie w ramach koncepcji elektroniki monomolekularnej.

Reasumując, problemem badawczym podejmowanym w pracy doktorskiej jest próba określenia w jakim stopniu możliwa jest realizacja proponowanych teoretycznie nowych koncepcji formowania układów logicznych na pasywowanych wodorem powierzchniach Ge(001):H oraz Si(001):H. W celu rozwiązania postawionego problemu badawczego w ramach pracy podjęto przede wszystkim próby wytworzenia nanostruktur z niewysyconych wiązań na obu rozpatrywanych powierzchniach z zadaną, atomową precyzją. Ta część pracy doktorskiej ma

pokazać, że realizacja proponowanych teoretycznie układów z niewysyconych wiązań jest możliwa doświadczalnie. Następnie w celu weryfikacji potencjalnych właściwości transportowych podjęto się charakteryzacji właściwości elektronowych uzyskanych nanostruktur z niewysyconych wiązań. W ostatnim etapie pracy, aby zweryfikować możliwość adresowania za pomocą niewysyconych wiązań molekuł organicznych zaadsorbowanych na uwodornionych półprzewodnikach, przebadano prototypowy układ hybrydowy: modelową organiczną molekułę oddziałującą z podwójnym niewysyconym wiązaniem na powierzchni Ge(001):H.

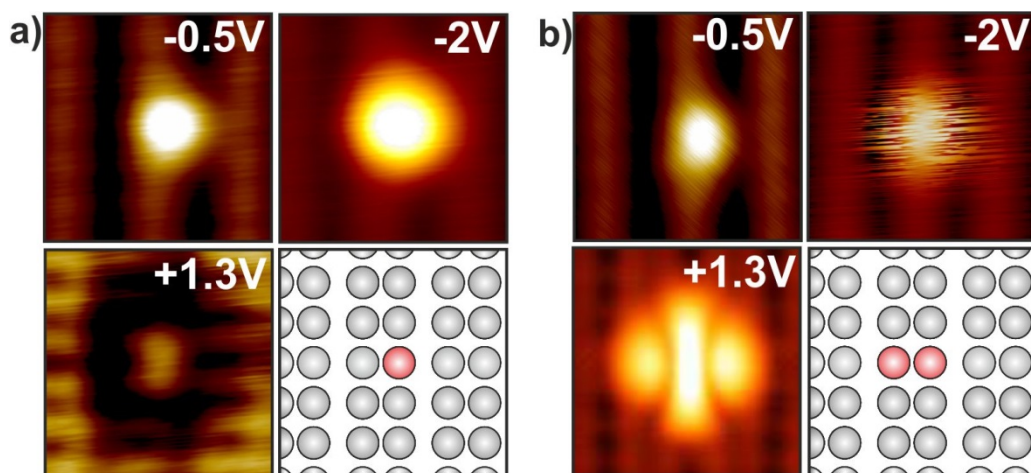
3. Zarys kontekstu naukowego pracy doktorskiej.

Przełomem w doświadczalnej realizacji idei elektroniki monomolekularnej było wynalezienie w 1981 roku przez Binniga i Rohrera pierwszego instrumentu z rodziny mikroskopów bazujących na architekturze sondy skaningowej (SPM): skaningowego mikroskopu tunelowego (STM) [9]. Ten moment zapoczątkował gwałtowny rozwój całej nanonauki, w tym również elektroniki monomolekularnej. Istotą tego nagłego rozwoju jest fakt, że za pomocą instrumentów SPM można nie tylko charakteryzować w przestrzeni rzeczywistej materię w skali atomowej, ale również manipulować nią.

Pierwsze tego typu eksperymenty, dotyczące manipulacji pojedynczymi adatomami na powierzchniach metalicznych, były przeprowadzane na początku lat 90tych [10]. W tym okresie zaczęto także po raz pierwszy charakteryzować uwodornioną powierzchnię (001) monokryształu krzemu za pomocą techniki STM [11]. Podejmowano także pierwsze próby desorpcji wodoru z Si(001):H przy użyciu mikroskopu STM [12, 13] oraz studiowano dynamikę pojedynczych natywnych niewysyconych wiązań na tej powierzchni w podwyższonych temperaturach [14]. W kolejnych latach zaczęto badania nad właściwościami nanostruktur z niewysyconych wiązań na powierzchni Si(001):H formowanych sztucznie w procesie desorpcji wodoru indukowanej ostrzem STM [5, 15-17]. Przykładowo w grupie profesora Wolkowa zapostulowano wykorzystanie układów z oddziałujących ze sobą pojedynczych niewysyconych wiązań do implementacji kubitów [17]. Należy zaznaczyć, że wszystkie powyższe badania STM nanostruktur z niewysyconych wiązań nie były prowadzone w układach doświadczalnych chłodzonych ciekłym helem, tzn. w temperaturach poniżej 10 K. Zaproponowane w związku z tym protokoły desorpcji wodoru wydają się nie dawać pełnej kontroli nad strukturą na poziomie pojedynczych wakancji wodorowych, co skutkuje defektami przy konstrukcji bardziej skomplikowanych układów [16]. Zastosowanie kriogenicznych temperatur, zapewniających odpowiednią stabilizację eksperymentu, może znacznie poprawić precyzję formowania zadanych struktur z niewysyconych wiązań. Co więcej, niedawno pokazano również, że najbardziej typowe defekty w postaci dodatkowych wakancji wodorowych mogą być naprawiane poprzez zastosowanie zaproponowanej przez Labidiego i innych metody [18]. W swojej pracy autorzy pokazują, że za pomocą ostrza STM można przeprowadzić kontrolowaną dysocjację molekuly H_2 i dokonać lokalnej adsorpcji wodoru na powierzchni krzemu (001).

Z kolei jedną z nielicznych grup charakteryzujących powierzchnię Si(001):H za pomocą techniki STM właśnie w kriogenicznych temperaturach jest grupa profesora Dujardin, która skupiła się jednak na właściwościach natywnych defektów na powierzchni Si(001):H, takich jak podwójnie uwodornione atomy krzemu [19] oraz pojedyncze i podwójne niewysyczone wiązania [20-22]. Dzięki zastosowaniu odpowiednio niskich temperatur w prowadzonych eksperymentach STM wykazali oni między innymi możliwość nielokalnego indukowania przeskoku atomu wodoru na sąsiadujące niewysyczone wiązanie [21], czy możliwość efektywnego naładowania pojedynczego niewysyczonego wiązania [22].

Z drugiej strony przedstawiona w pracy [16] idea zastosowania niewysyczonych wiązań na powierzchni Si(001):H do wytwarzania obwodów elektronicznych, była w ostatnim czasie badana w szeregu prac czysto teoretyczno-obliczeniowych [23-27]. Pokazano w nich, że dla pewnych geometrii atomowych drutów z niewysyczonych wiązań można rzeczywiście uzyskać efektywny transport ładunku w płaszczyźnie powierzchni. Co więcej, zaproponowano także możliwość implementacji bramek logicznych w skali atomowej dla specyficznych układów niewysyczonych wiązań na Si(001):H [6, 28]. W kontekście przytoczonych prac teoretycznych kluczowym aspektem doświadczalnym jest nie tylko określenie w jakim stopniu możliwa jest bezpośrednia realizacja postulowanych układów z niewysyczonych wiązań, ale także określenie ich właściwości elektronowych. W szczególności natywna geometria pojedynczych bądź podwójnych niewysyczonych wiązań ma fundamentalne znaczenie dla właściwości elektronowych i transportowych uformowanych z nich nanostruktur. Przykładowo, zgodnie z obliczeniami przedstawionymi w pracy [26], drut zbudowany z podwójnie niewysyczonych wiązań na powierzchni Si(001):H uformowany wzdłuż rzędów dimerów rekonstrukcji z niewykrzywionych par atomów Si posiada metaliczne stany elektronowe. Wykrzywienie geometrii dimerów względem płaszczyzny powierzchni, będące postulowaną natywną geometrią niewodornionych dimerów Si, powoduje otwarcie przerwy i zmianę właściwości transportowych opisywanego drutu. Należy zaznaczyć, że w przypadku niewysyczonych wiązań na powierzchniach Si(001):H oraz Ge(001):H występuje niezwykle silne sprzężenie pomiędzy geometrią a strukturą elektronową. Powoduje to sytuację, w której badania oparte jedynie na wynikach obliczeniowych bądź doświadczalnych są niewystarczające, a jedynie kompilacja obu podejść daje możliwość pełnej interpretacji właściwości badanych układów. Aby zilustrować złożoność badanego zagadnienia przedstawiono na **Rys.1** obrazy STM podstawowych jednostek strukturalnych



Rys.1

a) Obrazy STM pojedynczego niewysyconego wiązania na powierzchni $\text{Ge}(001):\text{H}$ o wymiarach $2 \times 2 \text{ nm}^2$ wykonane w 4 K dla różnych napięć wraz z odpowiednim modelem strukturalnym. Napięcia polaryzacji złącza STM zamieszczono na poszczególnych obrazach. W modelu strukturalnym szare koła odpowiadają atomom Ge posiadającym wodór, natomiast czerwone koło reprezentuje atom Ge z niewysyconym wiązaniem.

b) Obrazy STM podwójnego niewysyconego wiązania na powierzchni $\text{Ge}(001):\text{H}$ o wymiarach $2 \times 2 \text{ nm}^2$ wykonane w 4 K dla różnych napięć wraz z odpowiednim modelem strukturalnym. Napięcia polaryzacji złącza STM zamieszczono na poszczególnych obrazach. W modelu strukturalnym szare koła odpowiadają atomom Ge posiadającym wodór, natomiast czerwone koła reprezentują atomy Ge z niewysyconym wiązaniem.

układów z niewysyconych wiązań: pojedynczego (**Rys.1a**) oraz podwójnego (**Rys.1b**) niewysyconego wiązania na powierzchni Ge(001):H. Przede wszystkim należy zwrócić uwagę na drastyczną zmianę kontrastów danych struktur dla poszczególnych napięć złącza STM. W przypadku pojedynczego niewysyconego wiązania (**Rys.1a**) jasne maksimum dla obrazów STM wypełnionych stanów elektronowych próbki (ujemne napięcia) zmienia się w niewielkie maksimum otoczone czarnym obszarem „halo” dla obrazowania przy napięciu +1.3V. Zaobserwowany efekt jest związany ze zmianą stanu ładunkowego pojedynczego niewysyconego wiązania, którego stany elektronowe znajdują się w pobliżu energii Fermiego, w wyniku efektu ugięcia pasm spowodowanego oddziaływaniem z ostrzem STM. Ponieważ stany elektronowe związane z pojedynczym podwójnym niewysyconym wiązaniem (**Rys.1b**) nie znajdują się w pobliżu energii Fermiego, to w tym przypadku opisany efekt nie występuje. Jednak dla podwójnego niewysyconego wiązania natywna wykrzywiona geometria, objawiająca się asymetrycznym względem rzędów rekonstrukcji maksimum dla napięcia -0.5V, zmienia się w poszarpaną symetryczną strukturę dla wyższych ujemnych napięć. Ten efekt z kolei jest związany z indukowaniem przeskoków dimeru Ge za pomocą elektronów tunelujących przez złącze STM. Natomiast całkowicie symetryczny obraz dla dodatnich napięć może świadczyć o wyprostowaniu geometrii dimeru Ge pod wpływem oddziaływania z ostrzem STM.

Warto w tym momencie zaznaczyć, że w odróżnieniu od szeroko badanej uwodornionej powierzchni (001) krzemu, prac dotyczących odpowiadającej jej uwodornionej powierzchni (001) monokryształu germanu o identycznej strukturze krystalicznej jest stosunkowo niewiele. Jedynie dwie z nich traktują o indukowanej ostrzem STM desorpcji wodoru z Ge(001):H [29, 30], przy czym nie ma prac opisujących atomowo precyzyjny protokół do formowania nanostruktur z niewysyconych wiązań na tej powierzchni. Wykorzystanie powierzchni Ge(001):H wydaje się być niezwykle obiecujące w kontekście doświadczalnej weryfikacji postulowanych teoretycznie właściwości transportowych nanostruktur z niewysyconych wiązań. Charakteryzacja nanostruktur z niewysyconych wiązań za pomocą skaningowej spektroskopii tunelowej (*Scanning Tunneling Spectroscopy*, STS) jest wymagana do zrozumienia struktury elektronowej badanych układów. Należy podkreślić, że do tego momentu w literaturze ukazało się bardzo niewiele prac dotyczących charakteryzacji struktur z pojedynczych niewysyconych wiązań na powierzchniach Ge(001):H i Si(001):H przy pomocy techniki STS [20, 31]. W przypadku monokryształu krzemu ten fakt może być tłumaczony relatywnie dużą

objętościową przerwą wzbronioną (~ 1.2 eV) i zablokowaniem kanałów przewodnictwa objętościowego w kriogenicznych temperaturach. Ta sytuacja powoduje, że w powyższych warunkach istotne dla architektury układów stany elektronowe struktur z niewysyconych wiązań na powierzchni Si(001):H są bardzo trudne do obserwacji za pomocą STS. Ten problem może być rozwiązany przez zastosowanie powierzchni (001) germanu, materiału o mniejszej przerwie (~ 0.7 eV) i zwiększonej ruchliwości nośników a posiadającej podobne właściwości strukturalne oraz elektronowe.

Jak już wspomniano w **rozdziale 2** innym istotnym aspektem zastosowania powierzchni uwodornionych półprzewodników jest fakt, że monowarstwa wodoru może odpręgać elektronowo duże organiczne molekuly od wpływu podłoża [7], co zostało ostatnio wykazane przez Bellec i innych dla powierzchni Si(001):H oraz molekuly pentacenu [8]. Ten wynik doświadczalny skłonił do rozważań nad projektowaniem hybrydowych układów opartych na koncepcji elektroniki monomolekularnej na powierzchni Si(001):H, które zawierałyby duże organiczne molekuly adresowane nanostrukturami z niewysyconych wiązań. Jednak jak również można wywnioskować z powyższej pracy [8], pomimo stosowania kriogenicznych temperatur podczas prowadzenia eksperymentów LT-STM/STS, molekuly organiczne bez specjalnych grup funkcyjnych na powierzchni Si(001):H są niezwykle mobilne. Powoduje to trudności w wytworzeniu i późniejszej charakteryzacji takich prototypowych dla elektroniki monomolekularnej układów hybrydowych. Ponieważ stany elektronowe atomów Ge związane z niewysyconymi wiązaniami rozciągają się bardziej w przestrzeni niż odpowiadające im stany atomów Si, co powinno bardziej stabilizować zaadsorbowane na nich molekuly organiczne, zastosowanie powierzchni Ge(001):H może także w tym wypadku okazać się dobrym rozwiązaniem.

Możliwość desorpcji wodoru i tworzenia dobrze zdefiniowanych nanostruktur z niewysyconych wiązań na powierzchniach Ge(001):H oraz Si(001):H jest również przedmiotem badań grup wykorzystujących inne koncepcje niż opisywana elektronika monomolekularna. Jedną z nich jest już wspomniana grupa profesora Wolkowa, zajmująca się przede wszystkim właściwościami pojedynczych niewysyconych wiązań na powierzchni Si(001):H w kontekście wykorzystania ich do implementacji kubitów [17, 32, 33]. Wśród innych grup należy także wymienić tutaj grupę profesor Simmons. W ramach prowadzonych przez tę

grupę badań tworzone są za pomocą litografii STM zdefiniowane struktury z niewysyconych wiązań na powierzchniach Ge(001):H [29, 30] i Si(001):H [34-36]. Następnie wykorzystując ich zwiększoną aktywność chemiczną adsorbują się na nich molekuły PH₃, które po wygrzaniu rozpadają się, pozostawiając atomy fosforu wbudowane w strukturę półprzewodnika. W ten sposób wywarzane są lokalnie domieszkowane obszary na powierzchni, które następnie są pokrywane odpowiednimi warstwami homoepitaksjalnymi. Za pomocą tak bardzo silnie i lokalnie domieszkowanych obszarów w objętości kryształów Ge oraz Si można tworzyć i charakteryzować ciekawe obiekty fizyczne takie jak kropki kwantowe czy przewodzące nanodruty.

4. Krótki opis badań składających się na pracę doktorską.

Wszystkie badania prowadzone w ramach pracy doktorskiej wykonano w laboratorium Zakładu Fizyki Nanostruktur i Nanotechnologii na Wydziale FAIS Uniwersytetu Jagiellońskiego. Eksperymenty przeprowadzono w systemie ultra wysokiej próżni (*Ultra High Vacuum*, UHV) o bazowym ciśnieniu na poziomie 5×10^{-11} mbar. Zasadniczą część pracy doktorskiej stanowią pomiary SPM, które wykonywano za pomocą niskotemperaturowego mikroskopu LT-STM/AFM firmy Omicron GmbH operującego w temperaturach ciekłego helu (4.5 K) oraz ciekłego azotu (77 K).

Przed wszystkim na potrzeby prowadzonych badań opracowano metodę preparatyki uwodornionych powierzchni Ge(001):H oraz Si(001):H o atomowo perfekcyjnych obszarach koniecznych do formowania układów logicznych w skali atomowej. Powierzchnie Ge(001):H oraz Si(001):H przygotowywano na dwa odmienne sposoby. W przypadku germanu próbki w postaci monokryształów eksponujących płaszczyznę (001) przygotowywano standardową procedurą składającą się z wygrzewania wraz z bombardowaniem powierzchni jonami Ar^+ . Jakość powierzchni Ge(001) sprawdzano wstępnie za pomocą dyfrakcji niskoenergetycznych elektronów (*Low Energy Electron Diffraction*, LEED), a następnie za pomocą techniki LT-STM. Dzięki powyższej procedurze uzyskano powierzchnie Ge(001) z atomowo płaskimi tarasami o rozmiarach lateralnych rzędu kilkudziesięciu nanometrów. Powierzchniowe atomy Ge układały się w rzędy dimerów, których wzajemne ułożenie mogło odpowiadać dwóm możliwym niskotemperaturowym rekonstrukcjom: $c(4 \times 2)$ lub $p(2 \times 2)$. Tak przygotowane próbki wystawiano na działanie strumienia atomowego wodoru. W czasie procesu uwodorniania powierzchni próbki monokryształu germanu utrzymywano w podwyższonej temperaturze w celu zapobiegnięcia procesowi tworzenia się di- i tri- wodorków germanu na powierzchni. W ten sposób uzyskiwano uwodornioną powierzchnię Ge(001):H o rekonstrukcji (2×1) z trzema typami pojedynczych defektów w skali atomowej: wakancjami powierzchniowych atomów Ge oraz pojedynczymi i podwójnymi niewysyconymi wiązaniami (odpowiedni brak jednego bądź dwóch atomów wodoru na dimerze Ge). Szczegółowy opis preparatyki oraz charakteryzacji powierzchni Ge(001) oraz Ge(001):H znajduje się w publikacjach [Kolmer, PRB 2012; Kolmer, ME 2013; Kolmer, Springer 2013].

Powierzchnię Si(001):H o rekonstrukcji (2×1) otrzymywano poprzez otwarcie „kanapki” składającej się z dwóch atomowo płaskich, uwodornionych monokryształów krzemu o terminacji (001) złączonych ze sobą za pomocą oddziaływań van der Waalsa. Uwodornione powierzchnie Si(001):H tworzące „kanapkę” zostały przygotowane chemicznie przez grupę z instytutu LETI-CEA w Grenoble (Francja). Procedura preparatyki zastosowana przez współpracowników z LETI-CEA jest w pełni kompatybilna z metodami używanymi w przemyśle mikroelektronicznym. W ramach pracy doktorskiej scharakteryzowano przygotowane w opisany sposób powierzchnie Si(001):H-(2×1) za pomocą LT-STM. Wykazano, że opisana innowacyjna metoda preparatyki uwodornionych podłoży Si(001):H daje odpowiednio duże, atomowo perfekcyjne obszary na powierzchni, które mogą być wykorzystane do testowania układów logicznych w skali atomowej. Jest to wynik niezwykle istotny i daje możliwość integracji atomowych bądź molekularnych układów logicznych na powierzchni pasywowanych wodorem półprzewodników ze standardowymi, obecnie używanymi metodami tworzenia układów scalonych. Szczegółowy opis preparatyki oraz charakteryzacji powierzchni Si(001):H znajduje się w publikacji [Kolmer, ASS 2014].

Posiadając uwodornione powierzchnie Ge(001):H i Si(001):H można przejść do kolejnego zadania badawczego pracy doktorskiej, którym było wytwarzanie struktur z niewysyconych wiązań z precyzją atomową. Aby osiągnąć ten cel za pomocą mikroskopu STM niezbędna jest odpowiednia stabilność pracy tego urządzenia, którą zapewniają kriogeniczne temperatury. Jak wspomniano w **rozdziale 3** w przypadku powierzchni Ge(001):H metody desorpcji wodoru o wymaganej na potrzeby tych badań precyzji nie zostały przedstawione do tej pory. W ramach pracy doktorskiej opracowano nową procedurę zapewniającą atomową zdolność rozdzielczą w formowaniu zadanych struktur z niewysyconych wiązań. Pokazano, że korzystając z zaproponowanego protokołu można tworzyć zadane nanostruktury z podwójnych niewysyconych wiązań na Ge(001):H odpowiadające postulowanym teoretycznie brąmom logicznym. Ciekawym i istotnym wynikiem w kontekście projektowania układów z niewysyconych wiązań, który został uzyskany na wstępnym etapie charakteryzacji wytworzonych struktur z niewysyconych wiązań na Ge(001):H za pomocą techniki LT-STM jest fakt, że natywna geometria struktur z podwójnych niewysyconych wiązań wykazuje wygięcie dimerów germanowych względem płaszczyzny powierzchni. Efekt możliwego wygięcia geometrii dimerów, mający konsekwencje dla struktury elektronowej, nie był do tej pory

uwzględniany w czysto teoretycznych pracach dotyczących projektowania układów z niewysyconych wiązań na powierzchni Si(001):H.

Kolejnym etapem badań prowadzonych w ramach pracy doktorskiej jest weryfikacja podstawowych założeń prac teoretycznych dotyczących właściwości transportowych nanostruktur z niewysyconych wiązań. W tym celu zbadano również właściwości elektronowe tego typu struktur. Przeprowadzono badania spektroskopowe używając techniki STS. Widma STS dla wybranych nanostruktur z niewysyconych wiązań pokazują, że związane z nimi stany elektronowe rzeczywiście pojawiają się w przerwie energetycznej Ge(001):H. Co więcej, ich położenie przesuwa się do wnętrza przerwy energetycznej wraz ze zwiększaniem rozmiarów struktury. W ramach pracy doktorskiej zbadano za pomocą STS liniowe struktury zbudowane z podwójnych niewysyconych wiązań o długościach do 5 dimerów, które były zorientowane zarówno w poprzek jak i wzdłuż rzędów rekonstrukcji powierzchni. Dzięki współpracy z grupą profesora Joachima z instytutu IMRE w Singapurze uzyskane wyniki doświadczalne STM/STS zostały wsparte obliczeniami teoretycznymi. Zasyulowano między innymi transmisję elektronów przez złącze: *ostrze STM – niewysycone wiązania – powierzchnia Ge(001)*, uzyskując widma transmisji T(E) oraz obrazy STM odpowiadające danym eksperymentalnym. W rezultacie przedyskutowano efekty prowadzące do sprzężeń pomiędzy niewysyconymi wiązaniami w poszczególnych strukturach, które prowadzą do opisywanego przesunięcia ich stanów elektronowych w funkcji lateralnych rozmiarów struktury. Szczegółowy opis tworzenia zadanych struktur z niewysyconych wiązań z atomową precyzją na powierzchni Ge(001):H znajduje się w publikacjach [Kolmer, PRB 2012; Kolmer, ME 2013]. Szczegółowy opis charakterystyki właściwości elektronowych nanostruktur z niewysyconych wiązań znajduje się w publikacji [Kolmer, PRB 2012].

Metodę desorpcji wodoru stosowaną dla powierzchni Ge(001):H można także wykorzystać w przypadku powierzchni Si(001):H. Należy ją jednak odpowiednio zmodyfikować ze względu na większą energię wiązania pomiędzy atomami wodoru i krzemu. Powoduje to między innymi, że w wypadku Si(001):H po zastosowaniu opracowanej procedury desorbowany jest pojedynczy atom wodoru, w odróżnieniu od powierzchni Ge(001):H, dla której są to zazwyczaj dwa wodory. Ta różnica pomiędzy oboma uwodornionymi podłożami pokazuje, że złożoność możliwych do realizacji struktur z niewysyconych wiązań na powierzchni Si(001):H

może być większa. Szczegółowy opis procedury tworzenia struktur z niewysyconych wiązań na Si(001):H oraz opis charakterystyki właściwości elektronowych krótkich nanostruktur z niewysyconych wiązań na tej powierzchni przedstawione są w publikacji [Kolmer, ASS 2014].

Ostatnim zadaniem badawczym zawartym w pracy doktorskiej jest próba uzyskania na powierzchni uwodornionego półprzewodnika prototypowego układu zawierającego duże, organiczne molekuly. Celem tego etapu pracy jest wykazanie możliwości sprzężenia organicznych molekuł z niewysyconymi wiązaniami na powierzchni w kontekście adresowania układów monomolekularnych przez struktury z niewysyconych wiązań. W związku z powyższym naparowano na powierzchnię Ge(001):H molekuly *trinaphthylene* („Y”). Te poliaromatyczne węglowodory, składające się z siedmiu pierścieni fenyłowych ułożonych w kształt litery Y, zaprojektowano specjalnie na potrzeby elektroniki monomolekularnej, jako potencjalne bramki logiczne. Molekuly stosowane w pracy zostały zsyntetyzowane w instytucie ICIQ w Tarragonie (Hiszpania). Ostatnio pokazano doświadczalnie, że rzeczywiście pojedyncza molekula „Y” może zachowywać się na powierzchni Au(111) jak bramka logiczna NOR [37].

Po naparowaniu molekuly „Y” adsorbują jedynie na defektach powierzchni Ge(001):H, takich jak na przykład krawędzie tarasów czy pojedyncze i podwójne niewysycone wiązania. W ramach pracy pokazano, że pojedyncze molekuly można stabilnie obrazować techniką STM w 4 K również na w pełni uwodornionych obszarach powierzchni. Wyniki charakterystyki molekuł tego typu potwierdzają przede wszystkim, że monowarstwa wodoru na powierzchni Ge(001):H efektywnie izoluje stany molekularne od wpływu podłoża. Co więcej, zaobserwowano wyraźny efekt wpływu sprzężenia molekuly z podwójnym niewysyconym wiązaniem na obrazowane za pomocą technik STM stany molekularne. Dzięki obliczeniom wykonanym w grupie z instytutu IMRE w Singapurze ustalono, że stan podstawowy molekuly „Y” może zostać zaobserwowany w obrazie STM tylko w przypadku molekuly podpiętej do podwójnego niewysyconego wiązania na powierzchni Ge(001):H. Dzięki sprzężeniu *molekula – niewysycone wiązania* uzyskuje się wtedy dostęp do stanów powierzchni Ge(001). Ten fundamentalny wynik pokazuje, że koncepcja adresowania molekuł organicznych przez sprzężenie się z ich stanami elektronowymi za pomocą niewysyconych wiązań na powierzchniach pasywowanych wodorem półprzewodników jest możliwa do zrealizowania. Szczegółowy opis charakterystyki molekuł *trinaphthylene* na powierzchni Ge(001):H znajduje się

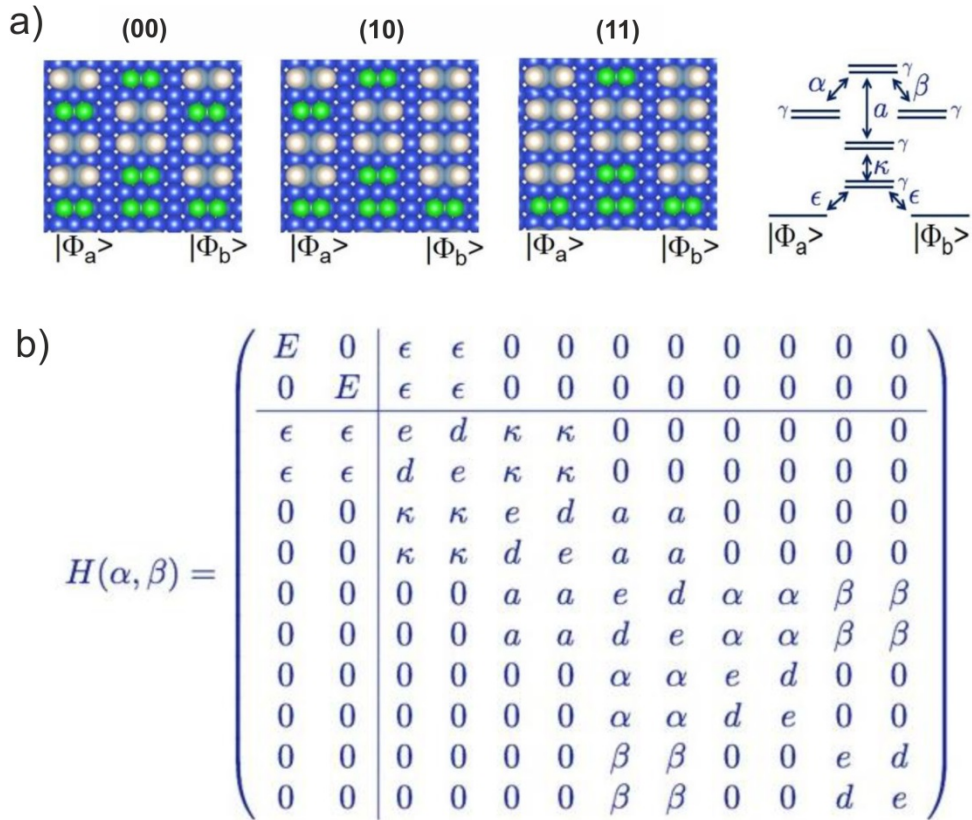
w publikacjach [**Kolmer, Springer 2013; Godlewski, ACS Nano 2013**]. Szczegółowy opis oddziaływania molekuly z podwójnym niewysyconym wiązaniem i jego wpływ na obrazowane stany elektronowe molekuly *trinaphthylene* w eksperymencie STM zawarty jest w publikacji [**Godlewski, ACS Nano 2013**].

5. Podsumowanie oraz wnioski z pracy doktorskiej.

Przede wszystkim wyniki uzyskane w ramach pracy doktorskiej pokazują, że korzystając z opracowanej metody desorpcji wodoru przy użyciu techniki STM można w kriogenicznych temperaturach uzyskać atomową precyzję w konstruowaniu układów z niewysyconych wiązań na powierzchniach Ge(001):H oraz Si(001):H. Ten rezultat potwierdza, że teoretycznie rozważane struktury z niewysyconych wiązań mogą zostać rzeczywiście wytworzone na powierzchni, co stanowi podstawę do dalszych badań nad właściwościami transportowymi nanostruktur z niewysyconych wiązań i ich potencjalnego zastosowania do tworzenia układów logicznych.

Dodatkowo w ramach pracy doktorskiej pokazano doświadczalnie, że stany elektronowe związane z niewysyconymi wiązaniami powstają w przerwie wzbronionej uwodornionego półprzewodnika. Dzięki zastosowaniu powierzchni Ge(001):H, która ma mniejszą przerwę wzbronioną niż odpowiadająca jej powierzchnia Si(001):H, zarejestrowano bezpośrednio za pomocą techniki STS stany elektronowe związane z niewysyconymi wiązaniami. Pozwoliło to na zbadanie wpływu sprzężeń pomiędzy niewysyconymi wiązaniami w różnych konfiguracjach na odpowiadające im stany elektronowe.

Znajomość sprzężeń pomiędzy niewysyconymi wiązaniami jest kluczowa dla projektowania układów z niewysyconych wiązań o zadanych właściwościach transportowych. Znając sprzężenia pomiędzy niewysyconymi wiązaniami można tworzyć z nich układy logiczne w oparciu o koncepcję *Quantum Hamiltonian Computing* (QHC) [38], w której ewolucja stanu kwantowego układu jest wykorzystana do implementowania klasycznych bramek logicznych. Przykładowy projekt bramki NOR/OR na powierzchni Si(001):H oparty o tę koncepcję zaprezentowany jest na **Rys.2a**. Zgodnie z konwencją przyjętą w pracy [6] za sygnał odpowiadający jedynce logicznej przyjęto obsadzenie podwójnego niewysyconego wiązania w strukturze bramki wodorem. Zeru odpowiada natomiast brak dwóch atomów wodoru. Sprzężenia pomiędzy stanami γ tworzącymi bramkę opisano w modelu ciasnego wiązania i przedstawiono w postaci parametrów: α , β , a , κ , ϵ . W takim opisie ewolucja układu uwarunkowana jest macierzą Hamiltonianu przedstawioną na **Rys.2b**, w której parametry α i β zależą od wartości logicznych na wejściach bramki (obecność bądź brak odpowiednich atomów



Rys.2

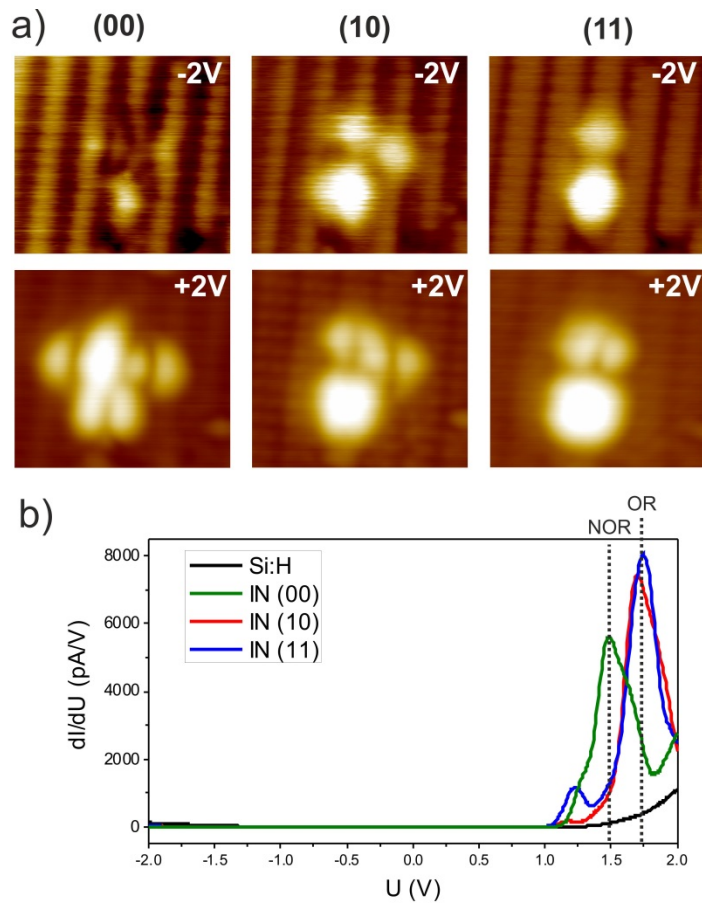
a) Model strukturalny oraz schemat stanów kwantowych i odpowiednich sprzężeń między nimi dla bramki logicznej OR/NOR zrealizowanej w koncepcji QHC na powierzchni Si(001):H. Opisy poszczególnych wartości logicznych zamieszczono w górnej części rysunku.

b) Hamiltonian QHC w przybliżeniu ciasnego wiązania odpowiadający za ewolucję układu z niewysyconych wiązań realizującego bramkę OR/NOR. Rysunek przekopiowany dzięki uprzejmości prof. Joachima z raportu rocznego 2013 projektu AtMol (<http://www.atmol.eu>).

wodoru). Okres charakterystycznych oscylacji Rabiego pomiędzy stanem wejściowym $|\phi_a\rangle$ a wyjściowym $|\phi_b\rangle$ determinuje propagację sygnału (informacji) przez strukturę i jest kontrolowany przez zanik odpowiednich sprzężeń α lub β .

Wykorzystując protokół zawarty w pracy doktorskiej przedstawioną bramkę OR/NOR zrealizowano doświadczalnie na powierzchni Si(001):H, co jest zaprezentowane na serii obrazów STM na **Rys.3a**. Tak jak opisano powyżej, desorpcja dwóch atomów wodoru z powierzchni zmienia odpowiednie sygnały wejściowe. Należy w tym momencie zaznaczyć, że bezpośrednia weryfikacja właściwości transportowych nanostruktur z niewysyconych wiązań nie była tematem podejmowanym w pracy doktorskiej. Do pomiarów lateralnego transportu ładunku przez nanostruktury wymagane jest użycie wielopróbnikowego instrumentu STM. Powoduje to szereg nierozważanych w pracy doktorskiej komplikacji i problemów badawczych związanych przede wszystkim ze skontaktowaniem się z badanymi obiektami w skali atomowej [39]. Z tego względu podjęto próbę charakteryzacji wytworzonej struktury z niewysyconych wiązań w geometrii wertykalnej, wykorzystując do tego celu metodę zaproponowaną w pracy [37]. Za pomocą pojedynczego ostrza STM i techniki STS zbadano przesunięcie stanów elektronowych w centralnej części bramki podczas zmiany wartości logicznych wejść. Wyniki zostały zaprezentowane na wykresie na **Rys.3b**. Można zauważyć wyraźną ewolucję stanów elektronowych na krawędzi pasma przewodnictwa. Wykonując odczyty sygnału dI/dU dla zadanych napięć +1.5 V i +1.75 V uzyskuje się odpowiednio charakterystyki odpowiadające bramkom logicznym NOR i OR. Powyższy wynik, pokazuje, że zaprezentowana w pracy doktorskiej metodologia tworzenia nanostruktur z niewysyconych wiązań na powierzchniach Si(001):H i Ge(001):H oraz zbadane właściwości sprzężeń pomiędzy nimi mogą zostać wykorzystane do tworzenia prototypowych układów logicznych na tych powierzchniach.

Dodatkowo w ramach pracy doktorskiej wykazano, że stosując nowatorski proces preparatyki uwodornionych powierzchni Si(001):H, kompatybilny z obecnie wykorzystywaną technologią wytwarzania wafli półprzewodnikowych na potrzeby przemysłu elektronicznego, można otrzymać atomowo czyste podłoża. Liczba pojedynczych defektów na monoatomowych tarasach tak uzyskanych powierzchni Si(001):H nie odbiega od typowej liczby defektów otrzymywanych po standardowej preparatyce powierzchni Si(001):H w laboratoryjnych warunkach UHV. Jak pokazano w pracy, jakość przygotowanych w ten sposób podłoży



Rys.3

a) Obrazy STM wykonane w 77 K dla różnych konfiguracji bramki logicznej, której model strukturalny został zaprezentowany na Rys2a. Opisy poszczególnych wartości logicznych odpowiadających danej strukturze zamieszczono w górnej części rysunku. Napięcia polaryzacji złącza STM zamieszczono na poszczególnych obrazach, wartość prądu tunelowego wynosiła 10pA.

b) Wykresy STS dI/dU dla powierzchni Si(001):H oraz poszczególnych struktur przedstawionych na Rys.3a. Zaznaczono napięcia, dla których następuje odczyt sygnału wyjściowego z widma STS.

Si(001):H jest wystarczająca do tworzenia zadanych, prototypowych struktur z niewysyconych wiązań i badania ich właściwości elektronowych czy transportowych. Przedstawiony wynik powoduje, że realnym wydaje się zintegrowanie w przyszłości układów z niewysyconych wiązań na powierzchniach pasywowanych wodorem półprzewodników ze standardowymi układami mikroelektronicznymi stosowanymi obecnie. Należy zaznaczyć, że w szerokim kontekście potencjalnych zastosowań, kompatybilność nowych rozwiązań z obecnie stosowaną technologią CMOS jest niezwykle istotna i może wręcz decydować o wdrożeniu danej koncepcji do praktycznej realizacji.

Ostatnim zadaniem badawczym wykonanym w ramach pracy doktorskiej było wytworzenie prototypowego układu monomolekularnego na powierzchniach pasywowanych wodorem półprzewodników. Ten cel został osiągnięty dla molekuł *trinaphthylene* („Y”) na powierzchni Ge(001):H. Po pierwsze pokazano, że monowarstwa wodoru efektywnie odpręga stany molekularne od wpływu podłoża. Ten wynik jest niezwykle istotny w kontekście praktycznego wykorzystania układów monomolekularnych, ponieważ pokazuje, że zadane podczas etapu projektowania i syntezy molekuł właściwości elektronowe nie zostaną zaburzone po jej zdeponowaniu na powierzchni. Dodatkowo wykazano, że podpięcie molekuly „Y” do podwójnego niewysyconego wiązania w istotny sposób wpływa na jej sprzężenie ze stanami elektronowymi powierzchni Ge(001). Efekt uzyskania efektywnego sprzężenia elektronowego pomiędzy molekułami *trinaphthylene* a niewysyconymi wiązaniami na powierzchni pasywowanego wodorem półprzewodnika otwiera perspektywę wykorzystania układów z niewysyconych wiązań do adresowania molekuł organicznych o zadanych właściwościach.

Reasumując, badania przedstawione w ramach pracy doktorskiej stanowią doświadczalną realizację prototypowych układów atomowych i molekularnych na powierzchniach pasywowanych wodorem półprzewodników. W świetle prezentowanych w pracy doktorskiej wyników podłoża Si(001):H i Ge(001):H rzeczywiście stanowią perspektywiczną platformę do wytwarzania układów logicznych opartych na idei elektroniki monomolekularnej.

Bibliografia

1. Aviram, A. and M.A. Ratner, *Molecular Rectifiers*. Chemical Physics Letters, 1974. **29**(2): p. 277-283.
2. Joachim, C., J.K. Gimzewski, and A. Aviram, *Electronics using hybrid-molecular and mono-molecular devices*. Nature, 2000. **408**(6812): p. 541-8.
3. Prauzner-Bechcicki, J.S., S. Godlewski, and M. Szymonski, *Atomic- and molecular-scale devices and systems for single-molecule electronics*. physica status solidi (a), 2012. **209**(4): p. 603-613.
4. Hallam, T., et al., *Use of a scanning electron microscope to pattern large areas of a hydrogen resist for electrical contacts*. Journal of Applied Physics, 2007. **102**(3): p. 034308.
5. Soukiassian, L., et al., *Atomic-scale desorption of H atoms from the Si(100)-2x1:H surface: Inelastic electron interactions*. Physical Review B, 2003. **68**(3).
6. Kawai, H., et al., *Dangling-bond logic gates on a Si(100)-(2 x 1)-H surface*. J Phys Condens Matter, 2012. **24**(9): p. 095011.
7. Ample, F. and C. Joachim, *The chemisorption of polyaromatic hydrocarbons on Si(100)H dangling bonds*. Surface Science, 2008. **602**(8): p. 1563-1571.
8. Bellec, A., et al., *Imaging Molecular Orbitals by Scanning Tunneling Microscopy on a Passivated Semiconductor*. Nano Letters, 2009. **9**(1): p. 144-147.
9. Binnig, G., et al., *Surface Studies by Scanning Tunneling Microscopy*. Physical Review Letters, 1982. **49**(1): p. 57-61.
10. Eigler, D.M. and E.K. Schweizer, *Positioning Single Atoms with a Scanning Tunneling Microscope*. Nature, 1990. **344**(6266): p. 524-526.
11. Boland, J., *Evidence of pairing and its role in the recombinative desorption of hydrogen from the Si(100)-2x1 surface*. Physical Review Letters, 1991. **67**(12): p. 1539-1542.
12. Shen, T.C., et al., *Atomic-Scale Desorption through Electronic and Vibrational-Excitation Mechanisms*. Science, 1995. **268**(5217): p. 1590-1592.
13. Foley, E.T., et al., *Cryogenic UHV-STM study of hydrogen and deuterium desorption from Si(100)*. Physical Review Letters, 1998. **80**(6): p. 1336-1339.
14. McEllistrem, M., M. Allgeier, and J.J. Boland, *Dangling bond dynamics on the silicon (100)-2x1 surface: Dissociation, diffusion, and recombination*. Science, 1998. **279**(5350): p. 545-548.
15. Hitosugi, T., et al., *Jahn-Teller distortion in dangling-bond linear chains fabricated on a hydrogen-terminated Si(100)-2 x 1 surface*. Physical Review Letters, 1999. **82**(20): p. 4034-4037.
16. Soukiassian, L., et al., *Atomic wire fabrication by STM induced hydrogen desorption*. Surface Science, 2003. **528**(1-3): p. 121-126.
17. Haider, M., et al., *Controlled Coupling and Occupation of Silicon Atomic Quantum Dots at Room Temperature*. Physical Review Letters, 2009. **102**(4).
18. Labidi, H., L. Kantorovich, and D. Riedel, *Atomic-scale control of hydrogen bonding on a bare Si(100)-2x1 surface*. Physical Review B, 2012. **86**(16).
19. Bellec, A., et al., *Dihydride dimer structures on the Si(100):H surface studied by low-temperature scanning tunneling microscopy*. Physical Review B, 2008. **78**(16).
20. Bellec, A., D. Riedel, and G. Dujardin, *Electronic properties of the n-doped hydrogenated silicon (100) surface and dehydrogenated structures at 5 K*. Physical Review B, 2009. **80**(24).
21. Bellec, A., et al., *Nonlocal Activation of a Bistable Atom through a Surface State Charge-Transfer Process on Si(100)-(2x1):H*. Physical Review Letters, 2010. **105**(4).
22. Bellec, A., et al., *Reversible charge storage in a single silicon atom*. Physical Review B, 2013. **88**(24).

23. Kawai, H., et al., *Conductance decay of a surface hydrogen tunneling junction fabricated along a Si(001)-(2×1)-H atomic wire*. Physical Review B, 2010. **81**(19).
24. Robles, R., et al., *Energetics and stability of dangling-bond silicon wires on H passivated Si(100)*. J Phys Condens Matter, 2012. **24**(44): p. 445004.
25. Kepenekian, M., et al., *Electron transport through dangling-bond silicon wires on H-passivated Si(100)*. J Phys Condens Matter, 2013. **25**(2): p. 025503.
26. Kepenekian, M., et al., *Surface-state engineering for interconnects on H-passivated Si(100)*. Nano Letters, 2013. **13**(3): p. 1192-5.
27. Kepenekian, M.I., et al., *Leakage current in atomic-size surface interconnects*. Applied Physics Letters, 2013. **103**(16): p. 161603.
28. Ample, F., et al., *Single OR molecule and OR atomic circuit logic gates interconnected on a Si(100)H surface*. J Phys Condens Matter, 2011. **23**(12): p. 125303.
29. Scappucci, G., et al., *A complete fabrication route for atomic-scale, donor-based devices in single-crystal germanium*. Nano Letters, 2011. **11**(6): p. 2272-9.
30. Scappucci, G., et al., *Atomic-scale patterning of hydrogen terminated Ge(001) by scanning tunneling microscopy*. Nanotechnology, 2009. **20**(49): p. 495302.
31. Ye, W., et al., *Scanning tunneling spectroscopy and density functional calculation of silicon dangling bonds on the Si(100)-2×1:H surface*. Surface Science, 2013. **609**: p. 147-151.
32. Livadaru, L., et al., *Dangling-bond charge qubit on a silicon surface*. New Journal of Physics, 2010. **12**(8): p. 083018.
33. Pitters, J.L., et al., *Tunnel coupled dangling bond structures on hydrogen terminated silicon surfaces*. J Chem Phys, 2011. **134**(6): p. 064712.
34. Fuhrer, A., et al., *Atomic-Scale, All Epitaxial In-Plane Gated Donor Quantum Dot in Silicon*. Nano Lett, 2009. **9**(2): p. 707-710.
35. Weber, B., et al., *Ohm's law survives to the atomic scale*. Science, 2012. **335**(6064): p. 64-7.
36. Fuechsle, M., et al., *Spectroscopy of few-electron single-crystal silicon quantum dots*. Nat Nanotechnol, 2010. **5**(7): p. 502-505.
37. Soe, W.H., et al., *Manipulating Molecular Quantum States with Classical Metal Atom Inputs: Demonstration of a Single Molecule NOR Logic Gate*. ACS Nano, 2011. **5**(2): p. 1436-1440.
38. Renaud, N. and C. Joachim, *Design and stability of NOR and NAND logic gates constructed with three quantum states*. Physical Review A, 2008. **78**(6).
39. Joachim, C., et al., *Multiple atomic scale solid surface interconnects for atom circuits and molecule logic gates*. J Phys Condens Matter, 2010. **22**(8): p. 084025.

Przedruki artykułów składających się na pracę doktorską.

Artykuły umieszczono w następującej kolejności:

1. [Kolmer, PRB 2012] M. Kolmer, S. Godlewski, H. Kawai, B. Such, F. Krok, M. Saeys, C. Joachim, M. Szymonski, *Electronic properties of STM-constructed dangling-bond dimer lines on a Ge(001)-(2×1):H surface*, Physical Review B, **86**, 125307 (2012);
2. [Kolmer, ME 2013] M. Kolmer, S. Godlewski, J. Lis, B. Such, L. Kantorovich, M. Szymonski, *Construction of atomic-scale logic gates on a surface of hydrogen passivated germanium*, Microelectronic Engineering, **109**, 262–265 (2013);
3. [Kolmer, ASS 2014] M. Kolmer, S. Godlewski, R. Zuzak, M. Wojtaszek, C. Rauer, A. Thuaire, J.M. Hartmann, H. Moriceau, C. Joachim, M. Szymonski, *Atomic scale fabrication of dangling bond structures on hydrogen passivated Si(001) wafers processed and nanopackaged in a clean room environment*, Applied Surface Science, **288** 83– 89 (2014);
4. [Kolmer, Springer 2013] M. Kolmer, S. Godlewski, B. Such, P. De Mendoza, C. De Leon, A. M. Echavarren, H. Kawai, M. Saeys, C. Joachim, M. Szymonski, *SPM imaging of trinaphthylene molecular states on a hydrogen passivated Ge(001) surface*, Springer series “Advances in Atom and Single Molecule Machines”, vol.3, ISBN 978-3-642-38808-8, 105-114 (2013);
5. [Godlewski, ACS Nano 2013] S. Godlewski, M. Kolmer, H. Kawai, B. Such, R. Zuzak, M. Saeys, P. De Mendoza, A.M. Echavarren, C. Joachim, M. Szymonski, *Contacting a conjugated molecule with a surface dangling bond dimer on a Ge(001):H surface allows imaging of the hidden ground electronic state*, ACS Nano, **7 (11)**, 10105-10111 (2013).

Electronic properties of STM-constructed dangling-bond dimer lines on a Ge(001)-(2×1):H surfaceMarek Kolmer,¹ Szymon Godlewski,^{1,*} Hiroyo Kawai,^{2,†} Bartosz Such,¹ Franciszek Krok,¹ Mark Saeys,^{2,3} Christian Joachim,^{2,4} and Marek Szymonski¹¹*Department of Physics of Nanostructures and Nanotechnology, Institute of Physics, Jagiellonian University, Reymonta 4, PL 30-059 Krakow, Poland*²*Institute of Materials Research and Engineering, 3 Research Link, Singapore 117602, Singapore*³*Department of Chemical and Biomolecular Engineering, National University of Singapore, 4 Engineering Drive 4, Singapore 117576, Singapore*⁴*Nanosciences Group & MANA Satellite, CEMES-CNRS, 29 rue Jeanne Marvig, F-31055 Toulouse, France*

(Received 25 April 2012; revised manuscript received 3 August 2012; published 6 September 2012)

Atomically precise dangling-bond (DB) lines are constructed dimer-by-dimer on a hydrogen-passivated Ge(001)-(2×1):H surface by an efficient scanning tunneling microscope (STM) tip-induced desorption protocol. Due to the smaller surface band gap of the undoped Ge(001) substrate compared to Si(001), states associated with individually created DBs can be characterized spectroscopically by scanning tunneling spectroscopy (STS). Corresponding dI/dV spectra corroborated by first-principle modeling demonstrate that DB dimers introduce states below the Ge(001):H surface conduction band edge. For a DB line *parallel* to the surface reconstruction rows, the DB-derived states near the conduction band edge shift to lower energies with increasing number of DBs. The coupling between the DB states results in a dispersive band spanning 0.7 eV for an infinite DB line. For a long DB line *perpendicular* to the surface reconstruction rows, a similar band is not formed since the interdimer coupling is weak. However, for a short DB line (2–3 DBs) perpendicular to the reconstruction rows a significant shift is still observed due to the more flexible dimer buckling.

DOI: [10.1103/PhysRevB.86.125307](https://doi.org/10.1103/PhysRevB.86.125307)

PACS number(s): 73.20.At, 68.37.Ef

I. INTRODUCTION

Silicon Si(001):H and germanium Ge(001):H hydrogen-passivated surfaces are promising platforms for the atomic-scale fabrication of mesoscopic electronic devices¹ and for the construction of atomic-scale surface electronic circuits.^{2,3} The desorption of surface hydrogen atoms using the scanning tunneling microscope (STM) tip creates very localized dangling-bond (DB) electronic states within the surface band gap of those materials.^{1,4–8} These nanostructures can be used as interconnects in molecular electronics devices stabilized on a surface,⁹ create DB logic circuits based on quantum interferences,² or act as qubits for the surface miniaturization of quantum computers.^{6–8} The formation of single, double DBs,^{10–19} and long DB lines^{3,4,20} on a Si(001):H surface, as well as selective *in situ* doping by PH₃ gas has been studied by STM techniques both at room temperature and at low temperatures (LT).^{1,5,8,20–22} Although it has been theoretically predicted that DB lines running parallel and perpendicular to the Si(001):H dimer rows will have very different electronic transport properties,^{23,24} those properties have not yet been characterized spectroscopically. It is important to quantify the difference between the DB lines in both directions in order to design efficient atomic-scale devices using DBs.² Specifically, it is crucial to determine the maximum and minimum length of DB line interconnects between surface molecular devices,⁹ as well as to investigate the surface tunneling leakage current²⁴ in both directions. However, due to the larger surface band gap, it is challenging to spectroscopically characterize the states introduced by DB nanostructures in the surface band gap of Si(001):H. As we demonstrate in this paper, the smaller surface band gap of Ge(001):H makes it possible to precisely track the gradual shift in the energy levels of the DB states as a function of number of DBs using scanning tunneling

spectroscopy (STS), as DB lines are created dimer-by-dimer.

We report an efficient STM protocol to construct pre-designed DB nanostructures on a Ge(001):H surface. First, short atomic lines containing 1–5 DB dimers are fabricated. Near the bottom of the Ge(001):H surface conduction band edge, the progressive introduction of DB electronic states is studied using LT-STM dI/dV spectroscopy. Short DB dimer lines introduce electronic states in the gap. Those states can be used to design DB logic gates.² When the length of DB lines increases beyond 3 DB dimers, a conduction channel gradually develops below the bottom of the Ge(001):H conduction band edge for DB lines parallel to the reconstruction rows.

II. EXPERIMENTAL AND COMPUTATIONAL DETAILS

The Ge samples used in the STM/STS measurements were cut from undoped Ge(001) wafers (TBL Kelpin Crystals, *n*-type, ~45 Ω cm). After insertion into the UHV system, the samples were first sputtered and annealed for 15 min (Ar⁺, 600 eV, 1020 K). The sputtering cycles were repeated until a clean $c(4\times 2)/p(2\times 2)$ surface was obtained as confirmed by low energy electron diffraction (LEED) and LT-STM measurements. Then hydrogen passivation was performed using a home-built hydrogen cracker to provide atomic hydrogen. During the passivation procedure, the samples were kept at 485 K and the hydrogen pressure was maintained at 1×10^{-7} mbar. The base pressure of the STM chamber was in the low 10^{-10} mbar range. All STM/STS measurements were performed at 5 K (liquid helium). Before construction of the DB dimer lines, the bare Ge(001) and Ge(001):H surface structures were characterized by comparing the experimental and calculated STM images. The electronic properties of DB dimer

lines were analyzed in detail using density functional theory (DFT) surface electronic structure calculations and dI/dV spectra calculated using the surface Green-function matching (SGFM) method.²⁵ The STM images and dI/dV spectra were calculated for structures optimized using DFT²⁶ with the Perdew-Burke-Ernzerhof (PBE) functional,²⁷ as implemented in the Vienna *ab initio* simulation package (VASP) (see Appendix A). STM images were calculated using the SGFM method²⁵ with an extended Huckel molecular orbital (EHMO) Hamiltonian. The parameters in the EHMO Hamiltonian were fitted to accurate DFT band structures. The HSE06 functional was used to fit the parameters since it provides a more accurate description of the Ge band gap than the PBE functional (see Appendix A). The STM junction was modeled as a semi-infinite W(111) slab, a Ge-terminated STM tip, a nine-layer Ge(001):H surface with the DB nanostructures, and the semi-infinite Ge(001) bulk, as illustrated in Fig. 9. Our approach takes into account the coupling between the surface and the tip and their couplings to the bulk electronic states. This approach provides a realistic description of the ballistic electron transport across the STM junction, while minimizing the computational cost.

III. RESULTS AND DISCUSSION

Starting from a Ge(001):H surface, atomically controlled H extractions were performed by pulsing the STM tip bias voltage. First, the tip was approached over the hydrogen dimer selected for extraction with the STM feedback loop set on a $I = 1$ nA tunneling current intensity and a $V = -0.5$ V bias voltage. The tip apex was positioned over the dimer according to the Ge(001):H filled-state STM image [see Fig. 1(a)]. Subsequently, the feedback loop was turned off and the desorption process started with a V pulse set up at $+1.6$ V. The desorption of the hydrogen dimer was detected when a sudden rise of the tunneling current was observed in the $I(t)$ characteristic. The procedure was repeated step-by-step until the targeted DB dimer pattern was constructed. The above protocol allows for the efficient construction of a predesigned DB nanostructure with atom-by-atom precision, unlike methods based on a fast tip movement along surface dimer rows at a constant speed.^{3,4,20} Figure 1 illustrates an atomically controlled dimer-by-dimer desorption leading to the construction of a short 2 DB dimer line parallel to the Ge(001):H rows. Here, unlike in the case of the Si(001):H surface, our STM tip V pulse protocol extracts a pair of H atoms per pulse instead of a single H.

Following this protocol, short lines consisting of 1 to 3 DB dimers were constructed in both directions, as presented in Fig. 2 (left column). DFT calculations show that infinite DB lines perpendicular and parallel to the Ge(001):H rows buckle by 0.81 and 0.89 Å, respectively. Along the perpendicular direction, the buckling of DB dimers is similar to the buckling of an isolated DB dimer, and in-phase buckling (a down-up-down-up sequence) is more stable than out-of-phase buckling (a down-up-up-down sequence) by 20 meV/dimer. The small energy difference suggests that the buckling is rather flexible for the perpendicular direction. For DB lines parallel to the Ge(001):H rows, out-of-phase buckling, where neighboring DB dimers are buckled in opposite directions, as

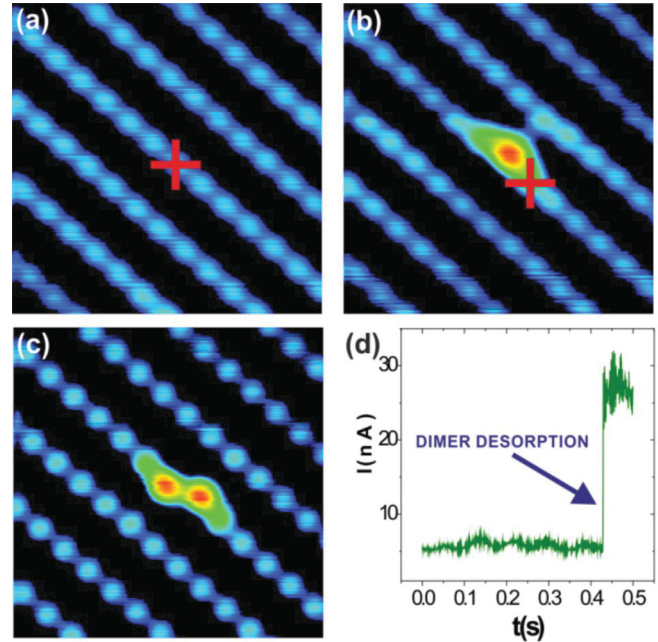


FIG. 1. (Color online) STM tip induced fabrication of a DB line running along the surface reconstruction rows. Red crosses indicate the positions of the tip during the dimer desorption processes: (a) filled-state STM image (-0.5 V, 1 nA, 4 nm \times 4 nm) of the hydrogenated Ge(001) surface before desorption, (b) single DB dimer, (c) two neighboring DB dimers forming the DB line, and (d) typical $I(t)$ characteristic recorded during the desorption process.

it is in the $c(4 \times 2)$ and $p(2 \times 2)$ reconstructions of the bare Ge(001) surface, is more stable than in-phase buckling, where neighboring DB dimers are buckled in the same direction, by 120 meV/dimer. The calculated STM images for short lines of 1, 2, and 3 DB dimers in both directions [Fig. 2, second column] agree well with the experimental STM images [Fig. 2, first column]. In order to compare the images in more detail, the corrugations over the DBs were also plotted. As presented in Fig. 2 (third column), each calculated constant current line scan agrees well with the corresponding experimental line scan. The small differences in the corrugations can be attributed to details of tip apex electronic structure, as well as to differences in buckling between short and infinite DB lines. The detailed comparison between experimental and calculated STM images furthermore highlights the different surface atomic structure of DB dimer lines constructed on a Ge(001):H surface and on a Si(001):H surface. As reported by Bellec *et al.*, isolated DB dimers do not appear buckled on a Si(001):H surface.¹²

To characterize the electronic properties of each surface, the electronic band structures of the Ge(001):H surface and of the bare Ge(001) surface were calculated [Fig. 3]. The fully hydrogenated Ge(001):H surface is predicted to have a 1.1 eV surface electronic band gap, while the bare Ge(001) surface has a 0.6 eV surface band gap [Figs. 3(a) and 3(d), respectively]. The Ge(001):H surface gap decreases when DB dimer lines are created on the surface due to the electronic states introduced by the DB dimers near the bottom of the Ge(001):H conduction band edge. These bands result from the antibonding π^* states of the Ge(001) DB dimers. The corresponding bonding π states are located well below the top of the valence band

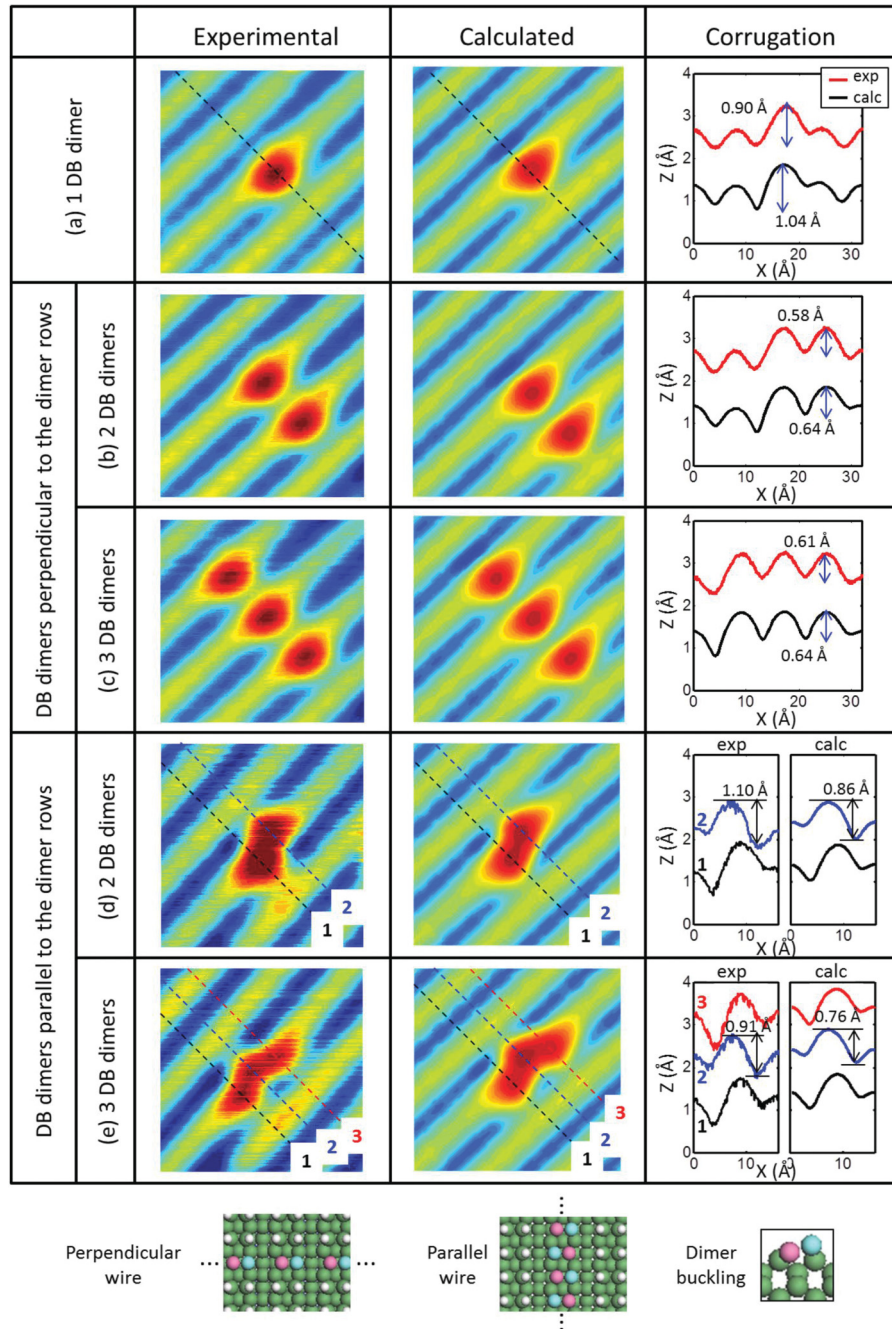


FIG. 2. (Color online) Experimental and calculated STM images of the Ge(001)-(2 \times 1):H surface with (a) 1 DB dimer, (b) and (c) 2 and 3 DB dimers aligned perpendicular to the dimer rows, and (d) and (e) 2 and 3 DB dimers aligned parallel to the dimer rows. The corrugations over the DB dimers are also shown for each case. All STM images acquired at -0.5 V, 1.0 nA, 3 nm \times 3 nm. The atomic structures of the DB line perpendicular and parallel to the dimer rows are shown to illustrate the line directions.

edge, and they do not affect the width of the band gap. The band structures for infinite DB lines on Ge(001):H in both the perpendicular and the parallel direction are shown in Figs. 3(b) and 3(c), respectively. In both cases, a new π^* conduction band is created near the bottom of the Ge(001):H conduction band. A significant dispersion of 0.67 eV is however only found for the parallel DB dimer line [Fig. 3(c)].

To investigate how the DB dimer states shift gradually in the Ge(001):H surface band gap as the length of DB line increases, dI/dV spectra were measured and transmission spectra $T(E)$ were calculated for DB lines with various lengths. All STS measurements were performed in a mode with the feedback loop turned on between every two $I(V)$ characteristics to determine the tip position. The $I(V)$ characteristics were automatically collected using a grid covering a 2.5 nm \times

2.5 nm surface area, and the corresponding dI/dV spectra were obtained by differentiating the $I(V)$ curves averaged previously over the area of the DBs only. The dI/dV spectra were simulated by calculating the electronic transmission spectra through the tunnel junction used for the constant current image calculations [Fig. 2], which consists of the W tip, the Ge tip apex, the Ge(001):H surface, and the Ge(001) bulk [see Appendix A, Fig. 9]. The tip apex was placed 7 Å above the Ge(001):H surface.

First, the dI/dV spectra for the bare Ge(001) surface and for the fully hydrogenated Ge(001):H surface were measured and compared with calculated $T(E)$ spectra. The experimental dI/dV spectra clearly show that the surface band gap increases upon surface hydrogenation from 0.25 eV for the bare Ge(001) surface to about 0.85 eV for Ge(001):H [light blue and green

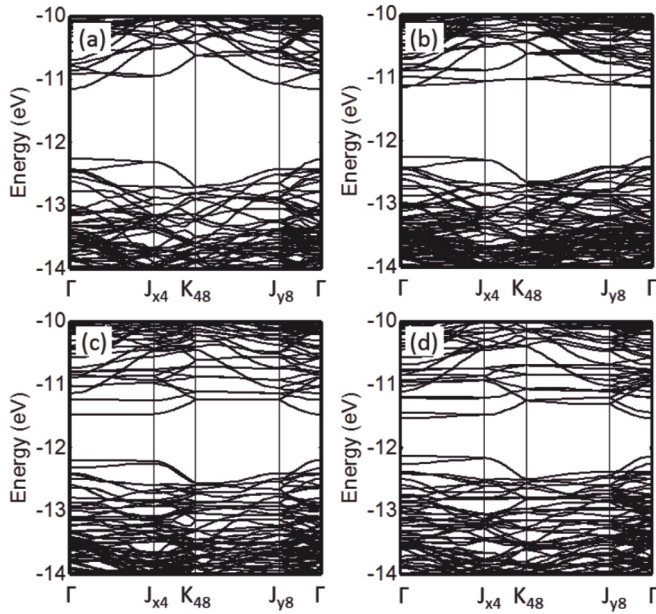


FIG. 3. Band structures of (a) a fully passivated Ge(001)-(2 \times 1):H surface, (b) infinite DB line perpendicular to the dimer rows with seven H-passivated dimers between two DB lines, (c) infinite DB line parallel to the dimer rows, where the DB dimers are buckled out-of-phase along the dimer row, and (d) a clean Ge(001)- $c(4\times 2)$ surface. A nine-layer slab was used to model the Ge surfaces.

curves in Fig. 4(a), respectively]. The calculated $T(E)$ spectra [Fig. 4(b)] follow the same trend, in agreement with the calculated bare Ge(001)- $c(4\times 2)$ and Ge(001):H surface band structures [Figs. 3(a) and 3(d), respectively]. The band gap

for the dI/dV and $T(E)$ spectra differs slightly from the calculated band structures, because a nine-layer slab was used for the band structure calculations while a semi-infinite structure was used in the transport calculations. Note that $T(E)$ was calculated for a single point instead of averaging over the DB area. Therefore, the relative heights and widths of the $T(E)$ resonance peaks are different from the experimental dI/dV spectra.

Next, experimental dI/dV spectra and calculated $T(E)$ spectra are compared for DB lines with 1, 2, 3, and 5 DB dimers in both the perpendicular and the parallel direction. For DB lines in both directions, the experimental dI/dV spectra and the calculated $T(E)$ spectra show large nonzero conductances at energies below the Ge(001):H surface conduction band edge [Fig. 4]. Although these nonzero conductances are found within the Ge(001):H surface gap, they can be detected in the measurements and in the calculations because the Ge bulk band gap is smaller than the 0.85 eV Ge(001):H surface band gap. Note that a large resonance peak appears 0.9 eV above the Fermi level even for a single DB dimer [blue resonance, Figs. 4(a) and 4(c)], clearly showing the DB dimer state introduced below the conduction band edge. This single DB dimer resonance peak is also described well by the calculations [blue resonance peak, Figs. 4(b) and 4(d)]. No resonance peaks are observed near the valence band edge.

For DB lines parallel to the dimer rows, it is expected that the dI/dV resonances are observed below the conduction band edge, and that the resonances will gradually span the 0.6 eV energy difference between the Ge(001):H and the bare Ge(001) conduction band edge as the length of the DB line increases. This is because each DB dimer introduces an additional π^*

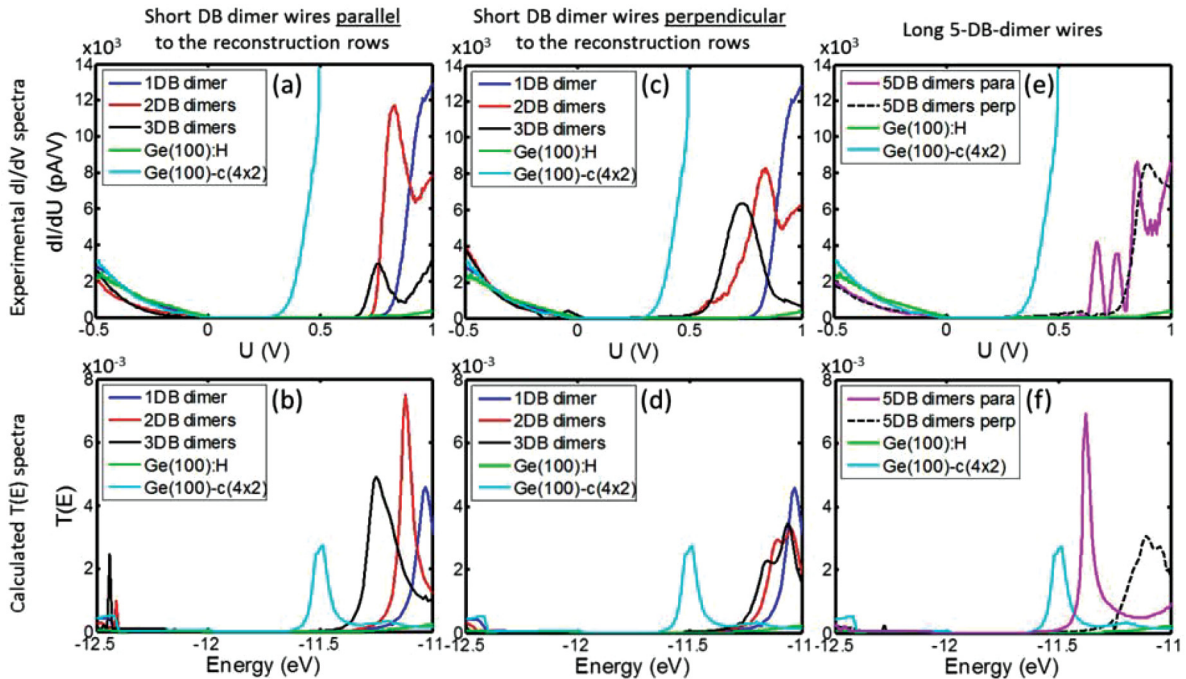


FIG. 4. (Color online) (a), (c), and (e) Experimental dI/dV and (b), (d), and (f) calculated $T(E)$ spectra for a fully hydrogenated Ge(001)-(2 \times 1):H, DB lines containing 1, 2, 3, and 5 DB dimers aligned parallel and perpendicular to the Ge(001):H dimer rows and clean Ge(001) surface with $c(4\times 2)$ reconstruction [STS feedback loop at 0.5 nA and -0.5 V for all cases except for 2 and 3 DB dimers in (a) and 5 DB dimers in (e), where 0.3 nA and -0.5 V setpoint was used].

and an infinitely long DB dimer line results in a dispersive π^* band as shown in Fig. 3(c). For short DB lines composed of 2 and 3 dimers, the dI/dV resonances indeed gradually shift towards lower energies compared to the resonance peak for a single DB dimer [Fig. 4(a), red and black resonances], which is also observed in the calculated $T(E)$ spectra [Fig. 4(b), red and black resonances]. When the number of DB dimers increases to 5, the dI/dV resonances shift further to lower energies [Fig. 4(e), pink resonance], gradually approaching the conduction band edge of the bare Ge(001) surface [Fig. 4(e), light blue resonance]. The $T(E)$ spectra show the same trend [Figs. 4(b) and 4(f)]. For DB lines parallel to the dimer rows, the gradual shift of the resonance peaks results from the significant electronic couplings between the nearest-neighbor DB dimer states [see Appendix B, Figs. 10]. Note that only one resonance is observed in the $T(E)$ spectrum for the 5 DB dimer line [Fig. 4(f), pink resonance], whereas a few peaks are observed in the dI/dV plot [Fig. 4(e)]. This is because the tip position is fixed above the central DB dimer for the $T(E)$ calculation, whereas the dI/dV plot is averaged over the DB line. Since each $T(E)$ peak results from a different DB dimer along the DB line, different peaks are enhanced in the $T(E)$ depending on the tip position. In all cases, no significant shift was observed in the valence band edge.

Similar to DB lines parallel to the dimer rows, the resonance peaks shift to lower energies for lines of 2 and 3 DB dimers perpendicular to the dimer rows. However, the shift in the measured dI/dV spectra is larger than the shift in the calculated $T(E)$ spectra [Figs. 4(c) and 4(d)]. For perpendicular DB lines, the shift in the $T(E)$ resonances due to coupling between DB states is expected to be small because the band structure for an infinite perpendicular DB line shows only a nondispersive π^* band located at the edge of Ge(001):H conduction band [Fig. 3(b)]. This difference between the measured and calculated shifts, however, results from a competition between surface atomic structure relaxation towards their infinite configurations and interdimer electronic interactions along those DB lines. Since the interdimer distance is larger for a perpendicular DB line, the buckling of the dimers for short 2 and 3 DB dimer lines is more flexible than for short parallel DB lines. For example, when the buckling of the perpendicular DB dimers is reduced by 25%, the DB-derived states shift down by almost 0.1 eV, and show a resonance shift similar to the one observed in the dI/dV spectra [Fig. 4(c)]. This flexibility hence causes the dI/dV shifts for short perpendicular DB lines to be similar to those observed for short parallel DB lines. However, when the length of the perpendicular DB line exceeds 3 DB dimers, the buckling becomes less flexible and approaches the buckling for the infinite DB line. Therefore, when the number of DB dimers is increased to 5, the resonance peak in both the dI/dV and the $T(E)$ spectra shifts up in energy, and becomes close to the position for a single DB dimer [dashed black resonance, Figs. 4(e) and 4(f)]. This behavior is very different from the trend observed for the parallel DB line with 5 DB dimers.

IV. CONCLUSIONS

In conclusion, we have developed an efficient protocol to construct atomically precise DB nanostructures on a

Ge(001):H platform, by selective dimer-by-dimer hydrogen desorption. Unlike on Si(001):H, the DB states on Ge(001):H can be characterized by STS methods on an undoped substrate. Comparison of first-principles calculations with high-resolution STM images confirms that the DB dimers are stabilized in buckled configurations, in contrast to isolated DBs on Si(001):H. The creation and gradual shift of DB electronic states as a function of the number of DB dimers has been probed by STS measurements. We demonstrate experimentally that the DB electronic states are introduced in the Ge(001):H gap differently for DB lines running perpendicular and parallel to the surface reconstruction rows. DB lines parallel to the surface reconstruction rows display a stronger inter-DB dimer electronic coupling, resulting in a dispersive conduction band spanning 0.7 eV for an infinite parallel DB line. Surprisingly, the DB states show similar shifts for short DB lines regardless of their orientation, which can be explained by different physics. For DB lines parallel to the dimer rows, the shift is caused by electronic coupling between neighboring DB dimer states, while for perpendicular DB lines, the corresponding shift results from the more flexible buckling of the DB dimers. This is confirmed spectroscopically for longer perpendicular DB lines, where the DB-derived peak shifts back to a higher energy when the DB buckling settles, while for parallel DB lines the peak continues to shift towards lower energies until the coupling saturates and the full range of the band structure is covered. The presence of states in the Ge(001):H surface band gap together with the ability to split them in both surface directions for 2 and 3 DB dimers provides a powerful tool to build surface atomic-scale logic gates with a minimum number of DBs. Indeed, one can play with those dimer states which, as we have shown, are also interacting in the case of short (3 DB dimers) perpendicular lines.² The best approach to interconnect those gates is to construct DB dimer lines parallel to the Ge(001):H rows and to apply a bias voltage higher than + 0.5 V to access the new π^* surface conduction states. The electronic behavior of short DB lines in both directions is of great importance for the design of DB quantum Hamiltonian atomic-scale logic gates, which up to now had only been accessible on a single molecule basis. Furthermore, we have demonstrated that by varying the number of neighboring DBs, the new electronic states located within the intrinsic band gap of the hydrogenated surface can be tuned, which can be utilized to control the charge state of DB quantum dots.

ACKNOWLEDGMENTS

This research was supported by the 7th Framework Programme of the European Union Collaborative Project ICT (Information and Communication Technologies) “Atomic Scale and Single Molecule Logic Gate Technologies” (ATMOL), Contract No. FP7-270028 and by the Visiting Investigatorship Programme “Atomic scale Technology Project” from the Agency of Science, Technology, and Research (A*STAR). The experimental part of the research was carried out with equipment purchased with financial support from the European Regional Development Fund in the framework of the Polish Innovation Economy Operational Program (Contract No. POIG.02.01.00-12-023/08).

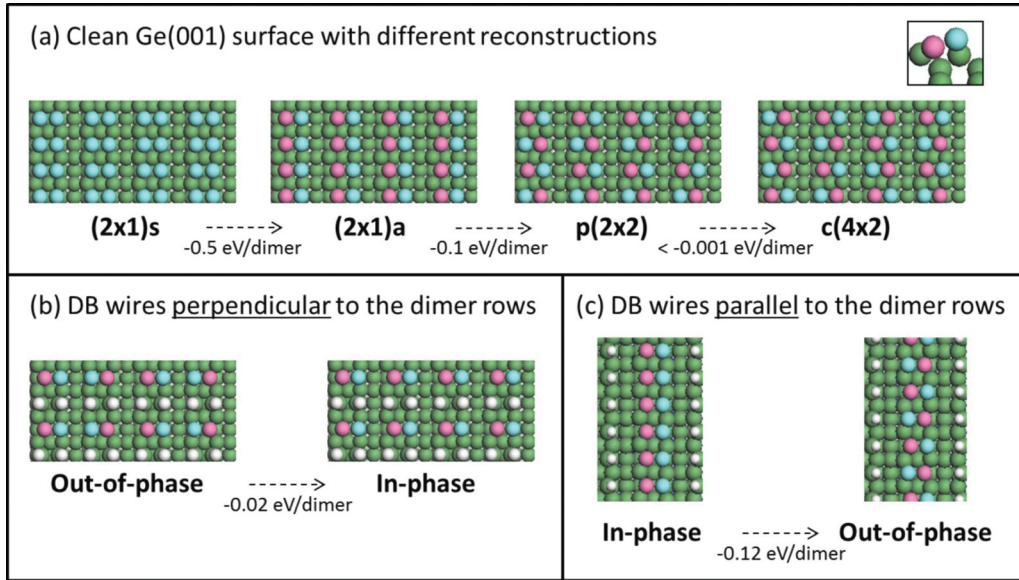


FIG. 5. (Color online) Atomic structure and stability of (a) four different surface reconstruction of Ge(001): $(2 \times 1)s$, $(2 \times 1)a$, $p(2 \times 2)$, and $c(4 \times 2)$, (b) two different buckling configurations for the DB wire perpendicular to the dimer rows, and (c) two different buckling configurations for the DB wire parallel to the dimer rows.

APPENDIX A

Four possible surface reconstructions for Ge(001) are shown in Fig. 5. Among the different surface reconstructions, the most stable reconstruction is $c(4 \times 2)$, but since the

difference in energy between $c(4 \times 2)$ and $p(2 \times 2)$ is very small, it is expected that both reconstructions will be observed in the experimental STM image of a clean Ge(001) surface. When the Ge(001) surface is fully hydrogenated, the Ge(001):H surface dimers are symmetric with one H atom per Ge atom. For the DB

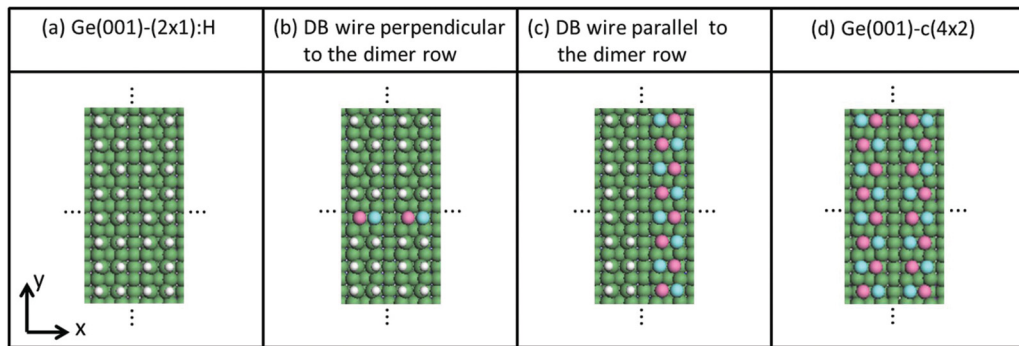


FIG. 6. (Color online) The surface atomic structures used in the band structure calculations shown in Fig. 3.

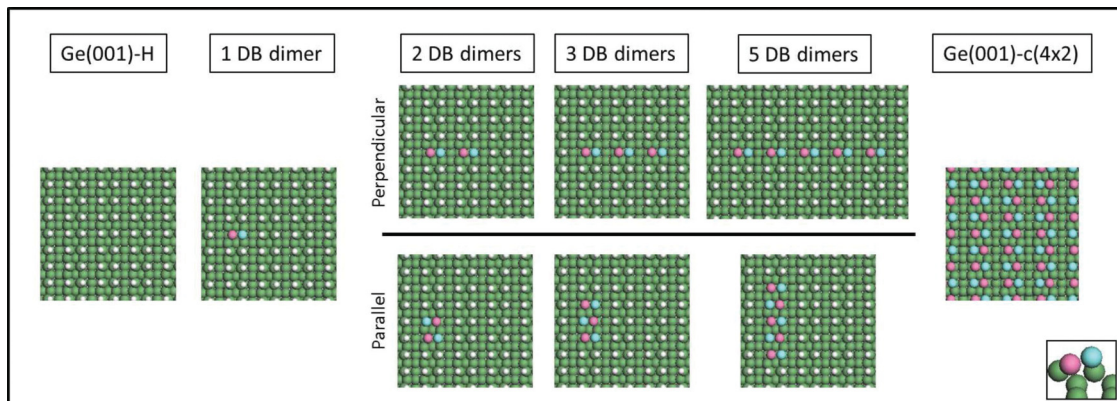


FIG. 7. (Color online) The surface atomic structures used in the image calculations [Fig. 2] and $T(E)$ spectra [Fig. 4].

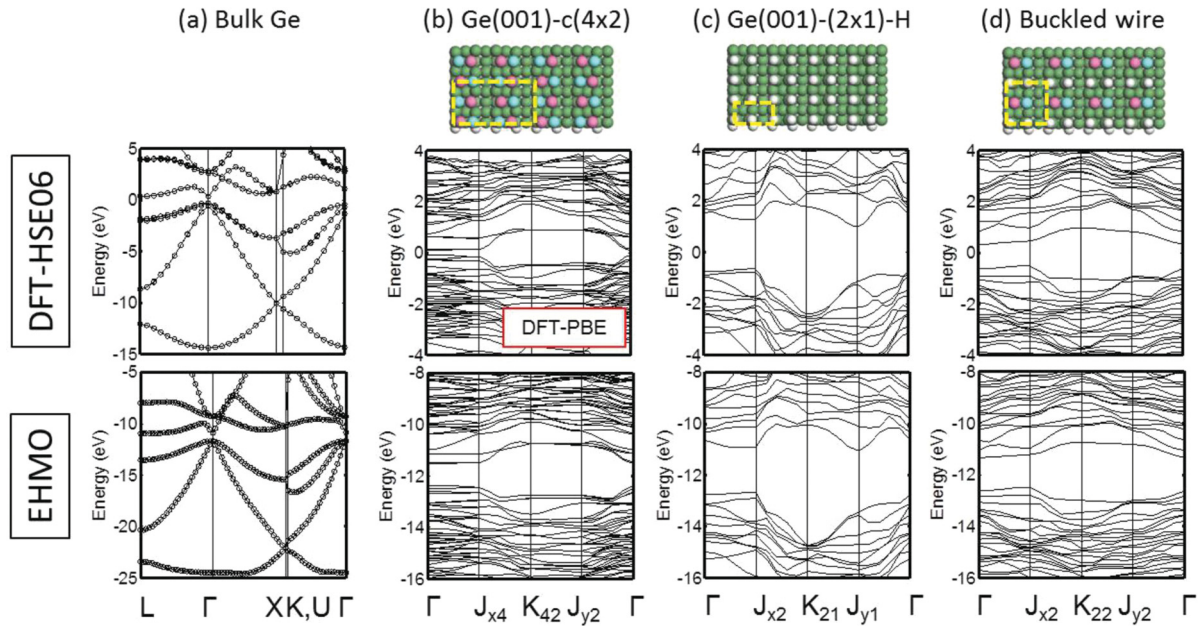


FIG. 8. (Color online) DFT-HSE06 (top row) and EHMO (bottom row) band structures for (a) bulk Ge, (b) Ge(001)- $c(4 \times 2)$, (c) Ge(001)- (2×1) -H, and (d) Ge(001)- (2×1) -H surface with buckled wire perpendicular to the dimer rows. The Brillouin zone for each band structure is indicated by the dashed lines on the atomic structure.

wire perpendicular to the dimer rows, the in-phase buckling configuration is slightly more stable than the out-of-phase configuration, but due to the small difference in stability (0.02 eV/dimer), both configurations were observed in STM measurements [Fig. 5(b)]. For the DB wire parallel to the dimer rows, the out-of-phase buckling configuration is more stable

than the in-phase configuration by 0.12 eV/dimer, consistent with the energy difference between the $(2 \times 1)a$ and the $p(2 \times 2)$ reconstruction [Fig. 5(c)].

The surface structures for the band structures in Fig. 3 are shown in Fig. 6. The same (4×8) unit cell was used for all band structure calculations to allow direct comparison.

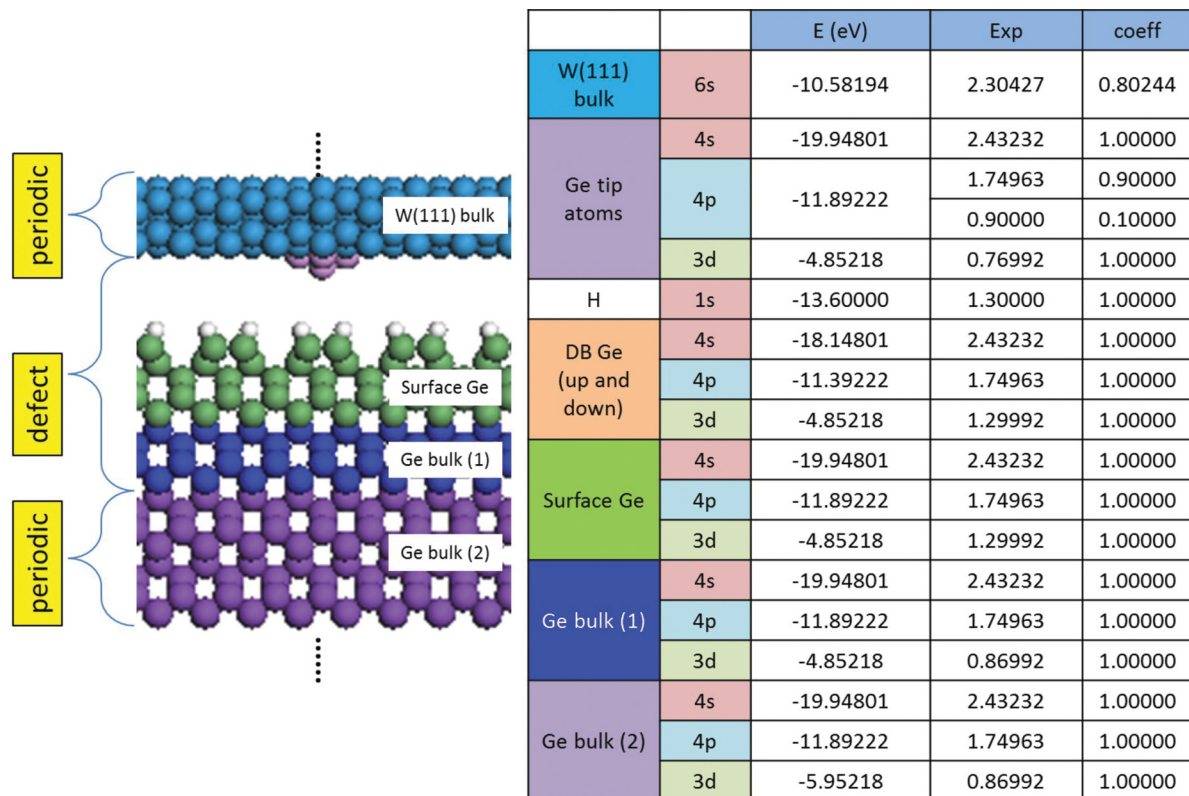


FIG. 9. (Color online) The atomic configuration and EHMO parameters used in the STM image and $T(E)$ calculations.

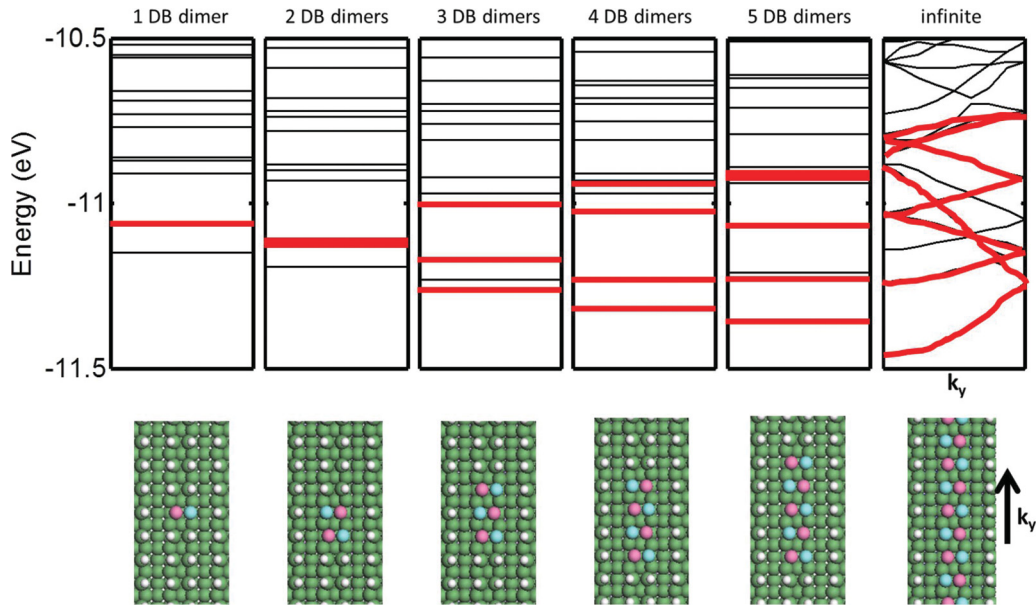


FIG. 10. (Color online) Energy spectra (Γ point) showing the DB states (red lines) for 1, 2, 3, 4, and 5 DB dimers parallel to the dimer rows. The band structure for an infinite line of DB dimers parallel to the dimer rows (k_y) is also shown for comparison.

The surface atomic structures of the calculated images in Fig. 2 and $T(E)$ spectra in Fig. 4 are also shown [Fig. 7]. As mentioned in Sec. II, the parameters in the EHMO Hamiltonian used in the STM image and $T(E)$ calculations were fitted to DFT-HSE06 band structures. In Fig. 8, the DFT-HSE06 and fitted EHMO band structures for bulk Ge and different Ge surfaces are compared, showing the reasonable agreement. Note that the DFT-PBE instead of DFT-HSE06 was used for $c(4 \times 2)$ configuration due to the computational limitation. The atomic configuration and EHMO parameters used in the STM image and $T(E)$ calculations are shown in Fig. 9.

APPENDIX B

As the number of DBs increases, the number of DB states near the conduction band edge increases, and they are dispersed due to the coupling between the DB dimer states. The range of the states for a short line of DBs parallel to the dimer rows eventually evolves to a band as the DB line becomes infinitely long [Fig. 10]. For a line of DBs perpendicular to the dimer rows, the dispersion of the DB states is much smaller than for the parallel direction [Fig. 11].

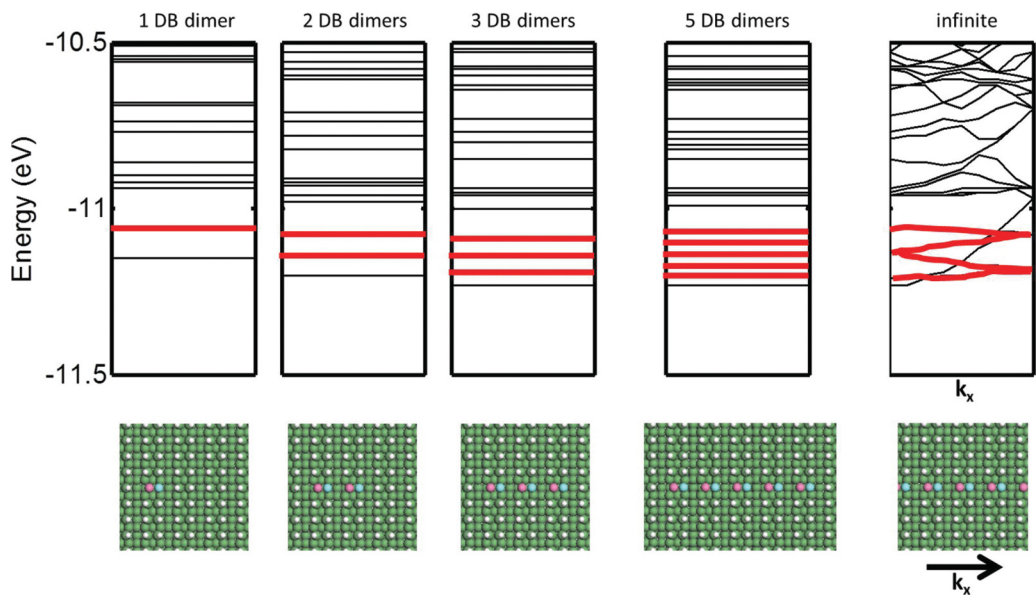


FIG. 11. (Color online) Energy spectra (Γ point) showing the DB states (red lines) for 1, 2, 3, and 5 DB dimers perpendicular to the dimer rows. The band structure for an infinite line of DB dimers perpendicular to the dimer rows (k_x) is also shown for comparison.

*szymon.godlewski@uj.edu.pl

†kawaih@imre.a-star.edu.sg

- ¹M. Fuechsle, S. Mahapatra, F. A. Zwanenburg, M. Friesen, M. A. Eriksson, and M. Y. Simmons, *Nat. Nanotechnol.* **5**, 502 (2010).
- ²H. Kawai, F. Ample, Q. Wang, Y. K. Yeo, M. Saeys, and C. Joachim, *J. Phys.: Condens. Matter* **24**, 095011 (2012).
- ³L. Soukiassian, A. J. Mayne, M. Carbone, and G. Dujardin, *Surf. Sci.* **528**, 121 (2003).
- ⁴T. Hitosugi, S. Heike, T. Onogi, T. Hashizume, S. Watanabe, Z. Q. Li, K. Ohno, Y. Kawazoe, T. Hasegawa, and K. Kitazawa, *Phys. Rev. Lett.* **82**, 4034 (1999).
- ⁵B. Weber, S. Mahapatra, H. Ryu, S. Lee, A. Fuhrer, T. C. G. Reusch, D. L. Thompson, W. C. T. Lee, G. Klimeck, L. C. L. Hollenberg, and M. Y. Simmons, *Science* **25**, 64 (2012).
- ⁶M. B. Haider, J. L. Pitters, G. A. DiLabio, L. Livadaru, J. Y. Mutus, and R. A. Wolkow, *Phys. Rev. Lett.* **102**, 046805 (2009).
- ⁷J. L. Pitters, I. A. Dogel, and R. A. Wolkow, *ACS Nano* **5**, 1984 (2011).
- ⁸J. L. Pitters, L. Livadaru, M. B. Haider, and R. A. Wolkow, *J. Chem. Phys.* **134**, 064712 (2011).
- ⁹F. Ample, I. Duchemin, M. Hliwa, and C. Joachim, *J. Phys.: Condens. Matter* **23**, 125303 (2011).
- ¹⁰A. Bellec, F. Ample, D. Riedel, G. Dujardin, and C. Joachim, *Nano Lett.* **9**, 144 (2009).
- ¹¹A. Bellec, D. Riedel, G. Dujardin, O. Boudrioua, L. Chaput, L. Stauffer, and P. Sonnet, *Phys. Rev. Lett.* **105**, 048302 (2010).
- ¹²A. Bellec, D. Riedel, G. Dujardin, O. Boudrioua, L. Chaput, L. Stauffer, and P. Sonnet, *Phys. Rev. B* **80**, 245434 (2009).
- ¹³T. Hitosugi, T. Hashizume, S. Heike, H. Kajiyama, Y. Wada, S. Watanabe, T. Hasegawa, and K. Kitazawa, *Appl. Surf. Sci.* **130**, 340 (1998).
- ¹⁴J. J. Boland, *Phys. Rev. Lett.* **67**, 1539 (1991).
- ¹⁵D. Chen and J. J. Boland, *Phys. Rev. B* **65**, 165336 (2002).
- ¹⁶K. Bobrov, G. Comtet, G. Dujardin, and L. Hellner, *Phys. Rev. Lett.* **86**, 2633 (2001).
- ¹⁷L. Soukiassian, A. J. Mayne, M. Carbone, and G. Dujardin, *Phys. Rev. B* **68**, 035303 (2003).
- ¹⁸T. C. Shen, C. Wang, G. C. Abeln, J. R. Tucker, J. W. Lyding, and P. Avouris, *Science* **268**, 1590 (1995).
- ¹⁹E. T. Foley, A. F. Kam, J. W. Lyding, and P. Avouris, *Phys. Rev. Lett.* **80**, 1336 (1998).
- ²⁰G. Scappucci, G. Capellini, W. C. T. Lee, and M. Y. Simmons, *Nanotechnology* **20**, 495302 (2009).
- ²¹G. Scappucci, G. Capellini, B. Johnston, W. M. Klesse, J. A. Miwa, and M. Y. Simmons, *Nano Lett.* **11**, 2272 (2011).
- ²²A. Fuhrer, M. Fuechsle, T. C. G. Reusch, B. Weber, and M. Y. Simmons, *Nano Lett.* **9**, 707 (2009).
- ²³S. Watanabe, Y. A. Ono, T. Hashizume, and Y. Wada, *Phys. Rev. B* **54**, R17308 (1996).
- ²⁴H. Kawai, Y. K. Yeo, M. Saeys, and C. Joachim, *Phys. Rev. B* **81**, 195316 (2010).
- ²⁵J. Cerda, M. A. Van Hove, P. Sautet, and M. Salmeron, *Phys. Rev. B* **56**, 15885 (1997).
- ²⁶G. Kresse and J. Hafner, *Phys. Rev. B* **47**, 558 (1993).
- ²⁷J. P. Perdew, K. Burke, and M. Ernzerhof, *Phys. Rev. Lett.* **77**, 3865 (1996).



Construction of atomic-scale logic gates on a surface of hydrogen passivated germanium

Marek Kolmer^a, Szymon Godlewski^a, Jakub Lis^a, Bartosz Such^a, Lev Kantorovich^b, Marek Szymonski^{a,*}

^a Centre for Nanometer-Scale Science and Advanced Materials, NANOSAM, Faculty of Physics, Astronomy, and Applied Computer Science, Jagiellonian University, Reymonta Str. 4, PL 30-059 Krakow, Poland

^b Department of Physics, King's College London, Strand, London WC2R 2LS, United Kingdom

ARTICLE INFO

Article history:

Available online 22 March 2013

Keywords:

Hydrogen passivated germanium
STM
Dangling bond nanostructures
Atomic-scale logic gates

ABSTRACT

We describe a complete protocol for atomically precise dangling bond (DB) logic gate construction on a hydrogenated Ge(001):H surface. Starting from the preparation of the reconstructed Ge(001) surface followed by its passivation with hydrogen atoms we end up with the platform for scanning tunneling microscopy (STM) atomic-scale lithography. Finally with the use of dimer-by-dimer STM tip-induced hydrogen desorption from the Ge(001) – (2 × 1):H surface the DB nanostructures of pre-designed form are fabricated. Furthermore, the STM tip manipulation provides the control over the buckling phase of a single DB dimer incorporated into the DB logic gate structure, which is of crucial importance for the final electronic properties of the system. Our results prove feasibility of DB atomic scale logic gate implementation on the passivated semiconductor surfaces.

© 2013 Elsevier B.V. All rights reserved.

1. Introduction

Miniaturization of the present electronic technology based on silicon devices nowadays approaches natural size limitations arising from quantum effects dominating the performance at the nanoscale. Therefore, all over the world new alternative solutions are sought for. Among them the idea of single molecules and atomic circuits performing logic operations seems to be an exciting one and has been the subject of several on-going experiments [1].

For the development of the monomolecular/atomic concept the suitable surfaces are required. One of the most promising ideas is based on the application of hydrogen passivated semiconductor surfaces. Its attractiveness arises from the possibility of creating sophisticated surface circuits by the controlled desorption of hydrogen atoms leading to formation of conductive nanostructures composed from dangling bonds [2–12]. Moreover the hydrogenated surfaces allow for combining atomic logic circuits with additional organic molecules that could be effectively decoupled from the underlying substrate.

In contrast to Si(001):H surface, there are only a few reports on STM tip-induced hydrogen desorption from a Ge(001):H surface [10–12]. In a recent paper, we demonstrated successful construction of atomically clean and ordered DB lines and also the first spectroscopic characterization of DB lines running across and along surface reconstruction rows [10]. We showed that upon desorption

of hydrogen atoms, the electronic states related to thus created DB structures appeared in the band gap of the Ge(001):H surface. The electronic coupling between short DB dimer lines provides a powerful tool to build surface atomic-scale logic gates. In this paper we demonstrate that our hydrogen extraction protocol can be applied for preparation of large well-defined DB structures containing several DB dimers. We show that STM tip induced desorption and further manipulation enables effective control over the DB structure geometry up to a single DB, including also variation of the DB dimer buckling configuration. Such a precision in construction of DB structures is of crucial importance for their electronic properties [3,10], governing the functionality of DB logic devices. Therefore reported data prove the feasibility of the proposed [3] DB atomic scale logic gates implementation on the passivated semiconductors.

2. Experiment

The experiments were carried out in an ultra-high vacuum (UHV) system with the base pressure of 5×10^{-11} mbar. The STM measurements were performed with the Omicron low temperature scanning probe microscope (LT STM). The samples were cut from Ge(001) undoped wafers (TBL Kelpin Crystals) and after introduction into the UHV system were first annealed for 6 h at 800 K. Subsequently the cycles of 1 keV Ar⁺ sputtering and annealing at 1040 K for 15 min were repeated until clean well-reconstructed surfaces were obtained, as checked by low energy electron diffraction (LEED) and STM. Hydrogen passivation was performed with

* Corresponding author. Tel./fax: +48 12 6635560.

E-mail address: marek.szymonski@uj.edu.pl (M. Szymonski).

use of a home built hydrogen cracker providing atomic hydrogen. The Ge sample temperature during the passivation was 480 K. The STM imaging was carried out at cryogenic temperature of around 4 K (liquid helium) with electrochemically etched polycrystalline tungsten tips used as probes. For image processing and STM data analysis SPIP and WSxM [13] software were used.

To help interpreting experimental results, we simulated STM images of the bare $\text{Ge}(001) - c(4 \times 2)$ and $\text{Ge}(001):\text{H} - (2 \times 1)$ surfaces using *ab initio* calculations based on the density functional theory. The geometries of both systems were optimized with the SIESTA code [14] applying the generalized gradient approximation for the exchange and correlation [15]. Rather thick slabs containing 10 layers of germanium were required to obtain the converged geometry and electronic structure of the surface [10]. Subsequently, STM images were calculated using the Tersoff–Hamman approximation [16] and the Vienna *ab initio* simulation package (VASP) code [17].

3. Results and discussion

A starting platform for DB-based logic gate construction is the crystalline, almost defect free surface of $\text{Ge}(001)$. The $\text{Ge}(001)$ surface itself is very reactive and UHV conditions are needed to avoid quick contamination of the sample. At cryogenic temperatures the (001) surface has two stable reconstructions, $c(4 \times 2)$ and $p(2 \times 2)$, consisting of Ge dimer rows separated by a distance of 0.8 nm. Each single Ge dimer is tilted with respect to the surface plane. Every two successive Ge dimers along the row are separated by 0.4 nm and they are buckled in opposite directions. This buckling associated with a small effective charge transfer from the lower Ge atom to the upper one stabilizes both surface geometries. The $p(2 \times 2)$ and $c(4 \times 2)$ reconstructions correspond to in-phase and out-of-phase buckling of two neighboring Ge dimer rows, respectively. From the DFT calculations the $c(4 \times 2)$ structure is more sta-

ble than $p(2 \times 2)$, but the small energy difference of about 1 meV/dimer between the two reconstructions suggests that both configurations are almost equally possible; as a result, for moderate STM junction biases both phases are observed at low temperature [10]. Furthermore, it is possible to control the surface reconstruction state by changing the Ge dimer buckling with the use of the STM manipulation technique [18,19]. By applying positive or negative voltage pulses one can switch the $\text{Ge}(001)$ reconstruction from $p(2 \times 2)$ to $c(4 \times 2)$ or vice versa. In Fig. 1A and B experimental and calculated STM filled state images of a $\text{Ge}(001) - c(4 \times 2)$ surface are presented. Each red protrusion corresponds to an upper Ge atom in buckled dimers, which stick out from the surface plane. Dark depletions are related to lower Ge atoms in the dimers. The out of phase buckling of two adjacent surface rows resulting in a formation of a (4×2) reconstruction is clearly seen.

The second step in the protocol of DB logic gate formation is a hydrogenation of the $\text{Ge}(001)$ surface. This process is done by exposure of the surface to a hydrogen atom source. As the result the surface is passivated by the monolayer of hydrogen atoms, which form a stable monohydride (2×1) phase. In this particular structure each Ge DB is filled with one H atom, meaning that there are two H atoms bonded to a single Ge dimer. The process of hydrogenation is performed for a sample kept at elevated temperature of around 470 K in order to avoid multihydride formation on the surface and its further etching. Filled state experimental and calculated STM images of the $\text{Ge}(001):\text{H}$ surface are depicted in Fig. 1D and E, respectively. As is clearly seen, the resulting surface geometry is now symmetric with respect to the reconstruction rows. This is due to the fact, that there is no buckling of hydrogenated Ge dimers. For images obtained with the -0.5 V surface bias voltage, the rows of reconstruction are seen as lines of single protrusions running along the dimer rows. These protrusions are separated by 0.4 nm along the reconstruction rows. DFT calculations reveal that the maxima in the images correspond to the position

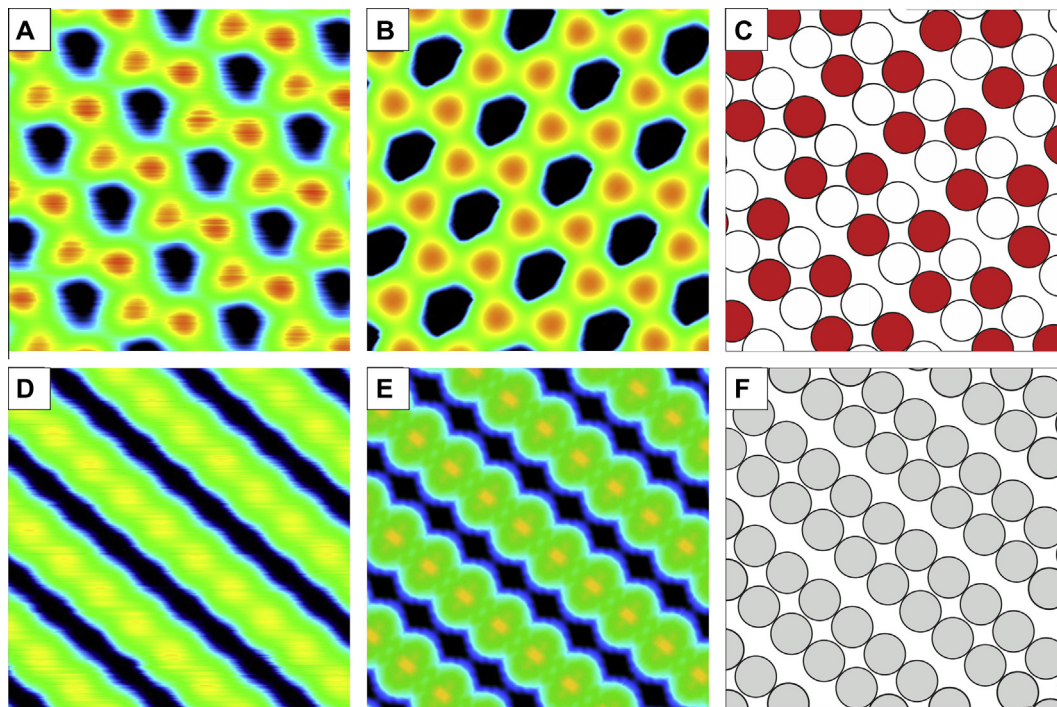


Fig. 1. Experimental constant current (A) and calculated (B) filled state STM images of a $\text{Ge}(001) - c(4 \times 2)$ surface. Experimental (D) and calculated (E) filled state STM images of $\text{Ge}(001):\text{H} - (2 \times 1)$ surface. All images are $3 \times 3 \text{ nm}^2$ and are obtained for -0.5 V sample bias. For experimental images the tunneling current is 1 nA. Note a very good agreement between experimental and calculated images. The corresponding models of surfaces are presented in (C) and (F). Red and white circles represent Ge atoms with up and down buckling configuration. Gray circles represent hydrogenated Ge atoms. (For interpretation of the references to color in this figure legend, the reader is referred to the web version of this article.)

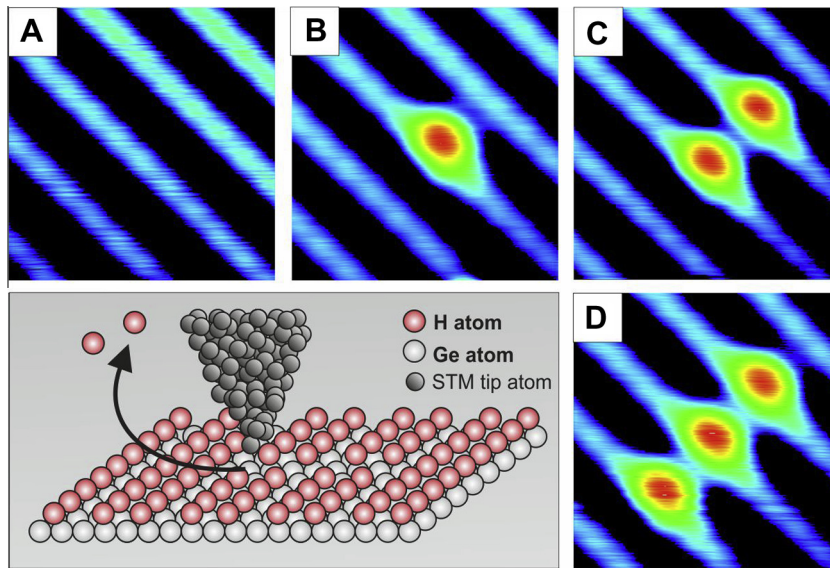


Fig. 2. Dangling bond nanostructures created by STM tip-induced hydrogen atom desorption from hydrogenated Ge(001) surface. Image (A) corresponds to perfectly hydrogenated surface, (B) to a single DB dimer, (C) to 2 DB dimer structure and (D) to 3 DB dimer line oriented across the Ge(001):H reconstruction rows. All STM images of $3 \times 3 \text{ nm}^2$ area are recorded with -0.5 V bias and 1 nA tunneling current. The schematic cartoon presents the idea behind the experiment.

between two H atoms located over each Ge dimer. The formation of atomic DB logic gates can be done only on a perfectly hydrogenated Ge(001):H surface area, such as presented in Figs. 1D and 2A, in order to avoid any influence of surface defects on final electronic properties of a given DB nanostructure. The next step of the DB logic circuit construction process is performed with the use of a newly developed STM vertical atom manipulation procedure [10]. First, the STM tip apex is located over a protrusion observed in the constant current filled state STM image. As mentioned, this corresponds to the location exactly over the center of a hydrogenated Ge dimer. Then, the STM feedback loop is switched off and the bias voltage is simultaneously increased by a positive value for a certain period of time. On the time scale of hundreds of milliseconds a sudden rise of the tunneling current is observed, which is related to a hydrogen desorption event. Images A and B in Fig. 2 present the same surface area before and after STM tip induced hydrogen desorption. The resulting asymmetric feature corresponds to a buckled Ge dimer, which lost *both* of its hydrogen atoms. Note that due to the increased local density of states (LDOS) related to Ge dimer dangling bonds this structure is observed in STM constant current mode as a protrusion instead of depletion, unlike the real surface morphology. The buckled configuration of the single bare Ge dimer with the buckling angle of about 19° was confirmed by comparing line-by-line the experimental and the calculated scans using the optimized dangling bond dimer structure on the Ge(001):H surface [10]. Our results indicate that by applying described protocol hydrogen dimers are desorbed and thus DB dimers are formed on the surface of Ge(001):H.

The presented procedure enables the creation of DB atomic scale lines and small circuits of any desired complexity. Images C and D in Fig. 2 show simple atomic structure with 2 and 3 DB dimers in length oriented perpendicularly to the reconstruction rows. Note that in this case all the DB dimers are buckled to the same side, what makes the DB line appearing as homogenous. Such a geometry corresponding to the $p(2 \times 2)$ reconstruction of the bare Ge(001) surface is more stable than alternating (across rows) buckling configuration. However, the calculated energy difference of 20 meV/dimer [10] is not high and the distorted structures oriented across the dimer rows can also be observed (see Fig. 3A). For long DB dimer structures oriented along the reconstruction

rows this is usually not the case, since the alternating buckling geometry observed for bare Ge(001) is strongly favored (120 meV/dimer).

In order to prove that our protocol is appropriate for surface atomic logic gate construction proposed theoretically in [3], we have focused the experiments on the construction of DB atomic scale structures extended over sizable areas. We have succeeded to construct very long DB wires consisting of more than 20 DBs with the length of up to 10 nm and 1 DB in width. However, described distortions caused by different buckling orientations of DB dimers start to be inevitable with increased lateral dimensions of a targeted DB nanostructure. To overcome this problem we propose the following procedure which should enable one to achieve the desired control over the DB dimer phase. It is based on the known mechanism of Ge(001) surface reconstruction change [18,19]. The STM tip manipulation protocol starts again with filled state imaging. As it was already mentioned, DB dimers for -0.5 V sample bias are typically represented as asymmetric protrusions. STM tip apex is placed in the center of a reconstruction row over the selected DB dimer. Note that it is the position on a side of the STM image maximum, which is related to the protruding DB. Then the STM feedback loop signal is turned off with the bias voltage changing to small positive values. Depending on the tip apex we usually use voltages of up to $+1 \text{ V}$. The application of described procedure is presented in Fig. 3A–D. A distorted DB wire consisting of 5 DB dimers is transformed into a homogenous structure in two controlled buckling phase change operations. The buckling phase of two neighboring DB dimers is of crucial importance for their electronic coupling and it also influences the electronic properties of the whole DB structure. The latter fact can be used in designing atomic switches controlled by the STM tip and is the subject of ongoing experiments. Described effect is nicely reflected in STM images in Fig. 3A and C, where increased LDOS on the central DB dimer is decreased after successful buckling phase transformation.

Since any even small surface DB circuit must also contain input electrodes, we propose to construct a small 2-input like small DB circuit by extracting the gate input atoms one lattice constant away from the DB line. This is presented in Fig. 3E with the corresponding atomic scale surface structure depicted in Fig. 3F. The

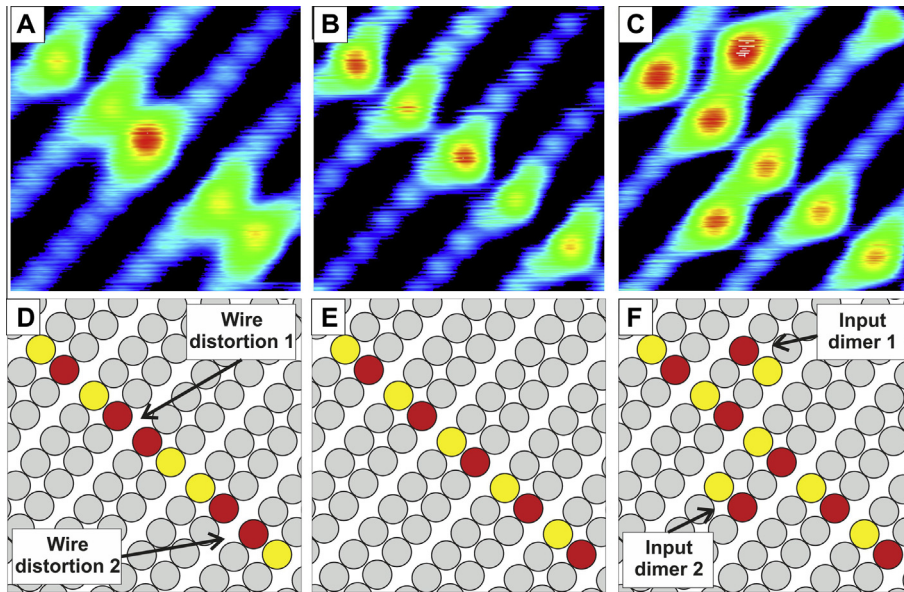


Fig. 3. DB wire fabricated on the Ge(001):H surface: (A) filled state STM image of DB line containing 5 DB dimers (10 DBs) with mixed DB dimer buckling configurations causing distortions in the line structure; (B) a structural model of the DB line presented in A, red and yellow circles correspond to upper and lower positions of Ge atoms in the bare Ge dimers, gray circles correspond to hydrogenated Ge surface atoms; (C) STM image showing the same DB line structure after induced manipulation with the STM tip yielding the same configuration of all DB dimer; (D) a structural model of the DB line presented in C; (E) STM image showing the same DB line structure but containing now two additional DB dimers (4 DBs) revealing stability of the entire structure, and (F) the corresponding structural model of the final structure. Image area: $3.5 \times 3.5 \text{ nm}^2$, tunneling current 1 nA, bias voltage -0.5 V . (For interpretation of the references to color in this figure legend, the reader is referred to the web version of this article.)

simple circuit shown in Fig. 3 is a very nice experimental demonstration that the atomic scale construction technology is beneficial for the design of surface logic gates based on DB nanostructures.

4. Conclusions

In conclusion, we have demonstrated that the hydrogenated Ge(001) surface may be used for construction of prototypical atomic-scale electronic circuits. The newly developed protocol allows for precise desorption of hydrogen atoms and provides unique technique for nanofabrication of circuits comprised of surface DB states.

Acknowledgments

This research was supported by the 7th Framework Programme of the European Union Collaborative Project ICT (Information and Communication Technologies) “Atomic Scale and Single Molecule Logic Gate Technologies” (ATMOL), contract number: FP7-270028. The experimental part of the research was carried out with equipment purchased with financial support from the European Regional Development Fund in the framework of the Polish Innovation Economy Operational Program (contract no. POIG.02.01.00-12-023/08).

References

- [1] J.S. Prauzner-Bechcicki, S. Godlewski, M. Szymonski, *Phys. Stat. Sol. A* 209 (2012) 603.
- [2] M. Fuechsle, S. Mahapatra, F.A. Zwanenburg, M. Friesen, M.A. Eriksson, M.Y. Simmons, *Nature Nanotechnol.* 5 (2010) 502.
- [3] H. Kawai, F. Ample, Q. Wang, Y. Kiat Yeo, M. Saeys, C. Joachim, *J. Phys. Condens. Matter* 24 (2012) 095011.
- [4] L. Soukiassian, A.J. Mayne, M. Carbone, G. Dujardin, *Surf. Sci.* 528 (2003) 121.
- [5] T. Hitosugi, S. Heike, T. Onogi, T. Hashizume, S. Watanabe, Z.Q. Li, K. Ohno, Y. Kawazoe, T. Hasegawa, K. Kitazawa, *Phys. Rev. Lett.* 82 (1999) 4034.
- [6] B. Weber, S. Mahapatra, H. Ryu, S. Lee, A. Fuhrer, T.C.G. Reusch, D.L. Thompson, W.C.T. Lee, G. Klimeck, L.C.L. Hollenberg, M.Y. Simmons, *Science* 25 (2012) 64.
- [7] M. Baseer Haider, J.L. Pitters, G.A. DiLabio, L. Livadaru, J.Y. Mutus, R.A. Wolkow, *Phys. Rev. Lett.* 102 (2009) 046805.
- [8] J.L. Pitters, I.A. Dogel, R.A. Wolkow, *ACS Nano* 5 (2011) 1984.
- [9] L. Pitters, L. Livadaru, M. Baseer Haider, R.A. Wolkow, *J. Chem. Phys.* 134 (2011) 064712.
- [10] M. Kolmer, S. Godlewski, H. Kawai, B. Such, F. Krok, M. Saeys, C. Joachim, M. Szymonski, *Phys. Rev. B* 86 (2012) 125307.
- [11] G. Scappucci, G. Capellini, W.C.T. Lee, M.Y. Simmons, *Nanotechnology* 20 (2009) 495302.
- [12] G. Scappucci, G. Capellini, B. Johnston, W.M. Klesse, J.A. Miwa, M.Y. Simmons, *Nano Lett.* 11 (2011) 2272–2279.
- [13] I. Horcas, R. Fernandez, J.M. Gomez-Rodriguez, J. Colchero, J. Gomez-Herrero, A.M. Baro, *Rev. Sci. Instr.* 78 (2007) 013705.
- [14] J.M. Soler et al., *J. Phys. Condens. Matter* 14 (2002) 2745.
- [15] J.P. Perdew, K. Burke, M. Ernzerhof, *Phys. Rev. Lett.* 77 (1996) 3865.
- [16] J. Tersoff, D.R. Hamann, *Phys. Rev. B* 31 (1985) 805.
- [17] G. Kresse, J. Furthmuller, *Comput. Mater. Sci.* 6 (1996) 15 (see also *Phys. Rev. B* 54 (1996) 11169).
- [18] Y. Takagi, Y. Yoshimoto, K. Nakatsuji, F. Komori, *Surf. Sci.* 559 (2004) 1.
- [19] Y. Takagi, K. Nakatsuji, Y. Yoshimoto, F. Komori, *Phys. Rev. B* 75 (2007) 115304.



Atomic scale fabrication of dangling bond structures on hydrogen passivated Si(001) wafers processed and nanopackaged in a clean room environment

Marek Kolmer^a, Szymon Godlewski^a, Rafal Zuzak^a, Mateusz Wojtaszek^a, Caroline Rauer^b, Aurélie Thuaille^b, Jean-Michel Hartmann^b, Hubert Moriceau^b, Christian Joachim^c, Marek Szymonski^{a,*}

^a Centre for Nanometer-Scale Science and Advanced Materials, NANOSAM, Faculty of Physics, Astronomy and Applied Computer Science, Jagiellonian University, Reymonta Str. 4, PL 30-059 Krakow, Poland

^b CEA, LETI, Minatec Campus, 17, Avenue des Martyrs, 38 054 Grenoble Cedex 9, France

^c Nanosciences Group & MANA Satellite, CEMES-CNRS, 29 rue Jeanne Marvig, F-31055 Toulouse, France

ARTICLE INFO

Article history:

Received 29 July 2013

Received in revised form

19 September 2013

Accepted 20 September 2013

Available online 27 September 2013

Keywords:

Hydrogen passivated Si(001) surface

Dangling bond nanostructures

STM-tip-induced desorption

Nanopackaging

Low-temperature scanning tunneling

microscopy and spectroscopy (LT STM/STS)

ABSTRACT

Specific surfaces allowing the ultra-high vacuum (UHV) creation of electronic interconnects and atomic nanostructures are required for the successful development of novel nanoscale electronic devices. Atomically flat and reconstructed Si(001):H surfaces are serious candidates for that role. In this work such Si:H surfaces were prepared in a cleanroom environment on 200 mm silicon wafers with a hydrogen bake and were subsequently bonded together to ensure the surface protection, and allow their transportation and storage for several months in air. Given the nature of the bonding, which was hydrophobic with weak van der Waals forces, we were then able to de-bond them in UHV. We show that the quality of the de-bonded Si:H surface enables the “at will” construction of sophisticated and complex dangling bond (DB) nanostructures by atomically precise scanning tunneling microscope (STM) tip induced desorption of hydrogen atoms. The DB structures created on slightly doped Si:H samples were characterized by scanning tunneling microscopy and spectroscopy (STM/STS) performed at 4 K. Our results demonstrate that DB nanostructures fabricated on UHV de-bonded Si(001):H wafers could be directly incorporated in future electronics as interconnects and parts of nanoscale logic circuits.

© 2013 Elsevier B.V. All rights reserved.

1. Introduction

Silicon is the most often used material in the semiconductor industry for the fabrication of highly integrated electronic devices. As the minimum feature size of such devices decreases, new challenges concerning the fabrication technologies and design rules have to be overcome. For the manufacturing of nanometer-scale or even smaller devices, one ultimate solution implies the creation of silicon dangling bond (DB) circuits and connections through the scanning tunneling microscope (STM) desorption of hydrogen atoms on a hydrogenated silicon surfaces [1–5]. A reconstructed and atomically flat surface like Si(001):H is then required, as it can provide regular and aligned atomic rows and would thus be an ideal platform for STM-based lithography [6–9]. This technique enables the formation of well-defined, nanoscale DB patterns: from

single and double DBs [7,8,10–12] to DB lines and Si-nanopads [6,9,13–15].

An ultra-high vacuum (UHV) environment is however mandatory for the successful construction of DB structures on hydrogen passivated silicon surfaces. This implies very strict strategies for the preparation of high quality Si:H surfaces. Typical procedures involving the direct current flashing of silicon samples followed by their exposure to hydrogen atoms are both inappropriate for the preparation of Si:H surfaces at larger scale, and incompatible with substrates featuring devices and interconnects. In this work, we demonstrate that high quality reconstructed and hydrogen passivated silicon surfaces can be obtained in a cleanroom environment with less stringent standard microelectronics processes [16,17]. We focus on Si(001):H-(2 × 1) surface obtained on 200 mm wafers in a Reduced Pressure-Chemical Vapor Deposition (RP-CVD) epitaxy reactor. The reconstructed Si(001):H surface is then protected by a temporarily bonded Si:H cap wafer [18,19], which allows subsequent exposition of the bonded wafers to ambient conditions, their dicing and transportation. Using a high resolution scanning electron microscope (SEM), low energy

* Corresponding author. Tel.: +48 12 633 5524; fax: +48 12 633 7086.
E-mail address: marek.szymonski@uj.edu.pl (M. Szymonski).

electron diffraction (LEED), and cryogenic temperature scanning tunneling microscopy/spectroscopy (STM/STS), we demonstrate that Si(001)-(2 × 1):H surfaces are well protected by the temporary bonded cap. They indeed show atomically flat and reconstructed terraces after UHV de-bonding, enabling the creation of atomic-scale DB structures. Our results demonstrate that high quality Si(001):H-(2 × 1) surface wafers can be transferred ex situ and used several months after surface reconstruction and temporary bonding. Furthermore we used such de-bonded, slightly p-doped Si(001):H samples for the construction of DB structures at 4 K and their detailed characterization. This study shows that the Si(001):H surface preparation performed in cleanroom on 200 mm substrates and followed by nanopackaging and UHV de-bonding is appropriate for the fundamental research community and may also be considered for future nanoelectronic applications.

2. Experimental details

The experiments were carried out in a UHV system from Omicron Nanotechnology GmbH with a base pressure of 5×10^{-11} mbar. The UHV system consists of three interconnected chambers incorporating high resolution SEM, LEED optics and low temperature STM (LT-STM). All STM measurements were performed thanks to a Omicron LT-STM operating at the cryogenic temperature of 4 K with electrochemically etched polycrystalline tungsten tips used as probes. All values of bias voltage in STM experiments presented in the paper are given with respect to the sample. SPIP and WSxM [20] software's were used for image processing and STM data analysis.

2.1. Surface preparation, processing and nanopackaging

The Si:H bonded samples were prepared in the CEA-LETI, Grenoble cleanroom. They consisted in two reconstructed Si:H surfaces, prepared in a RP-CVD epitaxy reactor, bonded face to face thanks to weak van der Waals forces [19]. The Si(001) starting wafers were $\sim 725 \mu\text{m}$ thick and 200 mm in diameter. The wafers were slightly p-doped ($10^{15} \text{ at}/\text{cm}^3$ corresponding to a resistivity of $\sim 10.5 \Omega \text{ cm}$). In order to obtain Si(001):H-(2 × 1) reconstructed surfaces on 200 mm silicon wafers, a multistep process was developed and consisted in the combination of a wet chemical cleaning and a high temperature treatment. The wet chemical cleaning was based on a Caro bath, followed by either a "SC1" standard cleaning ($\text{H}_2\text{O}:\text{NH}_4\text{OH}:\text{H}_2\text{O}_2$) or a "Dynamic Diluted Clean" (DDC), based on desoxidation (HF) and re-oxidation (ozone wet solution) of the substrate [19]. Both cleaning processes led to the formation of a chemical oxide on the surface. The following high temperature treatment took place in a RP-CVD reactor and consisted in a first H_2 annealing at 1100°C , 20 Torr in order to remove the thin chemical oxide on the surface, an epitaxy of a thin Si buffer layer with dichlorosilane, and a final H_2 annealing at 950°C [18]. The wafers were directly bonded together right after this process. The hydrophobic state of the reconstructed surface was checked by measuring a contact angle of a water droplet on the surface of 89° . The 200 mm bonded substrates were then diced into 1 cm^2 samples in order to fulfill the STM tools requirements. These samples were subsequently de-bonded under UHV, which implies for bonding energies to be at the same time (i) strong enough to allow dicing and (ii) weak enough to allow de-bonding of structures without

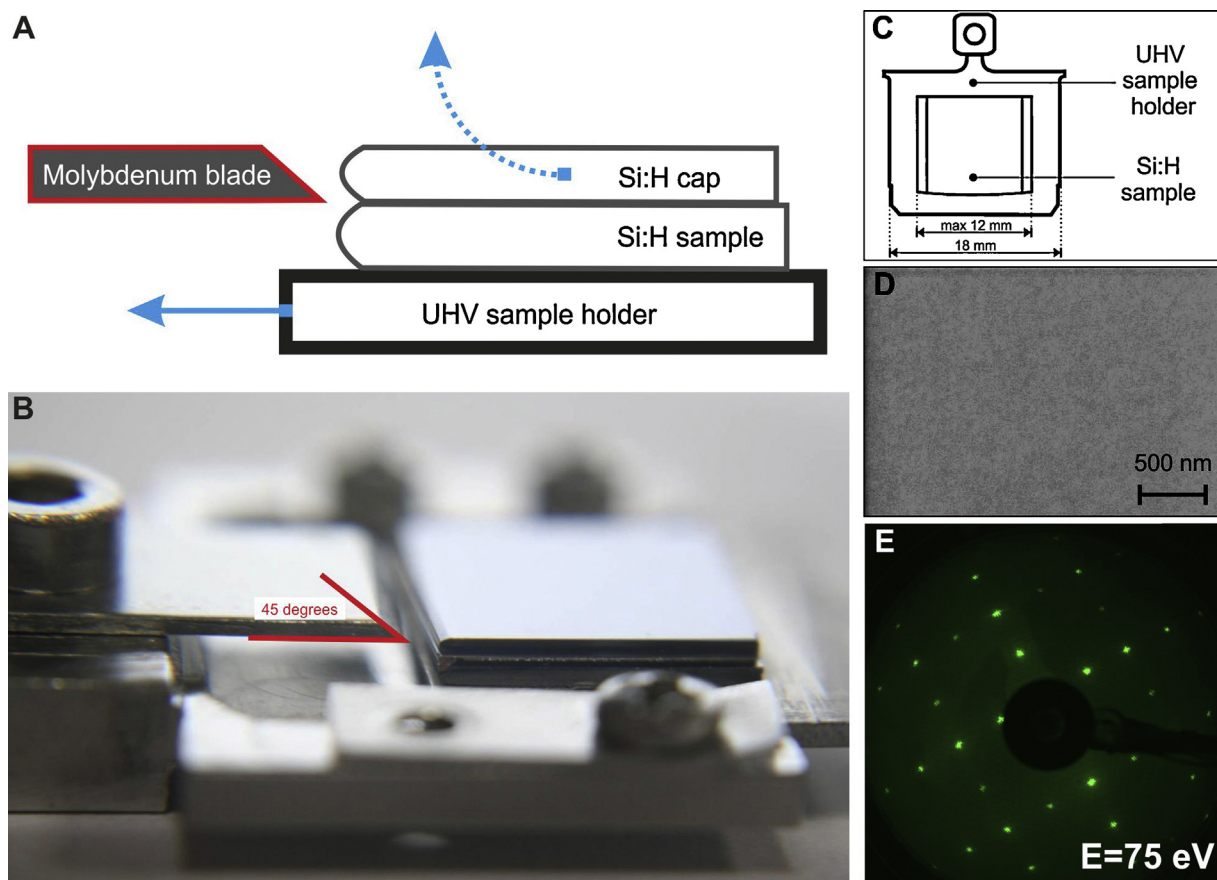


Fig. 1. (A)–(C) Schematic drawings (A, C) and photograph (B) of the bonded sample, UHV sample holder and the de-bonding tool used for opening it under UHV conditions. Blue arrows in (A) indicate the sample holder movement and corresponding Si:H cap removal during the opening procedure. (D) High resolution SEM micrograph of the de-bonded Si(001):H surface: magnification 50,000, EHT 5 kV and probe current 1 nA. (E) LEED pattern of the de-bonded Si(001):H surface. (For interpretation of the references to color in this figure legend, the reader is referred to the web version of the article.)

inducing damages on the reconstructed surfaces. The strength of the Si(001):H-(2 × 1) bonding was measured with the crack opening method [21]. A bonding energy value of 150 mJ/m² was measured at room temperature and stayed constant even after 200 °C annealing for 2 h. Such a bonding energy value revealed suitable both for sample dicing and subsequent damage free UHV de-bonding.

2.2. Sample de-bonding in UHV

Diced samples equipped with the natural wafer bevel were selected for the wafer opening. A dedicated UHV de-bonding tool,

designed and fabricated on purpose, was placed in the preparation chamber attached to the Omicron UHV system. It consisted in a blade mounted on a specially designed sample stage (Fig. 1A, B). The tool routine operation for the opening of the Si:H bonded samples prepared by CEA-LETI is presented in the movie available as a supplementary material (attached). For UHV opening and UHV-SEM/LEED/STM characterization, the samples were glued to the UHV holder using an indium (99.99%) layer less than 0.05 mm thick. It should be noted that once the two face to face bonded samples were separated, the standard experimental procedure used for Si:H surface characterization could be performed, as the wafer was already mounted on a standard Omicron sample holder (Fig. 1C),

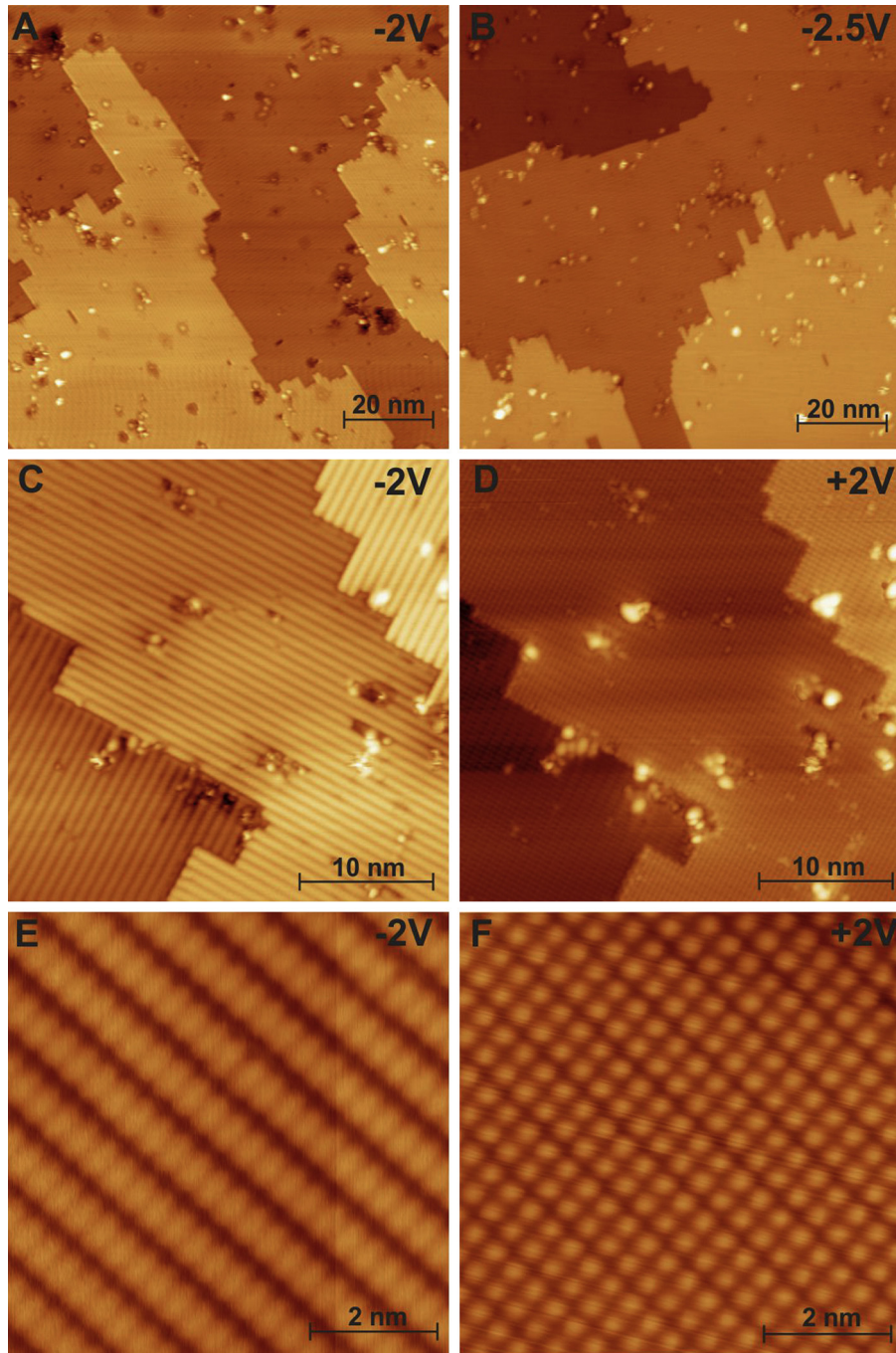


Fig. 2. (A)–(F) STM characterization of a de-bonded Si(100):H surface at 4 K. Filled state imaging: (A) –2 V, 10 pA, (B) –2.5 V, 20 pA and (C, E) –2 V, 100 pA. Empty states: (D, F) +2 V, 100 pA. The scan area is 100 nm × 100 nm (A, B), 35 nm × 35 nm (C, D) and 7 nm × 7 nm (E, F). Sharp atomic step edges and hydrogen terminated reconstruction rows are clearly visible.

and could be moved into other parts of the UHV system. The surface quality was checked after wafer de-bonding by means of high resolution SEM imaging with sub 10 nm resolution (Fig. 1D): no contrast was found on the de-bonded Si(001):H surfaces, leading to the conclusion that, at least within the resolution of SEM (10 nm, typically), the proposed de-bonding procedure has little or no impact on the quality of the Si:H surfaces. The origin of the few nm size defects evidenced by STM will be discussed later on. Moreover, this process preserves the surface reconstruction as demonstrated by the LEED pattern of UHV de-bonded samples (Fig. 1E): sharp, characteristic (2×1) and (1×2) spots are observed on the surface, even after storing of the bonded structures for a few months at room temperature and in ambient conditions.

3. Results and discussion

3.1. LT-UHV-STM characterization

For LT-UHV-STM characterization samples were transferred immediately after the de-bonding process to the LT-STM cryostat, where they were cooled down to 4K. LT-STM imaging was firstly performed on de-bonded samples to evaluate both the impact of the full packaging process at the atomic scale and the amount of surface defects. Results are shown on the representative $100 \text{ nm} \times 100 \text{ nm}$ and $35 \text{ nm} \times 35 \text{ nm}$ images presented in Fig. 2A–D. It is seen that the surface crystallographic structure of the hydrogenated Si(001):H is well preserved for large, flat and single-terrace areas. The high quality of the surface allows for surface DB structures construction by hydrogen atoms desorption with the use of a STM tip. The agglomeration of defects observed on the atomically clean terraces in Fig. 2A–D could be due to (i) the dichlorosilane chemistry (SiH_2Cl_2) used during the surface preparation process for Si buffer growth (Cl atoms would then be present on the surface) or (ii) the wafer de-bonding procedure itself. The average defect densities estimated from several STM scans on the de-bonded surfaces is about 1 defect per 50 nm^2 .

The high resolution STM $7 \text{ nm} \times 7 \text{ nm}$ scans (see Fig. 2E, F) of the de-bonded sample clearly show that the surface is passivated by a monolayer of hydrogen atoms, which form a stable monohydride (2×1) phase in which each Si surface atom is bound to one H atom. In particular, the empty state experimental STM images of the Si(001):H surface (Fig. 2F) reflect the resulting surface geometry with symmetric dimer features along the reconstruction rows. These features correspond to unbuckled hydrogenated Si dimers. For the filled state image (Fig. 2E) obtained with the -2 V surface bias voltage, the reconstruction rows are seen as lines of single protrusions running along the dimer rows. These protrusions are separated by 0.38 nm along the reconstruction rows and are attributed to pairs of hydrogen atoms.

We would like to underline that the atomic DB structures described thereafter were constructed on perfectly hydrogenated Si(001):H surface areas only, as those in Fig. 2E, F, in order to avoid any influence of surface defects on the final electronic properties of created structures.

3.2. DB nanostructures: STM construction and STS spectroscopy

The construction of individual DBs or pre-designed DB lines and/or atomic scale logic circuits was performed with the procedure already optimized on the Ge(001):H surface [22]. First, the STM tip apex was located over a protrusion observed in the constant current filled state (-2 V) STM image corresponding to the H atom to be removed. Then, the STM feedback loop was switched off and the bias voltage polarity was simultaneously reversed. Voltage was increased until values in the $2.5\text{--}3.5 \text{ V}$ range were reached

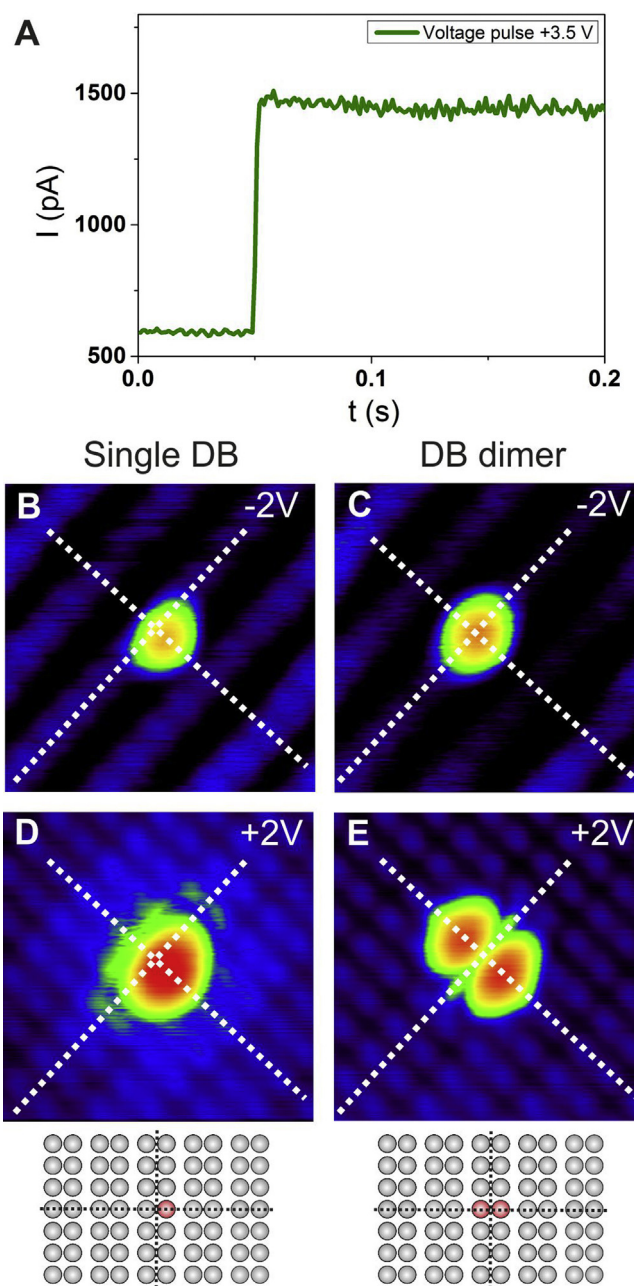


Fig. 3. (A) $I(t)$ characteristics recorded during the LT-UHV-STM tip induced desorption of a single H atom from Si(001)- (2×1) :H. The voltage pulse applied on the tip was $+3.5 \text{ V}$ with respect to the sample. (B)–(E) filled state (B,C) and empty state (D,E) STM images of the same $3.5 \text{ nm} \times 3.5 \text{ nm}$ surface area presenting single (B, D) and double (C, E) DBs, which are the result of consecutive STM tip induced hydrogen atom desorption. STM scanning parameters: 10 pA , -2 V for filled state and 10 pA , $+2 \text{ V}$ for empty state imaging. Structural models of presented structures are also shown. Gray and red circles depict hydrogenated and bare silicon atoms respectively. Dashed lines on STM scans and models highlight the positions of atoms.

for a certain period of time. On a hundreds of milliseconds time scale, a sudden rise of the tunneling current was observed, which is related to the hydrogen desorption event as shown in Fig. 3A. Our results indicate that, by applying the described protocol at cryogenic temperatures, single hydrogen atoms could predominantly be desorbed as shown in Fig. 3B–E, where single and double DBs were formed. Please note that, in this case, the DB dimer is obtained in two separate consecutive desorption events. With the use of this protocol, DB lines and small circuits can be constructed atom by atom on a Si(001):H surface with the desired complexity.

A single DB was observed in both filled and empty state STM images as a protrusion, located asymmetrically with respect to the reconstruction row of Si(001):H, as shown in Fig. 3B, D. Desorption of the second hydrogen atom from the Si dimer led to formation of an isolated DB dimer. This structure appears in Fig. 3C, E filled and empty state STM images as a symmetric protrusion for moderate imaging conditions (10 pA current, -2 V and $+2$ V biases). It shows a characteristic “butterfly” contrast in the empty state image. These observations are in agreement with previous STM measurements performed at RT [23], 80 K [24] and 5 K [11]. Interestingly, the buckled, asymmetric configuration of the isolated Si bare dimer, where it is tilted with respect to the surface plane by about 19° , is often considered as the native geometry [24]. Such buckled geometry of isolated bare Ge dimers was also reported for Ge(001):H surface [22]. Results shown in Fig. 3B, D demonstrate symmetric STM appearance of the isolated Si bare dimer. However scanning parameters used here may symmetrize the bare Si dimer STM images, which still leaves open the question of the native geometry of these structures on Si(001):H surfaces.

Extraction of hydrogen atoms from neighboring hydrogenated silicon dimers induces coupling between the already constructed

DBs. The coupling varies with the DB structure orientation, which can be considered as an advantage for the design and construction of atomic scale logic gates [4,22]. The interactions between neighboring DB dimers are expected to stabilize the buckled dimer configuration, as already observed for bare reconstructed silicon surface [25] and for short DB dimer lines formed on Ge(001):H surface [22]. However, this was not the case for the short DB dimer structures as presented in Fig. 4. Two DB dimers oriented along (Fig. 4A, C) and across (Fig. 4B, D) the reconstruction rows did not show a buckling and appeared symmetric at both bias polarizations. The characteristic empty state contrast of a single isolated DB dimer evolved toward four-lobe and three-lobe structures for parallel (Fig. 4C, E) and perpendicular (Fig. 4D, F) geometries, respectively. Note that, due to the weak interaction between DBs, central maxima of two perpendicularly oriented DB dimer structures appear brighter in Fig. 4D empty state STM image, what is clearly demonstrated by the corresponding STM height profile (Fig. 4F).

In order to associate a specific empty state contrast to a particular DB state and to follow the interaction between newly created DB dimers, we performed STS dI/dU analysis of perpendicularly oriented DB dimer lines with various lengths. All STS measurements were performed at 4 K in a mode where the feedback loop was turned on between every two $I(U)$ characteristics to determine the tip position. The $I(U)$ characteristics were automatically collected using a grid covering respective surface areas (Fig. 5A–C), and the corresponding dI/dU spectra were obtained by differentiating the $I(U)$ curves averaged previously over the area of the DB structure only (Fig. 5A–C).

The experimental dI/dU spectrum of a fully hydrogenated Si(001):H surface area is presented in Fig. 5D. It clearly shows that the measured surface band gap of slightly p-doped Si(001):H is about 2 eV for the STM feedback loop conditions maintaining the tip apex away from the surface to avoid any band bending effects.

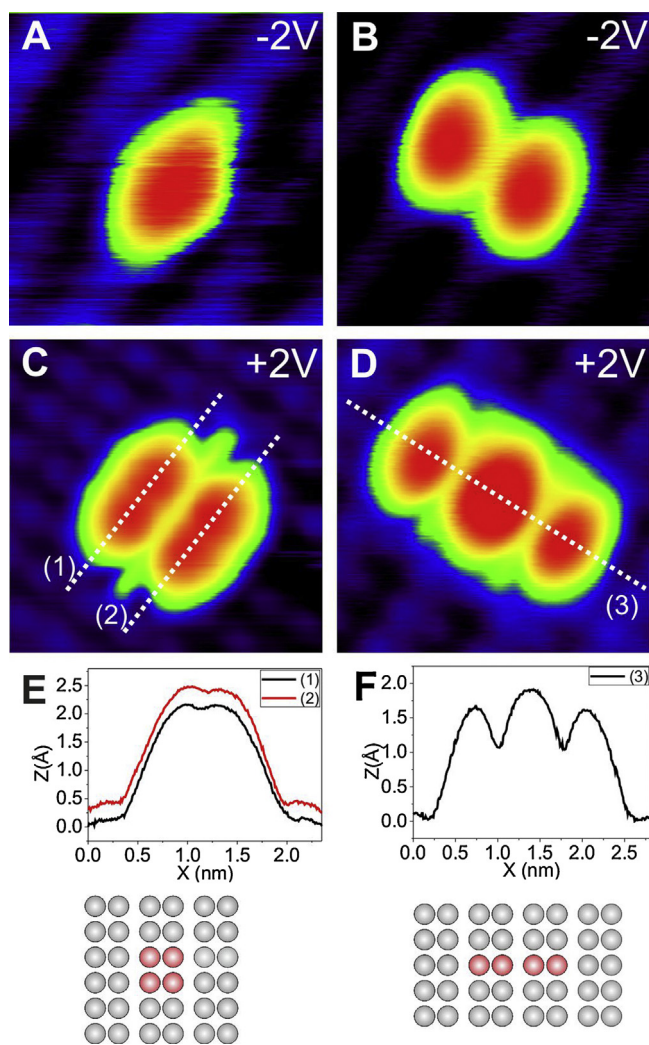


Fig. 4. (A)–(D) Filled state (A, B) and empty state (C, D) STM images of $2.5 \text{ nm} \times 2.5 \text{ nm}$ surface area presenting short lines of two DB dimers, which are oriented along (A, C) and across (B, D) reconstruction rows. STM scanning parameters: 10 pA, -2 V for filled state and 10 pA, $+2$ V for empty state imaging. (E), (F) Height profiles taken from the STM images (C) and (D). Structural models of presented structures are also shown. Gray and red circles depict hydrogenated and bare silicon atoms respectively.

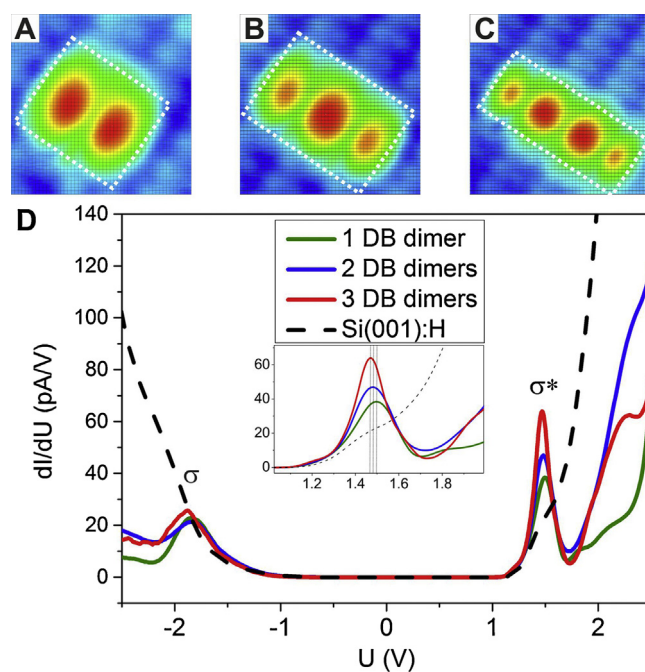


Fig. 5. (A)–(C) Empty state STM images ($+2$ V) taken before acquisition of STS dI/dU spectra presented in D with a 50×50 grid used in the STS experiment. The scan areas are $2 \text{ nm} \times 2 \text{ nm}$ (A), $2.5 \text{ nm} \times 2.5 \text{ nm}$ (B) and $3 \text{ nm} \times 3 \text{ nm}$ (C). (D) STS dI/dU spectra acquired at 4 K for a fully hydrogenated Si(001)-(2 \times 1):H surface and for DB lines containing 1, 2, and 3 DB dimers aligned perpendicularly to the Si(001):H dimer rows. Presented STS dI/dU spectra for various DB dimer structures were obtained by averaging over the rectangular areas marked on corresponding STM images in A–C. Inset: magnification presenting exact STS dI/dU σ^* peak positions.

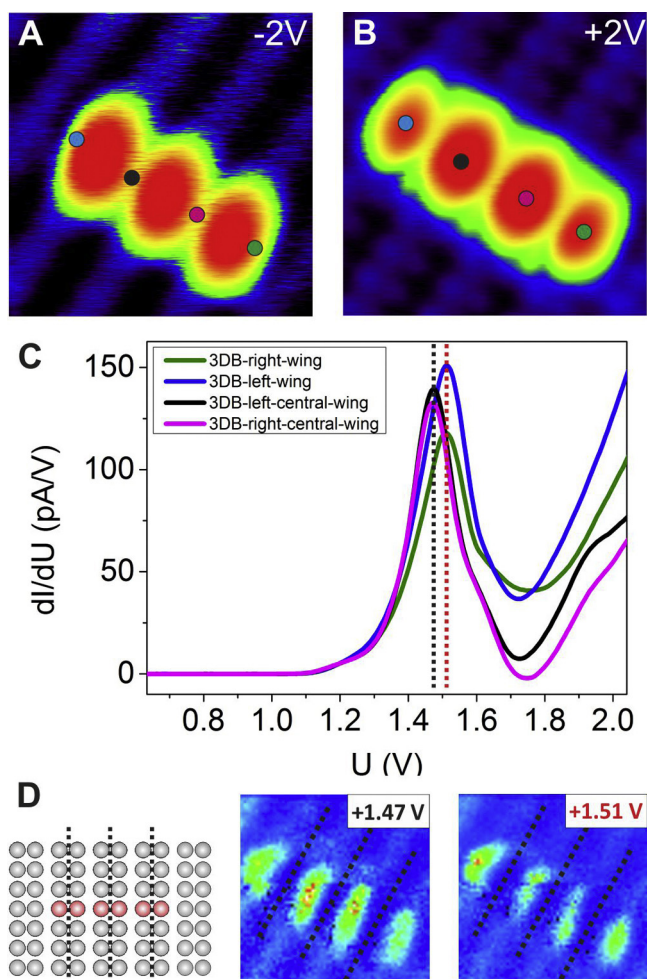


Fig. 6. (A), (B) Filled state (A) and empty state (B) STM images ($3.5 \text{ nm} \times 3.5 \text{ nm}$) of a 3 DB dimer line oriented across the reconstruction rows. The corresponding STM scanning parameters were 10 pA , -2 V for filled state and 10 pA , $+2 \text{ V}$ for empty state imaging. (C) STS dI/dU spectra acquired at 4 K of a 3 DB dimer line taken at different lateral positions indicated in the STM images (A) and (B). The 0.05 eV shift of the dI/dU peak position due to weak interaction between DB dimers is clearly seen. (D) Structural model of analyzed DB structure and lateral dI/dU maps obtained for voltages corresponding to both STS dI/dU peak positions.

Collected dI/dU spectra for DB dimer lines with different lengths show almost the same electronic structure. The $\text{Si}(001)\text{:H}$ surface gap slightly decreases when DB dimers are formed on the surface, due to the electronic states introduced by the DBs near the bottom of the $\text{Si}(001)\text{:H}$ conduction band edge. This is coming from the narrow states of the $\text{Si}(001)$ DB dimers, which are located at a $+1.5 \text{ eV}$ energy (Fig. 5) and which correspond to σ^* antibonding states of the Si dimer back bonds, as reported by Bellec et al. [11]. Such description of observed dI/dU maxima is also in agreement with STS data obtained for bare $\text{Si}(001)$ surface [26].

For negative sample biases, the states observed close to the valence band edge at around -1.8 eV may be associated to σ bonding states [11]. The π^* antibonding and π bonding states of DB dimers are located within the band gap of $\text{Si}(001)\text{:H}$ and are extremely hard to capture by STS due to the specific experimental conditions. Low doped silicon substrate and cryogenic temperature indeed cause the electronic filtering of these states by the band gap of bulk Si. The very small shift ($\sim 0.02 \text{ eV}$) of the σ^* antibonding states toward the center of the band gap, observed with the increasing number of DB dimers, is related to weak interactions between these DBs. In order to follow these interactions, we focused on the three DB dimers structure presented in Fig. 6A, B. The empty state STM

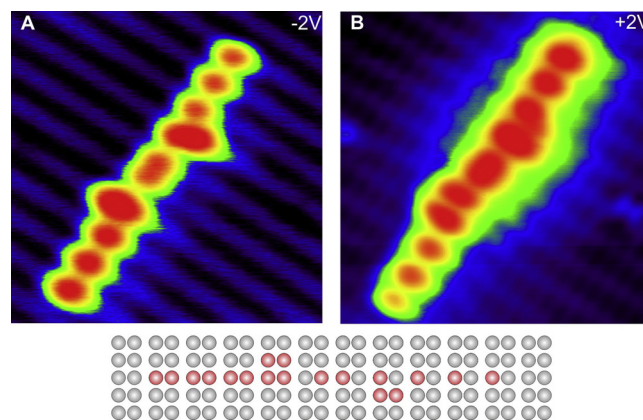


Fig. 7. Filled (A) and empty (B) state images of a more complex “gate like” DB structure, which consists of single DBs and DB dimers. The corresponding STM scanning parameters were 10 pA , -2 V for filled state and 10 pA , $+2 \text{ V}$ for empty state imaging. The structural model of the imaged structure is schematically shown below. Gray and red circles depict hydrogenated and bare silicon atoms respectively.

image in Fig. 6B clearly shows a four-lobe image with two larger central maxima. The STM image results from the convolution of “butterfly” contrasts from three isolated DB dimers. Fig. 6C presents the STS dI/dU spectra averaged over different locations on the DB structure. The peak position corresponding to the σ^* state is shifted by about 0.04 eV toward the center of the band gap for spectra collected on central maxima with respect to the ones collected on the “side wings” of the DB structure. This is also observed in the dI/dU maps extracted from the STS dI/dU experiment and presented in Fig. 6D. The dI/dU map obtained for $+1.47 \text{ eV}$ shows central peaks with higher apparent contrast compared to the side ones, whereas the situation is reversed for the map at $+1.51 \text{ eV}$. Moreover, the peak position of the σ^* state of the “side wings” of the three DB dimer structure is located at the same energy as the peak position of a single isolated DB dimer. Interactions among DBs, in the DB line oriented perpendicularly to the $\text{Si}(001)\text{:H}$ reconstruction rows, seem thus to be reflected in the shift of the σ^* state of the central DBs rather than in the ones of the sides of the DB structure. The STS dI/dU maps presented in Fig. 6D also clearly show that the characteristic “butterfly” empty state contrast of DB dimers is related to the energy state about $+1.5 \text{ eV}$ above the Fermi level.

Finally to illustrate that our UHV de-bonded Si:H surface is appropriate for the construction of surface atomic scale logic gates and interconnects as theoretically proposed [3–5], we have constructed DB atomic scale structures extending over more sizable dimensions. The example shown in Fig. 7, demonstrates that the controlled construction of a long and complex DB structure of nearly 20 DBs, with a length up to 10 nm is feasible. This is a nice experiment demonstrating that the atomic scale construction technology is effective for the fabrication of surface logic gates based on DB nanostructures, using as a substrate the 200 mm silicon wafer surface processed and nanopackaged in a cleanroom environment.

4. Conclusions

This work demonstrates the feasibility of preparing reconstructed 200 mm $\text{Si}(001)\text{:H}$ surfaces in a cleanroom environment with fabrication tools dedicated to the microelectronics industry. The protection of the $\text{Si}(001)\text{:H}$ surface by a temporarily bonded cap enables its storage and transportation in ambient conditions. After de-bonding under UHV, the $\text{Si}(001)\text{:H}$ surface remains perfectly reconstructed and atomically clean. We prove that the de-bonded $\text{Si}(001)\text{:H}$ surface quality is appropriate for the construction of DB nanostructures by STM tip induced hydrogen atom desorption. They were investigated in detail with cryogenic

temperature STM/STS. Our results show that Si(001):H wafers processed with standard microelectronics and nanopackaging tools are suitable as templates for the precise atomic scale construction of surface DB state circuits.

Acknowledgements

This research was supported by the 7th Framework Program of the European Union Collaborative Project ICT (Information and Communication Technologies) “Atomic Scale and Single Molecule Logic Gate Technologies” (ATMOL), contract number: FP7-270028. The UHV part of the experiment was carried out using equipment purchased with financial support from the European Regional Development Fund within the framework of the Polish Innovation Economy Operational Program (contract no. POIG.02.01.00-12-023/08). M.K. would like to acknowledge financial support received from the Polish National Science Center for preparation of his PhD dissertation on the basis of decision number: DEC-2013/08/T/ST3/00047.

Appendix A. Supplementary data

Supplementary data associated with this article can be found, in the online version, at <http://dx.doi.org/10.1016/j.apsusc.2013.09.124>.

References

- [1] C. Joachim, D. Martrou, M. Rezek, C. Troadec, D. Jie, N. Chandrasekhar, S. Gauthier, Multiple atomic scale solid surface interconnects for atom circuits and molecule logic gates, *Journal of Physics: Condensed Matter* 22 (2010) 084025.
- [2] J.S. Prauzner-Bechcicki, S. Godlewski, M. Szymonski, Atomic- and molecular-scale devices and systems for single-molecule electronics, *Physica Status Solidi (a)* 209 (2012) 603–613.
- [3] F. Ample, I. Duchemin, M. Hliwa, C. Joachim, Single OR molecule and OR atomic circuit logic gates interconnected on a Si(100)H surface, *Journal of Physics: Condensed Matter* 23 (2011) 125303.
- [4] H. Kawai, F. Ample, Q. Wang, Y.K. Yeo, M. Saeys, C. Joachim, Dangling-bond logic gates on a Si(100)-(2×1)-H surface, *Journal of Physics: Condensed Matter* 24 (2012) 095011.
- [5] M. Kepenekian, R. Robles, C. Joachim, N. Lorente, Surface-state engineering for interconnects on H-passivated Si(100), *Nano Letters* 13 (2013) 1192–1195.
- [6] J.W. Lyding, T.-C. Shen, J.S. Hubacek, J.R. Tucker, G.C. Abeln, Nanoscale patterning and oxidation of H-passivated Si(100)-2×1 surfaces with an ultrahigh vacuum scanning tunneling microscope, *Applied Physics Letters* 64 (1994) 2010–2012.
- [7] T.C. Shen, C. Wang, G.C. Abeln, J.R. Tucker, J.W. Lyding, P. Avouris, R.E. Walkup, Atomic-scale desorption through electronic and vibrational excitation mechanisms, *Science* 268 (1995) 1590–1592.
- [8] E. Foley, A. Kam, J. Lyding, P. Avouris, Cryogenic UHV-STM study of hydrogen and deuterium desorption from Si(100), *Physical Review Letters* 80 (1998) 1336–1339.
- [9] L. Soukiassian, A. Mayne, M. Carbone, G. Dujardin, Atomic wire fabrication by STM induced hydrogen desorption, *Surface Science* 528 (2003) 121–126.
- [10] M. Haider, J. Pitters, G. DiLabio, L. Livadaru, J. Mutus, R. Wolkow, Controlled coupling and occupation of silicon atomic quantum dots at room temperature, *Physical Review Letters* 102 (2009) 046805.
- [11] A. Bellec, D. Riedel, G. Dujardin, O. Boudrioua, L. Chaput, L. Stauffer, P. Sonnet, Electronic properties of the n-doped hydrogenated silicon (100) surface and dehydrogenated structures at 5 K, *Physical Review B* 80 (2009) 245434.
- [12] A. Bellec, D. Riedel, G. Dujardin, O. Boudrioua, L. Chaput, L. Stauffer, P. Sonnet, Nonlocal activation of a bistable atom through a surface state charge-transfer process on Si(100)-(2×1):H, *Physical Review Letters* 105 (2010) 048302.
- [13] T. Hitosugi, S. Heike, T. Onogi, T. Hashizume, S. Watanabe, Z. Li, K. Ohno, Y. Kawazoe, T. Hasegawa, K. Kitazawa, Jahn-Teller distortion in dangling-bond linear chains fabricated on a hydrogen-terminated Si(100)-2×1 surface, *Physical Review Letters* 82 (1999) 4034–4037.
- [14] M. Fuechsle, S. Mahapatra, F.A. Zwanenburg, M. Friesen, M.A. Eriksson, M.Y. Simmons, Spectroscopy of few-electron single-crystal silicon quantum dots, *Nature Nanotechnology* 5 (2010) 502–505.
- [15] B. Weber, S. Mahapatra, H. Ryu, S. Lee, A. Fuhrer, T.C.G. Reusch, D.L. Thompson, W.C.T. Lee, G. Klimeck, L.C.L. Hollenberg, M.Y. Simmons, Ohm's law survives to the atomic scale, *Science* 335 (2012) 64–67.
- [16] V. Loup, J.M. Hartmann, G. Rolland, P. Holliger, F. Laugier, Reduced pressure chemical vapour deposition of Si/Si_{1-x-y}Ge_xC_y heterostructures using a chlorinated chemistry, *Semiconductor Science and Technology* 18 (2003) 352–360.
- [17] C. Rauer, F. Rieutord, J.M. Hartmann, A.-M. Charvet, F. Fournel, D. Mariolle, C. Morales, H. Moriceau, Hydrophobic direct bonding of silicon reconstructed surfaces, *Microsystem Technologies* 19 (2013) 675–679.
- [18] Q.Y. Tong, U. Gösele, *Semiconductor wafer bonding: science and technology*, Wiley, New York, 1999.
- [19] H. Moriceau, O. Rayssac, B. Aspar, B. Ghyselen, The bonding energy control: an original way to debondable substrates, *Proceedings of the Electrochemical Society* 2003-19 (2003) 49–56.
- [20] I. Horcas, R. Fernández, J.M. Gómez-Rodríguez, J. Colchero, J. Gómez-Herrero, A.M. Baro, WSXM: a software for scanning probe microscopy and a tool for nanotechnology, *Review of Scientific Instruments* 78 (2007) 013705.
- [21] W.P. Maszara, G. Goetz, A. Caviglia, J.B. McKitterick, Bonding of silicon wafers for silicon-on-insulator, *Journal of Applied Physics* 64 (1988) 4943–4950.
- [22] M. Kolmer, S. Godlewski, H. Kawai, B. Such, F. Krok, M. Saeys, C. Joachim, M. Szymonski, Electronic properties of STM-constructed dangling-bond dimer lines on a Ge(001)-(2×1):H surface, *Physical Review B* 86 (2012) 125307.
- [23] J.J. Boland, Evidence of pairing and its role in the recombinative desorption of hydrogen from the Si(100)-2×1 surface, *Physical Review Letters* 67 (1991) 1539–1542.
- [24] D. Chen, J. Boland, Chemisorption-induced disruption of surface electronic structure: Hydrogen adsorption on the Si(100)-2×1 surface, *Physical Review B* 65 (2002) 165336.
- [25] R.A. Wolkow, Direct observation of an increase in buckled dimers on Si(001) at low temperature, *Physical Review Letters* 68 (1992) 2636–2639.
- [26] L. Perdigão, D. Deresmes, B. Grandidier, M. Dubois, C. Delerue, G. Allan, D. Stiévenard, Semiconducting surface reconstructions of p-Type Si(100) substrates at 5 K, *Physical Review Letters* 92 (2004) 216101.

Advances in Atom and Single Molecule Machines

Series Editor: Christian Joachim

Leonhard Grill

Christian Joachim *Editors*

Imaging and Manipulating Molecular Orbitals

Proceedings of the 3rd AtMol International
Workshop, Berlin 24–25 September 2012

 Springer

SPM Imaging of Trinaphthylene Molecular States on a Hydrogen Passivated Ge(001) Surface

Marek Kolmer, Szymon Godlewski, Bartosz Such, Paula de Mendoza, Claudia De Leon, Antonio M. Echavarren, Hiroyo Kawai, Mark Saeys, Christian Joachim and Marek Szymonski

Abstract We report on studies concerning individual trinaphthylene molecules (Y molecules) deposited and anchored on the hydrogenated Ge(001):H surface. The characterization of single Y molecules has been performed by means of cryogenic temperature STM imaging using conventional STM tungsten tips and tuning fork-based sensors. In the latter case, a qPlus sensor facilitated simultaneous STM and NC-AFM measurements and thus molecular states were probed by both tunneling current and atomic forces concurrently. We show that the molecules are physisorbed, thus weakly interacting with the substrate. Contrary to the measurements on hydrogenated silicon, for planar aromatic molecules on the hydrogenated germanium, both empty and filled molecular states could be probed by STM.

M. Kolmer (✉) · S. Godlewski · B. Such · M. Szymonski
Centre for Nanometer-Scale Science and Advanced Materials, NANOSAM, Faculty of Physics, Astronomy, and Applied Computer Science, Jagiellonian University, Reymonta 4, 30059 Krakow, Poland
e-mail: marek.kolmer@uj.edu.pl

P. de Mendoza · C. De Leon · A. M. Echavarren
Institute of Chemical Research of Catalonia (ICIQ), Avenida Països Catalans 16, 43007 Tarragona, Spain

H. Kawai · M. Saeys · C. Joachim
Institute of Materials Research and Engineering, 3 Research Link, Singapore 117602, Singapore

M. Saeys
Department of Chemical and Biomolecular Engineering, National University of Singapore, 4 Engineering Drive 4, Singapore 117576, Singapore

C. Joachim
Nanosciences Group & MANA Satellite, CEMES-CNRS, 29 rue Jeanne Marvig, F-31055 Toulouse, France

1 Introduction

Since further development of a conventional, CMOS-type electronic device is approaching fundamental limits at the nanoscale, several alternative routes are considered [1–3]. One possibility, called “monomolecular electronics,” is considering a device in which states of a single organic molecule are altered by close contact with another atom or a molecule, which play the role of inputs [4]. In order to extract output information from such a molecular (quantum) device, spectroscopic control of individual molecular states is needed, so at first, imaging and spectroscopy of states of the prospective molecules should be performed with atomic precision. Furthermore, the effect of external input stimulation on the molecular states of the device, for example with atomic-size defects, should be characterized with similar level of precision.

In order to facilitate molecular orbital imaging and spectroscopy based on the state-of-the-art use of modern nanotechnology tools, such as Scanning tunneling microscopy (STM) and Non-contact atomic force microscopy (Nc-AFM), electronic decoupling of the molecule in question from the underlying substrate is required. It is expected that proper isolation of such molecular entities could be achieved by application of passivated semiconductor surfaces, e.g., Si(001):H and Ge(001):H. A monolayer of hydrogen atoms may decouple molecules from a semiconductor surface as recently demonstrated by Bellec et al. [5], who imaged physisorbed pentacene molecules on hydrogen passivated silicon surfaces. Recorded images closely resemble the HOMO orbital contour of molecules and the dI/dU spectra provide additional confirmation of weak molecule substrate interaction. The STM image of the pentacene on the Si(001):H is shown in Fig. 1.

Similarly, also functionalized molecular platforms adsorbed on hydrogenated surfaces could be probed by STM technique as reported by Gruyters et al. [6], who measured iron phthalocyanine molecules on passivated silicon Si(111):H. The images recorded with different bias voltages provide insight into the electronic structure and are shown in Fig. 2.

Fig. 1 STM image of the pentacene molecule anchored on a step of the hydrogenated Si(001) surface; the image closely resembles the contour of molecule HOMO orbital. Reprinted with permission from Bellec et al. [5]

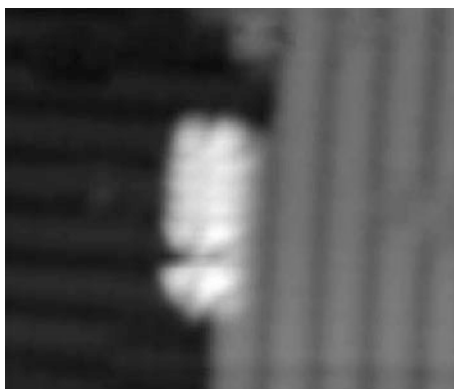
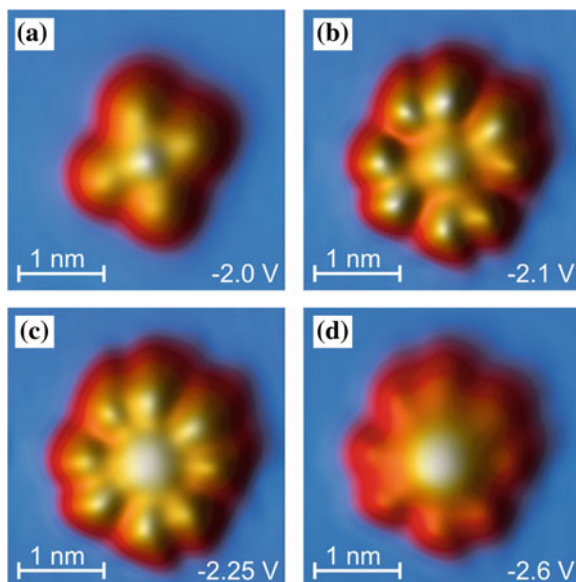


Fig. 2 STM filled-state images of the iron phthalocyanine molecule adsorbed on the hydrogenated Si(111) surface. Reprinted from Gruyters et al. [6] with permission



The application of passivated surfaces offers also the possibility to construct dangling-bond (DB) atomic-scale structures by STM tip-induced hydrogen desorption [7]. These DB structures may then serve as interconnects in molecular electronic devices. However, in principle the measurements of aromatic molecules on hydrogenated surfaces are extremely challenging due to high mobility of molecules. Moreover, the large band gap of the silicon substrate may hinder empty state probing especially if the states are hidden in the gap of the substrate. As a result only filled states are measured [5, 6].

Recent advances in quantum-chemical design and organic synthesis offer practical solutions toward fabrication of a suitable molecular logic gate. In general, we need planar aromatic molecules, which would physisorb on the passivated Ge(001):H and/or Si(001):H surface and should rather not be quite freely diffusing on those substrates but still the binding should allow for STM-tip induced manipulation over the surface. The molecules should have 3–4 branches allowing for anchoring them to dangling-bond defects (hydrogen monomer or dimer vacancies), so the lateral dimensions of the molecule branches should be correlated with a spacing of the reconstruction rows on the passivated surface.

One possibility is to use some symmetrical or non-symmetrical Y-shaped acenes, i.e., triphenylene-cored oligoacenes, as molecular gate building blocks. Therefore, in this study we decided to deposit a simple Y-shaped trinaphthylene, which could be considered as a prototypic molecule for the molecular logic gate devices. In our work, usage of hydrogen passivated Ge(001) allows for not only decoupling the molecules electronically (at least partially) from the low band gap substrate, but also offers an innovative way of producing interconnects by

H-extraction with the STM tip, as described recently in Ref. [7]. The DB wires fabricated by STM-tip-induced H-extraction could also form logic structures providing specific input for the molecule device.

2 Ge(001) Surface Preparation and Molecule Deposition

The experiment was carried out in an ultra-high vacuum (UHV) system containing preparation and cryogenic microscope chambers. The STM measurements were performed with the Omicron low temperature scanning probe microscope (LT-STM/AFM). The base pressure was in the low 10^{-10} mbar range. The preparation chamber was supplied with a noble gas ion gun, a homebuilt hydrogen cracker, and an infrared pyrometer. The surface quality was monitored with a low energy electron diffraction (LEED) setup. The Ge(001) undoped wafers (TBL Kelpin Crystals) were mounted on sample holders and were heated by direct current flowing through the sample. The samples were first annealed for 6 h at 800 K, and subsequently the 15 min cycles of 600 eV Ar^+ sputtering of the sample kept at 1040 K were repeated until a clean, well-defined surface was obtained, as checked by LEED and STM. The annealing temperature was controlled by the infrared pyrometer. Hydrogen passivation was performed with the use of a homebuilt hydrogen cracker providing atomic hydrogen. During passivation procedure the sample was kept at 485 K and the hydrogen pressure was maintained at 1×10^{-7} mbar. The STM imaging was carried out at reduced temperature of around 4 K (liquid helium) with etched tungsten tips used as probes. For image processing and STM data analysis SPIP and WSxM [8] software was used.

Figure 3 shows low temperature (liquid helium, 4 K) filled state STM images of Ge(001) (left panel) and hydrogen passivated Ge(001):H (right panel) surfaces. Ge(001) image exhibits clearly a mixed $c(4 \times 2)$ and $p(2 \times 2)$ surface

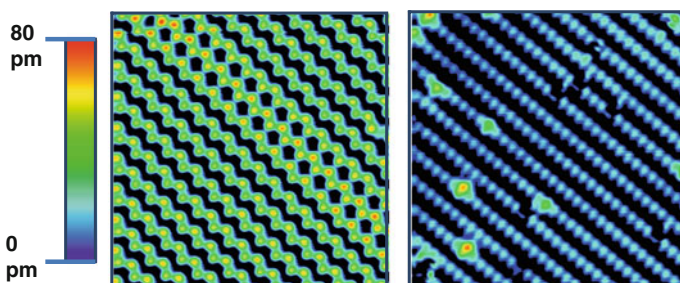
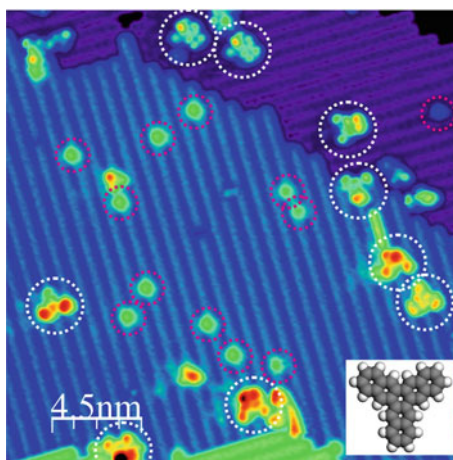


Fig. 3 Filled-state low temperature (4 K) STM images of the zig-zag dimer rows indicating mixed $c(4 \times 2)$ - and $p(2 \times 2)$ -Ge(001) surface reconstructions (*left panel*), and Ge(001)- (2×1) :H (*right panel*) surfaces; scan size $10 \times 10 \text{ nm}^2$, STM parameters $V = -0.5 \text{ V}$, and $I = 1 \text{ nA}$

Fig. 4 LT STM image (25×25 nm) of the hydrogen passivated Ge(001) surface with individual trinaphthylene molecules (Y). *White circles* mark single Y molecules and *red circles* indicate individual DBs. Tunneling current 2 pA, bias voltage -2.0 V. A scheme of the Y molecules is shown in the *inset*



reconstruction which arises from in-phase and out-of-phase buckling of neighboring Ge dimers. The hydrogenated surface is recorded as a ladder structure consisting of rows of Ge dimers passivated by hydrogen atoms. On the right panel image, one can distinguish three main types of intrinsic defects inevitably present on the surface. The brightest are attributed to surface double DBs (two dangling bonds on a Ge dimer), slightly smaller and less bright are single DBs (one dangling bond per Ge dimer). The third type recorded as dark depletion is ascribed to surface Ge atom vacancies. Note that the apparent height of surface double DBs is in principle identical to the height of surface Ge atoms on unpassivated surface.

In this work, low temperature scanning tunneling microscopy and non-contact atomic force microscopy (LT-STM/nc-AFM) measurements have been made on planar polyaromatic hydrocarbon molecules, namely the heptastarphene (trinaphthylene, Y) molecules deposited on the hydrogenated germanium surface. The Y molecules are prototypical 3 input/output molecules that could be applied in single molecule switches. The inset in Fig. 4 shows the scheme of Y molecule. Due to extremely high molecule mobility, Y molecules are evaporated on the sample which is removed from the microscope cryostat just before deposition. This procedure enables evaporation of molecules on the sample kept still at low temperature. The sample is inserted into the microscope cryostat immediately after molecule deposition. The molecules are evaporated at very low molecule flux with the evaporator kept at 450 K. A typical result of the deposition at relatively low dose is presented in Fig. 4, where LT-STM image (25×25 nm) of the hydrogen passivated Ge(001) surface with individual trinaphthylene molecules (Y) is shown.

3 Molecular State Imaging of Heptastarphene Molecules Anchored on the Ge(001):H Surface with LT-STM

The molecules deposited on the hydrogenated germanium sample are physisorbed, and thus only weakly interact with the substrate. Therefore, after evaporation the molecules are mobile and move across the surface. This results in trapping of the molecules by surface defects and step edges. Some molecules are trapped by unidentified defects and are strongly interacting with these defects. Therefore these molecules could not be manipulated with the use of the STM tip. However, the vast majority of the molecules could be found immobilized by the well-known surface defects, i.e., characterized previously DB dimers [7]. These molecules do not interact very strongly with the defects and could be manipulated with the use of the STM tip. The procedure of the tip-induced lateral manipulation enables us to detach the molecules from the DB dimers and to place the molecules on the fully hydrogenated surface. Therefore, we can probe both the properties of molecules immobilized by surface DBs and molecules physisorbed on the surface without any defects in the vicinity.

At liquid helium temperature the molecules physisorbed on the hydrogenated surface prove to be stable during measurements allowing for acquisition of STM images with different bias voltages. In Fig. 5a the STM images obtained at different bias voltages are shown. The images obtained for -3.0 and $+3.0$ V voltage settings exhibit intramolecular contrast proving that the submolecular resolution of physisorbed molecules could be achieved. For bias voltages between -2.4 and $+3.0$ V almost no intramolecular contrast is recorded indicating that no molecule states are available for tunneling electrons and the recorded image is simply the image of the hydrogenated surface with the image contrast modulated by the molecule. To analyze the details of the molecule–substrate interaction and the electronic structure we performed extensive calculations. The density functional theory (DFT)-based calculations show that the HOMO–LUMO gap of free gas phase molecule reaches approximately 3.24 eV (HSE06 functional). In Fig. 5b calculated STM image of the molecule physisorbed on the Ge(001):H is shown. The image closely resembles the experimental images acquired for -2.0 V

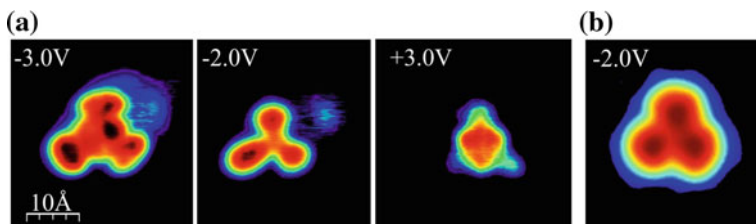


Fig. 5 **a** STM images of the physisorbed Y molecule acquired with different bias voltages denoted in the text. **b** Calculated STM image of Y molecule

indicating that the measurements are performed out of the resonances resulting in the imaging of the surface modified by the presence of the molecule.

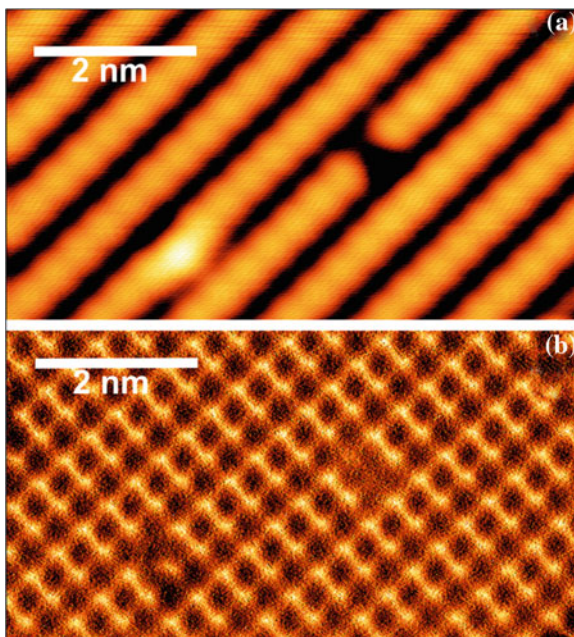
4 3D Molecular State Probing with Simultaneous Tunneling Current and Force Imaging with a qPlus Sensor

In recent years NC-AFM-related techniques have been developing very fast. One of the fields where fast progress is especially prominent is cryogenic NC-AFM. Following the footsteps of STM, for which going to low temperatures gave access to new fields in physics and chemistry, cryogenic NC-AFM is opening a range of new applications. There are some examples of highly successful NC-AFM experiments performed with the use of cantilever-based systems; however, the rapid growth of applications and accessibility of the field coincided with the introduction of quartz tuning forks as sensors. Additionally, a tuning fork can be equipped with a tip made of any material (for instance tungsten or Pt–Ir alloy) which can be connected to preamplifier by a separate lead allowing in principle for dual AFM/STM operation. Tuning forks are typically used in qPlus configuration—in which one of the prongs is glued to a ceramic holder while another, with a tip attached at its end, is oscillating freely.

Two consecutive images of the same area of the hydrogenated Ge(001):H surface taken with qPlus-based scanning probe microscope: topographic, constant current STM image, and constant height map of frequency shift are presented in Fig. 6a and b. The appearance of the STM image (Fig. 6a) is similar to the one presented in Fig. 3. The main features of the constant height image (Fig. 6b) are double rows of protrusions, i.e., positions where the tip had to adjust the frequency shift in order to maintain the required height. Note that Fig. 6b represents a map of the frequency shift, i.e., elevation indicates weaker attraction. The separation between the protrusions in a single row is about 0.37 nm, while the double rows are separated by 0.82 nm. Those values correspond quite closely to the postulated distances between hydrogen atoms adsorbed on a Ge dimer and the distance between dimer rows on the Ge(001) surface. Occasionally, defects can be observed on the surface, located over one of the hydrogen atoms in a dimer row. In the atomically resolved images, they are depicted as depressions.

Proper characterization of molecular adsorbates with the use of an NC-AFM based on qPlus sensor solution could provide an additional channel of information complementary to a standard STM study. In particular, possibility of simultaneous acquiring both the tunneling current and the detuning frequency maps for selected tip sensor heights above the surface opens new opportunities for 3D spectroscopy of molecular states. It is known that standard STS dI/dU spectroscopy for molecules adsorbed on surfaces provides information in which spatial distribution of the molecular state density is filtered by a specific surface band structure and the

Fig. 6 Two consecutive images of the same area of hydrogenated Ge(001):H surface taken with qPlus-based scanning probe microscope; **a** topographic, constant current STM image, $U = -0.5$ V, the color scale spans over 0.15 nm; **b** constant height map of frequency shift ($f_0 = 22,970$ Hz, $Q = 20,000$, $A = 500$ pm), color scale corresponds to the range from -1.1 to -0.1 Hz

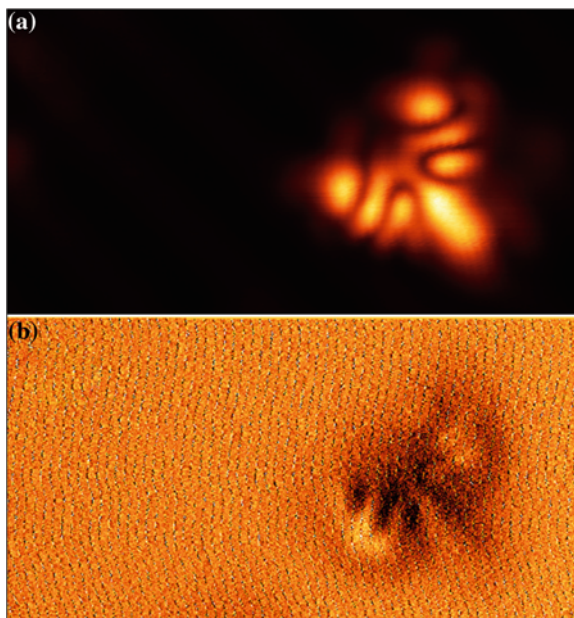


molecule-surface electronic coupling. For large surface band gaps and low level of coupling a large fraction of the density of states spectrum is not accessible in conventional STS measurements. This missing information could be retrieved by the proper analysis of the force maps measured by a qPlus sensor in parallel to tunneling current measurements.

In Fig. 7 the result of simultaneous STM/NC-AFM imaging of a single starphene molecule adsorbed at a defect on the Ge(001):H surface is shown. In this case, it is clear that the image is dominated by the interactions related to the density of electrons and hence is quite similar to the corresponding STM image. Till date it was impossible to approach the repulsive mode which could show the internal structure of a molecule, since binding to the surface is not strong enough and such an attempt resulted in uncontrolled manipulation of a molecule. However, since during the STM experiments a certain degree of control over location of the molecule on the surface (i.e. tip-induced manipulation) was achieved, further efforts will be undertaken to find a location stable enough to access molecular internal structure by the NC-AFM.

Fig. 7 Simultaneous imaging of “Y” molecule by STM and NC-AFM in constant height mode.

a 5×2.7 nm current image, $V = -0.5$ V, color scale corresponds to currents from 0 to 3.1 nA; **b** 5×2.7 nm frequency shift image, color scale corresponds to frequency shift from -1.0 to 0.4 Hz



5 Concluding Remarks

In this report we showed that a symmetric Y-shaped starphene, a prototypic molecule for the molecular logic gate devices, could be successfully anchored and imaged on the passivated semiconductor surface, namely Ge(001):H, using an STM/NC-AFM scanning probe operating at cryogenic temperatures (4 K). It appears that a uniform monohydrate layer provides sufficient electronic decoupling of the molecular states from the semiconductor substrate providing insight into internal structure of the molecular orbitals by scanning tunneling current spectroscopy and force spectroscopy with an NC-AFM qPlus sensor. The physisorbed molecules could also be manipulated with the STM tip. This could be utilized in the future for sampling of various levels of the molecule coupling to the passivated surface defects, both native and at will, created by analyzing STM images of the molecules at the relevant locations. Finally, possibility of simultaneous acquiring of both the tunneling current and the detuning frequency maps for selected tip sensor heights above the surface has been successfully explored.

Acknowledgments This research was supported by the 7th Framework Programme of the European Union Collaborative Project ICT (Information and Communication Technologies) “Atomic Scale and Single Molecule Logic Gate Technologies” (ATMOL), Contract No. FP7-270028. The experimental part of the research was carried out with equipment purchased with financial support from the European Regional Development Fund in the framework of the Polish Innovation Economy Operational Program (Contract No. POIG.02.01.00-12-023/08).

References

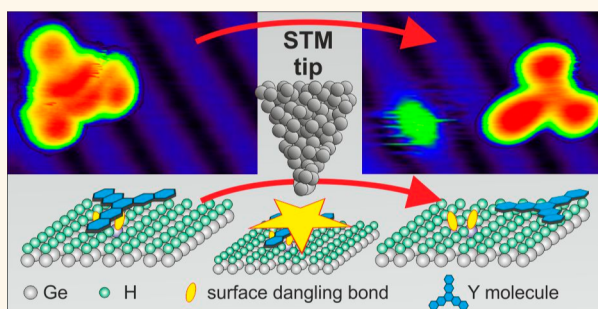
1. Fiurasek, J., et al.: Intramolecular Hamiltonian logic gates. *Physica E* **24**(3–4), 161–172 (2004)
2. Joachim, C., Gimzewski, J.K., Aviram, A.: Electronics using hybrid-molecular and mono-molecular devices. *Nature* **408**(6812), 541–548 (2000)
3. Prauzner-Bechcicki, J.S., Godlewski, S., Szymonski, M.: Atomic- and molecular-scale devices and systems for single-molecule electronics. *Phys. Status Solidi (a)* **209**, 603–613 (2012)
4. Soe, W.-H., Manzano, C., Renaud, N., De Mendoza, P., De Sarkar, A., Ample, F., Hliwa, M., Echavarren, A.M., Chandrasekhar, N., Joachim, C.: Manipulating molecular quantum states with classical metal atom inputs: demonstration of a single molecule NOR logic gate. *ACS Nano* **5**, 1436–1440 (2012)
5. Bellec, A., Ample, F., Riedel, D., Dujardin, G., Joachim, C.: Imaging molecular orbitals by scanning tunneling microscopy on a passivated semiconductor. *Nano Lett.* **9**, 144–147 (2009)
6. Gruyters, M., Pingel, T., Gopakumar, T.G., Néel, N., Schütt, Ch., Köhler, F., Herges, R., Berndt, R.: Electronic ground-state and orbital ordering of iron phthalocyanine on H/Si(111) unraveled by spatially resolved tunneling spectroscopy. *J. Phys. Chem. C* **116**, 20882–20886 (2012)
7. Kolmer, M., Godlewski, S., Kawai, H., Such, B., Krok, F., Saeys, M., Joachim, C., Szymonski, M.: Electronic properties of STM-constructed dangling-bond dimer lines on a Ge(001)-(2 × 1):H surface. *Phys. Rev. B* **86**, 125307 (2012)
8. Horcas, I., Fernández, R., Gómez-Rodríguez, J. M., Colchero, J., Gómez-Herrero, J., Baro, A. M.: WSXM: a software for scanning probe microscopy and a tool for nanotechnology. *Rev. Sci. Instr.* **78**, 013705 (2007)

Contacting a Conjugated Molecule with a Surface Dangling Bond Dimer on a Hydrogenated Ge(001) Surface Allows Imaging of the Hidden Ground Electronic State

Szymon Godlewski,^{†,‡,*} Marek Kolmer,^{†,‡} Hiroyo Kawai,^{‡,‡,*} Bartosz Such,[†] Rafal Zuzak,[†] Mark Saeys,^{‡,§} Paula de Mendoza,[‡] Antonio M. Echavarren,[‡] Christian Joachim,^{‡,||} and Marek Szymanski[†]

[†]Centre for Nanometer-Scale Science and Advanced Materials, NANOSAM, Faculty of Physics, Astronomy and Applied Computer Science, Jagiellonian University, Reymonta 4, PL 30-059, Krakow, Poland, [‡]Institute of Materials Research and Engineering, 3 Research Link, Singapore 117602, Singapore, [§]Department of Chemical and Biomolecular Engineering, National University of Singapore, 4 Engineering Drive 4, Singapore 117576, Singapore, ^{||}Institute of Chemical Research of Catalonia (ICIQ), Avenida Països Catalans 16, 43007 Tarragona, Spain, and ^{||}Nanosciences Group & MANA Satellite, CEMES-CNRS, 29 Rue Jeanne Marvig, F-31055 Toulouse, France. [#]S. Godlewski, M. Kolmer, and H. Kawai contributed equally to this work.

ABSTRACT Fabrication of single-molecule logic devices requires controlled manipulation of molecular states with atomic-scale precision. Tuning molecule–substrate coupling is achieved here by the reversible attachment of a prototypical planar conjugated organic molecule to dangling bonds on the surface of a hydrogenated semiconductor. We show that the ground electronic state resonance of a Y-shaped polyaromatic molecule physisorbed on a defect-free area of a fully hydrogenated surface cannot be observed by scanning tunneling microscopy (STM) measurements because it is decoupled from the Ge bulk states by the hydrogen-passivated surface. The state can be accessed by STM only if the molecule is contacted with the substrate by a dangling bond dimer. The reversibility of the attachment processes will be advantageous in the construction of surface atomic-scale circuits composed of single-molecule devices interconnected by the surface dangling bond wires.



KEYWORDS: hydrogenated semiconductor · organic molecule · single-molecule devices · atomic-scale contacts · scanning tunneling microscope · molecule manipulation · surface dangling bonds

Detailed knowledge of the electronic structure of individual molecules and the ability to manipulate their electronic states are the key ingredients for the construction of single-molecule logic circuits. One of the most powerful tools to visualize individual atoms and molecules, to probe their electronic properties, and to manipulate them with atomic-scale precision is the scanning tunneling microscope (STM).^{1–15} However, the use of an STM requires metallic or semiconducting substrates. As a result, originally designed electronic properties of free molecules are in general not retained after adsorption, due to electronic coupling of the molecular

electronic states with the surface. To overcome this problem, a passivating layer must be inserted between the molecules and the surface of the substrate to minimize those interactions. In recent years, several examples of molecules electronically decoupled by an ultrathin insulating layer on metals^{7,16} and on semiconductors¹⁷ have been reported, showing that even a monolayer of insulating material efficiently minimizes the electronic coupling. For example, Bellec *et al.* have shown that pentacene molecules are decoupled from the semiconductor bulk states by surface hydrogenation.¹⁸ The transport properties of molecules on the hydrogenated surface, however, can

* Address correspondence to szymon.godlewski@uj.edu.pl, kawai@imre.a-star.edu.sg.

Received for review August 14, 2013 and accepted October 22, 2013.

Published online October 22, 2013
10.1021/nn404254y

© 2013 American Chemical Society

be influenced by the surface dangling bonds (DBs), as demonstrated by Piva *et al.*¹⁹ Moreover, the ability to create²⁰ surface DBs on demand by extracting specific hydrogen atoms from the semiconductor surface allows in principle to create a planar atomic-scale contact between a physisorbed molecule and a DB.

In this paper, we demonstrate that a single tri-naphthylene (Y) molecule physisorbed on a hydrogenated semiconductor surface can be reversibly contacted with a single surface DB dimer. This molecule was selected because it was demonstrated to function as a NOR logic gate on a Au(111) surface.⁴ On a fully passivated Ge(001):H surface, its ground electronic state resonance cannot be recorded in the corresponding scanning tunneling spectroscopy (STS) dI/dV spectrum because it is very well decoupled from the semiconductor bulk states. However, when this molecule is manipulated to a native or specifically constructed DB dimer to increase its interaction with the Ge bulk electronic states through the DB states, the ground state tunneling resonance becomes observable. This leads to large differences in the recorded STM intramolecular contrast of this molecule when it is positioned on a surface DB dimer compared to the same molecule positioned on a fully hydrogenated surface.

RESULTS AND DISCUSSION

Physisorbed Molecules. Filtering the Ground Electronic State Resonance by a Hydrogenated Surface. Low-temperature STM measurements performed after molecule deposition show that all molecules are located either at the surface step edges or on defect-like native DBs (see Figure 1, molecule 2). This indicates that the interaction between the Y molecules and the Ge(001):H surface is very weak. The Y molecules are physisorbed on the surface and are highly mobile, as observed previously for pentacene molecules on Si(001):H.¹⁸ However, on Si(001):H the molecules were found only at step edges, while on Ge(001):H Y molecules can also be trapped by native DB defects. This is because a DB on Ge(001):H protrudes further into the vacuum than on Si(001):H. Therefore, a flat aromatic molecule can interact more strongly with a surface DB on Ge(001):H without any significant distortion of its planar structure. Still, Y molecules can be easily detached from DBs by STM lateral molecular manipulation. This procedure facilitates the identification of the native Ge(001):H surface defects that trap the Y molecule after adsorption (see Figure 1). The atomic structure of these surface defects is determined by a comparison between the appearance of a defect in an STM image, its STS characteristics, and the results of our recent studies of DB nanostructures constructed by STM tip-induced hydrogen desorption.²⁰

The characterization of the uncovered DB defect is indeed consistent with results obtained for an intentionally created DB dimer on Ge(001):H, demonstrating that, during deposition, Y molecules are stabilized by

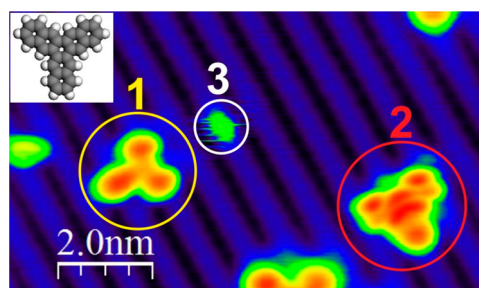


Figure 1. Filled state STM image of Y molecules on a hydrogenated Ge(001):H surface. (1) Y molecule physisorbed on a defect-free Ge(001):H surface. The molecule was intentionally detached from a DB dimer (3) and placed on a defect-free area by STM tip-induced manipulation. (2) Y molecule in an initial geometry immobilized by a surface DB dimer. Inset: Atomic structure of the Y molecule. STM imaging conditions: bias voltage -2.0 V, tunneling current 2 pA. The image is acquired at liquid helium temperature (4.5 K).

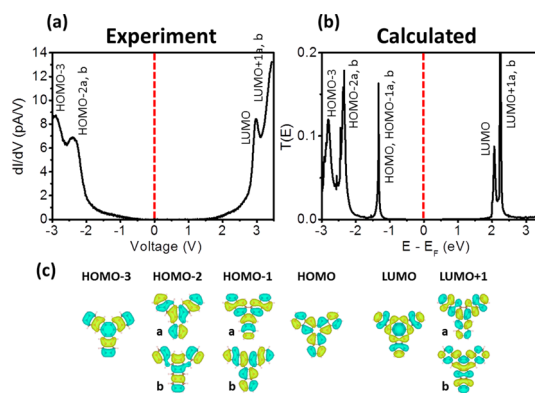


Figure 2. (a) STS spectra recorded over a physisorbed Y molecule on a defect-free Ge(001):H surface with indicated filled (-2.9 V; -2.4 V) and empty states ($+3.0$ V). (b) Transmission coefficient spectra, $T(E)$, calculated for a physisorbed Y molecule on Ge(001):H. (c) Extended Hückel molecular orbitals for the gas-phase Y molecule.

native DB dimers on Ge(001):H.²⁰ It is worth emphasizing that our ability to remove a Y molecule from a DB dimer and to place it on the defect-free part of the Ge(001):H surface is extremely advantageous. This allows for a detailed characterization of the electronic properties of a molecule without any perturbation of its electronic structure by substrate defects. Our measurements show that Y molecules placed on the hydrogenated surface by the STM tip are stable enough to perform both STM imaging and STS characterization at liquid helium temperature. Although initially all molecules are trapped by surface defects, we will first discuss the electronic states and STM image of a Y molecule physisorbed on a fully hydrogenated Ge(001) surface, followed by a discussion of the electronic states and STM image of a Y molecule on a DB dimer.

STS measurements are performed on Y molecules positioned on a defect-free area of the Ge(001):H surface. As shown in Figure 2a, two distinct peaks are recorded at approximately -2.4 and -2.9 V below the Ge bulk Fermi level. A single resonance is also recorded

at +3.0 V in the conduction band of bulk Ge. Contrary to previous experiments with conjugated molecules on hydrogenated semiconductor surfaces,^{18,21} the lowest excited state of the Y molecule can be probed with tunneling electrons on Ge(001):H. However, the apparent electronic gap between the first peak below and the first peak above the Fermi energy as measured by STS is approximately 5.4 eV, considerably larger than the HOMO–LUMO gap of 3.5 eV calculated for a gas-phase Y molecule. The electronic structure of a Y molecule physisorbed on defect-free Ge(001):H does not differ from a free molecule. In order to understand the large apparent gap between the STS peaks, the electronic transmission spectrum, $T(E)$, for a Y molecule physisorbed on Ge(001):H is calculated with the STM tip apex located above the Y molecule (Figure 2b). The $T(E)$ spectrum below the bulk Ge Fermi level comprises three peaks. The first resonance involves three molecular orbitals (MOs), HOMO, HOMO–1a, and HOMO–1b, which have nearly the same energy (separated by less than 0.05 eV). Note that these MOs are not located in the band gap of the Ge substrate. The second resonance originates from HOMO–2a and HOMO–2b, and the third resonance, which is the last peak within the energy window shown, is attributed to HOMO–3. The first resonance above the Fermi level corresponds to the LUMO and the second one to LUMO+1a and LUMO+1b (see Figure 2c for the spatial expansion and symmetry of those MOs for the isolated Y molecule). The calculated tunneling resonance gap of 3.5 eV is consistent with the HOMO–LUMO gap of a free Y molecule.

Interestingly, the first peak corresponding to HOMO, HOMO–1a, and HOMO–1b is calculated to be a very sharp Lorentzian resonance, implying that its contribution to the tunneling current intensity is very small. This is because the Y molecule is very well decoupled from the Ge bulk states by the hydrogen surface layer, and this decoupling is enhanced by the very small number of Ge bulk channels near the top of the valence band edge. Both effects limit the tunneling current in this energy range. Therefore, in this energy range, the tunneling current intensity is dominated by the tails of the HOMO–2a, HOMO–2b, and HOMO–3 resonances. Furthermore, for bias voltages down to –2.0 V, the STM images recorded for a Y molecule on a defect-free Ge(001):H do not exhibit any intramolecular contrast that would correspond to the HOMO/HOMO–1ab peak (see Figure 3a,b). The absence of the intramolecular contrast is apparent when these images are compared with the STM image of a Y molecule on a Au(111) surface measured at the ground state (HOMO) energy, which clearly shows the characteristic HOMO intramolecular features.⁴ These images rather reflect the Ge(001):H surface corrugation recorded through a planar Y molecule. The first HOMO/HOMO–1ab resonance is hence filtered by the tunneling junction, indicating that the interaction of those MOs with the Ge bulk states is

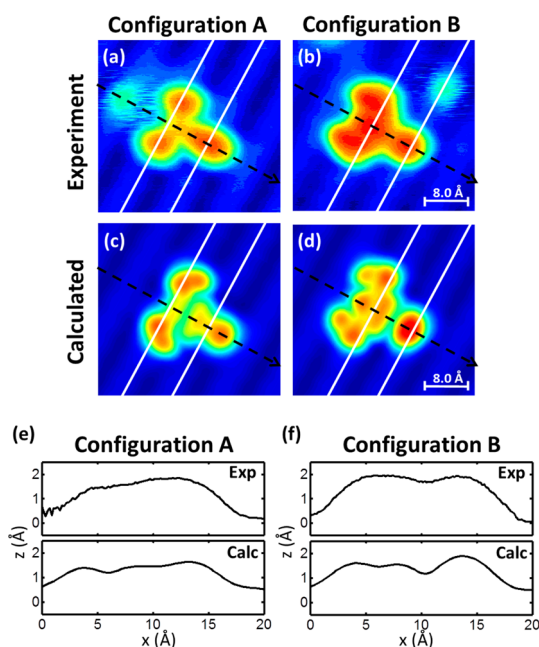


Figure 3. Two slightly different configurations (denoted as A and B) of physisorbed Y molecules on a defect-free Ge(001):H surface. (a and b) Filled state STM images. (c and d) STM images calculated when the HOMO/HOMO–1ab resonance is excluded. The presence of the Ge(001):H surface rows underneath the molecule, marked by white solid lines, results in the contrast variation over the molecule. The variation is different for configurations A and B, reflecting the positions of the hydrogenated surface rows. All images are acquired at –2.0 V bias voltage and 2 pA tunneling current. The bright green noisy features clearly visible in the experimental images correspond to the DB dimer. (e and f) Comparison of experimental and calculated corrugations of the Y molecule obtained along the black dashed lines shown in panels a–d.

so small that this resonance cannot be captured in the dI/dV spectra. The decoupling of these MO states from the Ge bulk states is also shown by the calculated MO structure, where almost no extension of Y MOs to the Ge bulk is observed (Figure 5g). This explains the very large apparent gap recorded for the Y molecule physisorbed on a defect-free Ge(001):H surface, even though those MOs are located neither in the intrinsic band gap of the Ge bulk nor in the surface band gap of the Ge(001):H surface.

Experimental STM images show that a Y molecule can physisorb in two slightly different configurations denoted as configurations A and B, respectively (Figure 3a,b). In both configurations, the Y molecule lies flat on the Ge(001):H surface with one Y arm perpendicular to the surface hydrogen dimer rows. The difference in the STM images arises from the slight displacement of the molecule perpendicular to those rows. In both cases, the structure of the Y molecule is not affected by the presence of the surface, and the resulting geometry resembles the gas-phase geometry. The results are in good agreement with previous theoretical calculations for polyacene molecules physisorbed on a fully hydrogenated Si(001) surface.^{22,23}

The calculated STM images for configurations A and B are presented in Figure 3c,d. The slight differences in

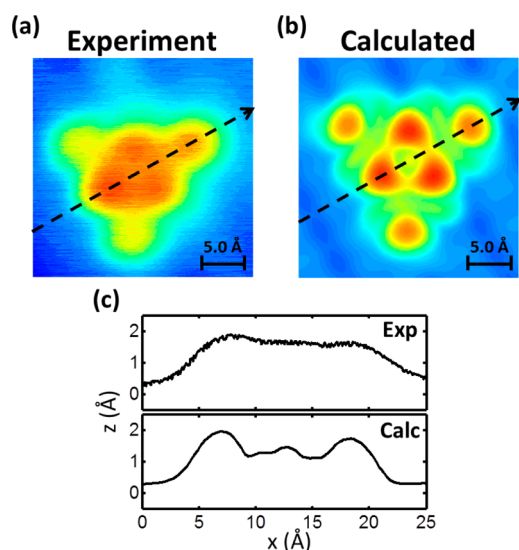


Figure 4. Excited state imaging. (a) Experimental empty state STM image of a Y molecule on defect-free Ge(001):H acquired at +3.5 V bias voltage and 2 pA tunneling current. (b) Calculated empty state STM image acquired at +2.1 V bias voltage and 2 pA tunneling current. (c) Comparison of experimental and calculated corrugation obtained along the black dashed lines in panels a and b.

the STM contrast between A and B originate from imaging of the Ge(001):H surface corrugation through the tails of the HOMO–2a, HOMO–2b, and HOMO–3 electronic state resonances. For example, the STM image of configuration A exhibits a higher contrast (conductance) for the arm perpendicular to hydrogenated surface rows (Figure 3c). The STM image of configuration B, where the central phenyl ring is located closer to the hydrogenated surface row, displays higher contrast (conductance) for the other arms and significantly lower conductance between these arms and the third arm (Figure 3d). The experimental and calculated surface corrugations of the physisorbed Y molecule are shown in Figure 3e,f.

The very weak coupling between the states of the Y molecule and the Ge bulk states is confirmed by STM imaging at a positive bias voltage (Figure 4). The STM image of a Y molecule on a Ge(001):H surface at +3.5 V resembles the images of a Y molecule physisorbed on Au(111) and on NaCl/Cu(111) surfaces, where three characteristic central lobes corresponding to a large conductance are observed near the LUMO resonance.^{4,24} These lobes correspond to the spatial expansion of the LUMO of the Y molecule. The similarity of the first excited state image on Ge(001):H and on Au(111) indicates that the Y molecule is physisorbed and not chemisorbed on a Ge(001):H surface, and therefore the coupling between the states of the Y molecule and the Ge bulk states is weak. The calculated image agrees reasonably well with the experimental image (Figure 4). The difference in bias voltages is due to the difference in the position of the LUMO in the experimental dI/dV and in calculated $T(E)$ spectra.

Y Molecule Contacted with a DB Dimer: Recoupling the Ground Electronic State Resonance to the Substrate.

The intramolecular STM corrugation changes significantly when one end of the Y molecule is placed intentionally over a DB dimer. The electronic coupling between the electronic states of the Y molecule and the Ge substrate states is enhanced due to coupling through the DB dimer states. These states protrude into the vacuum and are located close to the energy range of the HOMO, HOMO–1a, and HOMO–1b molecular states around 1.0 eV below the Fermi level. The difference in the spatial expansion and hybridization of the states of the Y molecule on Ge(001):H with and without DB dimer is shown in Figure 5f,g, respectively. Notice that initially all Y molecules are trapped by surface DB dimers and other surface defects. By manipulating a Y molecule away from the surface defect using the STM tip, one can confirm that the molecule was on a DB dimer. The Y molecule can then be manipulated back to the DB dimer to investigate how the DB dimer states are coupled to the states of the Y molecule. Through such precise contacting, the interaction between the states of the Y molecule and the DB dimer states recouples the HOMO/HOMO–1ab states of the Y molecule to the Ge(001) states and therefore to the Ge bulk states, allowing for STM imaging of this hidden ground electronic state. This is evident from the difference in contrast between the experimental STM images of a Y molecule on a defect-free Ge(001):H surface (Figure 3a,b) and of a Y molecule contacted by a DB dimer (Figure 5a). The experimental and calculated images of a Y molecule contacted by a DB dimer are compared in Figure 5a,b, with the corresponding corrugations in Figure 5d,e. The DB dimer is located at the intersection of the dashed lines A and B. The images agree reasonably well. The differences in the amplitudes can be attributed to details of tip apex electronic structure. Notice that when the Y molecule is contacted by a DB dimer, one arm of the molecule is parallel to the Ge(001):H dimer rows, whereas for the Y molecule on a defect-free Ge(001):H surface, one arm of the molecule is perpendicular to the Ge(001):H dimer rows.

We first compare the calculated images and corrugations of the Y molecule contacted with a DB dimer with the corrugation for a Y molecule on defect-free Ge(001):H (Figure 5b,c,e) for an identical configuration. When the Y molecule contacts the DB dimer, a higher conductance is expected because this structure resembles the structure where one end of a conjugated molecular wire contacts a metallic step edge. For such a structure, a high conductance at contact was indeed observed experimentally.^{25–27} The line scans across the Y molecule in contact with a DB dimer (solid lines in Figure 5e) clearly show a larger corrugation compared to the line scans without the DB dimer (dashed lines in Figure 5e). This higher conductance results from the

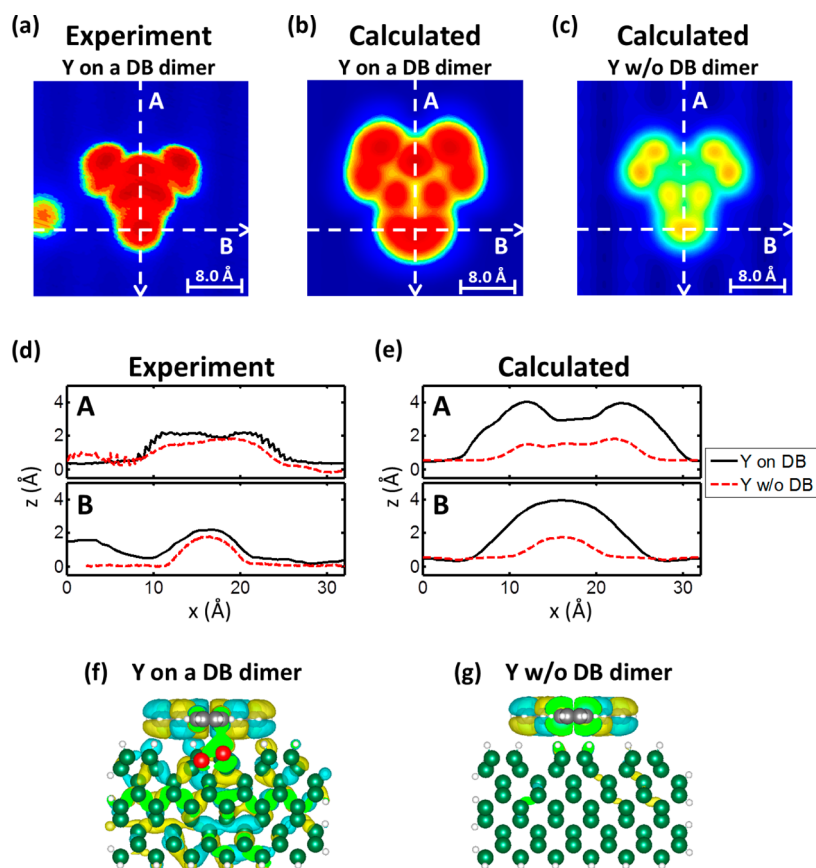


Figure 5. Y molecules on a DB dimer. (a) Filled state STM image of a Y molecule contacted by a DB dimer at -2.0 V and 2 pA. (b) Calculated STM image of a Y molecule contacted by a DB dimer. (c) Calculated STM image of a Y molecule on a Ge(001):H surface without a DB dimer. (d and e) Corrugation along the dashed lines A and B in panels a–c for calculated and experimental images. The black solid lines and red dashed lines correspond to the corrugation of a Y molecule on a DB dimer and on a fully hydrogenated Ge(001) surface, respectively. Note that the dashed lines in panel d show the corrugation of a Y molecule in configuration A shown in Figure 3a. (f) MO expansion, illustrating the coupling of the HOMO/HOMO–1ab states with the Ge bulk states *via* the DB dimer state. (g) MO expansion of a Y molecule on a fully hydrogenated Ge(001) surface, showing the decoupling of the HOMO/HOMO–1ab state from the Ge bulk states.

overlap between the DB dimer states and the MO states of the Y molecule, as shown in Figure 5f. The experimental STM image and line scan of the Y molecule on a fully hydrogenated Ge(001) surface and with one of the arms parallel to the surface H dimer rows could not be obtained due to the structural instability of this configuration. However, the experimental line scans of a Y molecule contacted by a DB dimer (solid lines in Figure 5d) have larger corrugations compared to the line scans of a Y molecule on a defect-free Ge(001):H in configuration A (dashed lines in Figure 5d), showing the same trend as the calculated results. Notice that the experimental line scan of configuration B (Figure 3f) cannot be used for comparison since the internal contrast of the Y molecule in configuration B is increased by the corrugation of the hydrogenated Ge(001) surface rows underneath the molecule.

To determine which state (HOMO, HOMO–1a, or HOMO–1b) contributes most to this contact conductance and therefore to the STM images, we have analyzed the symmetry of these states and of the experimentally recorded images. From the symmetry,

it is clear that the appearance of a single lobe at the Y-DB dimer contact point corresponds to the HOMO–1a (see Figure 2c). In addition, the lobes at the two other arms also resemble the symmetry of the HOMO–1a. Calculations also show that when the Y molecule contacts the DB dimer, the maximum of the transmission peak contains a dominant contribution from the HOMO–1a state. Notice that experimentally, the precise recording of the dI/dV spectra in the energy range of the HOMO/HOMO–1ab states is very delicate due to the instability of the Y molecule positioned on a DB dimer against higher currents and bias voltages, resulting in the uncontrolled detachment of Y molecules from the DB dimers during the acquisition of the STS spectrum. The STM images are recorded with an extremely small current, but this current is insufficient for STS measurements.

To resolve whether the Y molecule is adsorbed over a buckled or an unbuckled DB dimer, surface structure optimizations have been performed. Experiments show that a DB dimer is buckled at liquid helium temperature. However, when measured at increasing bias voltages,

the DB dimers flip frequently, as shown already in Figure 1. The stability of the buckled geometry is confirmed by calculations showing that the buckled geometry is 0.5 eV more stable than the unbuckled one. Thus, it is unlikely that the weak interaction with the Y molecule stabilizes the unbuckled geometry. Yet, the asymmetry of the buckled DB dimer under the Y molecule is not reflected in the experimental STM images. The symmetric appearance of the Y molecule positioned over a DB dimer seems to arise from either (1) oscillations of the DB dimer caused by tunneling electrons or (2) the filtering of the DB states by the bulk states of the Ge substrate, which provide an averaged symmetric contribution, similar to the recently reported symmetric appearance of buckled silicon dimers on a Si(001)-c(4×2) surface, where the buckling of the dimer is not apparent from the image when imaging is performed at a higher voltage.²⁸ To reproduce these effects in the calculated image, the images of the Y molecule on a DB dimer with two buckling configurations are calculated, and the average of the two images is obtained. This results in a symmetric image (Figure 5b) that agrees reasonably well with the experimental image.

METHODS

Experimental Details. All experiments are performed using a low-temperature Omicron GmbH STM operated at liquid helium (4.5 K) temperature in ultra-high-vacuum (UHV) conditions with a base pressure at the low 10^{-10} mbar range. The samples are cut from an undoped Ge wafer (TBL Kelpin Crystals, n-type, $\sim 45 \Omega\text{cm}$). After insertion into the UHV chamber, the substrate is prepared by subsequent cycles of Ar⁺ ion sputtering (600 eV, sputtering time: 10 min). During sputtering, the sample temperature is kept at 1020 K and controlled by an infrared pyrometer. The quality of the surface is checked by LEED and STM measurements. The surface hydrogenation procedure is performed using a home-built hydrogen cracker as described by Kolmer *et al.*²⁰ During the passivation procedure, the sample is kept at 485 K and the hydrogen pressure is maintained at 1×10^{-7} mbar. The triphenylene (Y) molecules are deposited from a three-cell Kentax effusion cell onto the sample, which is removed from the microscope cryostat just before the evaporation to keep the sample at cryogenic temperature. The molecular powder is purified before evaporation. The deposition is performed with the crucible at 450 K.

Calculation Scheme. To analyze the STM images, the electronic properties of a Y molecule adsorbed on a Ge(001):H surface are studied using theoretical approaches. The tunneling transmission coefficient, T(E), spectra (equivalent to the dI/dV experimental spectra) and the STM images are calculated using the surface Green-function matching (SGFM) method²⁹ with an extended Hückel molecular orbital (EHMO) Hamiltonian. The structures of Ge(001):H surfaces are optimized using the density functional theory (DFT) with the Perdew–Burke–Ernzerhof (PBE) functional³⁰ as implemented in the Vienna *ab initio* simulation package (VASP).^{31–34} The parameters in the EHMO Hamiltonian are fitted to accurate DFT band structures obtained with the HSE06 functional,^{35–37} which provides a more accurate description of the Ge band gap than the PBE functional.²⁰ The STM junction is modeled as described by Kolmer *et al.*²⁰ and takes into account all the electronic couplings inside the STM tunneling junction, including the coupling between the surface and the tip and the native couplings between the surface and the bulk electronic states.

CONCLUSIONS

In conclusion, we have shown that a large polyaromatic molecule physisorbed on a defect-free Ge(001):H surface can be imaged using STM. Because DB states on a Ge(001):H surface extend further into the vacuum compared to Si(001):H surface DBs, such molecules can be contacted with a DB dimer without significant distortion of their planar geometry. The ground electronic state of the physisorbed Y molecule on a defect-free Ge(001):H surface cannot be observed in the STM images due to the very weak electronic coupling of those states with the Ge bulk states through the Ge(001):H surface states. The ground electronic state becomes visible when the molecule is precisely positioned over a DB dimer, resulting in its direct STM observation. The reversibility of the electronic contact formation by LT-STM manipulation allows for a controlled coupling of a single conjugated molecule to a Ge substrate *via* a surface DB dimer, which can be native or precisely constructed using the STM tip. This opens up the possibility of constructing surface atomic-scale circuits using single-molecule devices and DB wires as interconnects.

Conflict of Interest: The authors declare no competing financial interest.

Acknowledgment. This research was supported by the 7th Framework Programme of the European Union Collaborative Project ICT (Information and Communication Technologies) “Atomic Scale and Single Molecule Logic Gate Technologies” (ATMOL), Contract No. FP7-270028, and by the Visiting Investigator Programme “Atomic Scale Technology Project” from the Agency of Science, Technology, and Research (A*STAR). The experimental part of the research was carried out with equipment purchased with financial support from the European Regional Development Fund in the framework of the Polish Innovation Economy Operational Program (Contract No. POIG.02.01.00-12-023/08). We acknowledge the A*STAR Computational Resource Centre (A*CRC) for the computational resources and support and the ICIQ Foundation for financial support. M.K. acknowledges financial support received from the Polish National Science Centre for preparation of his Ph.D. dissertation (Decision No. DEC-2013/08/T/ST3/00047).

REFERENCES AND NOTES

- Uhlmann, C.; Swart, I.; Repp, J. Controlling the Orbital Sequence in Individual Cu-Phthalocyanine Molecules. *Nano Lett.* **2013**, *13*, 777–780.
- Gross, L.; Moll, N.; Mohn, F.; Curioni, A.; Meyer, G.; Hanke, F.; Persson, M. High-Resolution Molecular Orbital Imaging Using a p-Wave STM Tip. *Phys. Rev. Lett.* **2011**, *107*, 086101.
- Mohn, F.; Schuler, B.; Gross, L.; Meyer, G. Different Tips for High-Resolution Atomic Force Microscopy and Scanning Tunneling Microscopy of Single Molecules. *Appl. Phys. Lett.* **2013**, *102*, 073109.
- Soe, W.-H.; Manzano, C.; Renaud, N.; de Mendoza, P.; De Sarkar, A.; Ample, F.; Hliwa, M.; Echavarren, A. M.; Chandrasekhar, N.; Joachim, C. Manipulating Molecular Quantum States with Classical Metal Atom Inputs: Demonstration of a Single Molecule NOR Logic Gate. *ACS Nano* **2011**, *5*, 1436–1440.

- Lafferentz, L.; Ample, F.; Yu, H.; Hecht, S.; Joachim, C.; Grill, L. Conductance of a Single Conjugated Polymer as a Continuous Function of Its Length. *Science* **2009**, *323*, 1193–1197.
- Liljeroth, P.; Repp, J.; Meyer, G. Current-Induced Hydrogen Tautomerization and Conductance Switching of Naphthalocyanine Molecules. *Science* **2007**, *317*, 1203–1206.
- Soe, W.-H.; Manzano, C.; De Sarkar, A.; Ample, F.; Chandrasekhar, N.; Renaud, N.; de Mendoza, P.; Echavarren, A. M.; Hliwa, M.; Joachim, C. Demonstration of a NOR Logic Gate Using a Single Molecule and Two Surface Gold Atoms to Encode the Logical Input. *Phys. Rev. B* **2011**, *83*, 155443.
- Gross, L.; Mohn, F.; Moll, N.; Liljeroth, P.; Meyer, G. The Chemical Structure of a Molecule Resolved by Atomic Force Microscopy. *Science* **2009**, *325*, 1110–1114.
- Swart, I.; Sonleitner, T.; Niedenfuehr, J.; Repp, J. Controlled Lateral Manipulation of Molecules on Insulating Films by STM. *Nano Lett.* **2012**, *12*, 1070–1074.
- Liljeroth, P.; Swart, I.; Paavilainen, S.; Repp, J.; Meyer, G. Single-Molecule Synthesis and Characterization of Metal–Ligand Complexes by Low-Temperature STM. *Nano Lett.* **2010**, *10*, 2475–2479.
- Mohn, F.; Repp, J.; Gross, L.; Meyer, G.; Dyer, M. S.; Persson, M. Reversible Bond Formation in a Gold-Atom–Organic-Molecule Complex as a Molecular Switch. *Phys. Rev. Lett.* **2010**, *105*, 266102.
- Pavlicek, N.; Fleury, B.; Neu, M.; Niedenfuehr, J.; Herranz-Lancho, C.; Ruben, M.; Repp, J. Atomic Force Microscopy Reveals Bistable Configurations of Dibenzo[a,h]thianthrene and their Interconversion Pathway. *Phys. Rev. Lett.* **2012**, *108*, 086101.
- Swart, I.; Sonleitner, T.; Repp, J. Charge State Control of Molecules Reveals Modification of the Tunneling Barrier with Intramolecular Contrast. *Nano Lett.* **2011**, *11*, 1580–1584.
- Olsson, F. E.; Paavilainen, S.; Persson, M.; Repp, J.; Meyer, G. Multiple Charge States of Ag Atoms on Ultrathin NaCl Films. *Phys. Rev. Lett.* **2007**, *98*, 176803.
- Repp, J.; Meyer, G.; Olsson, F. E.; Persson, M. Controlling the Charge State of Individual Gold Adatoms. *Science* **2004**, *305*, 493.
- Repp, J.; Meyer, G.; Stojkovic, S. M.; Gourdon, A.; Joachim, C. Molecules on Insulating Films: Scanning-Tunneling Microscopy Imaging of Individual Molecular Orbitals. *Phys. Rev. Lett.* **2005**, *94*, 026803.
- Such, B.; Goryl, G.; Godlewski, S.; Kolodziej, J. J.; Szymonski, M. PTCDA Molecules on a KBr/InSb System: a Low Temperature STM Study. *Nanotechnology* **2008**, *19*, 475705.
- Bellec, A.; Ample, F.; Riedel, D.; Dujardin, G.; Joachim, C. Imaging Molecular Orbitals by Scanning Tunneling Microscopy on a Passivated Semiconductor. *Nano Lett.* **2009**, *9*, 144–147.
- Piva, P. G.; DiLabio, G. A.; Pitters, J. L.; Zikovsky, J.; Rezek, M.; Dogel, S.; Hofer, W. A.; Wolkow, R. A. Field Regulation of Single-Molecule Conductivity by a Charged Surface Atom. *Nature* **2005**, *435*, 658–661.
- Kolmer, M.; Godlewski, S.; Kawai, H.; Such, B.; Krok, F.; Saeys, M.; Joachim, C.; Szymonski, M. Electronic Properties of STM-Constructed Dangling-Bond Dimer Lines on a Ge(001)-(2×1):H Surface. *Phys. Rev. B* **2012**, *86*, 125307.
- Gruyters, M.; Pingel, T.; Gopakumar, T. G.; Néel, N.; Schütt, Ch.; Köhler, F.; Herges, R.; Berndt, R. Electronic Ground-State and Orbital Ordering of Iron Phthalocyanine on H/Si(111) Unraveled by Spatially Resolved Tunneling Spectroscopy. *J. Phys. Chem. C* **2012**, *116*, 20882–20886.
- Ample, F.; Joachim, C. The Chemisorption of Polyaromatic Hydrocarbons on Si(100)H Dangling Bonds. *Surf. Sci.* **2008**, *602*, 1563–1571.
- Tsetseris, L.; Pantelides, S. T. Atomic-Scale Mechanisms of Selective Adsorption and Dimerization of Pentacene on Si Surfaces. *Appl. Phys. Lett.* **2005**, *87*, 233109.
- Guillermet, O.; Gauthier, S.; Joachim, C.; de Mendoza, P.; Lauterbach, T.; Echavarren, A. STM and AFM High Resolution Intramolecular Imaging of a Single Decastaphene Molecule. *Chem. Phys. Lett.* **2011**, *511*, 482–485.
- Langlais, V. J.; Schlittler, R. R.; Tang, H.; Gourdon, A.; Joachim, C.; Gimzewski, J. K. Spatially Resolved Tunneling along a Molecular Wire. *Phys. Rev. Lett.* **1999**, *83*, 2809.
- Moresco, F.; Gross, L.; Alemani, M.; Rieder, K.-H.; Tang, H.; Gourdon, A.; Joachim, C. Probing the Different Stages in Contacting a Single Molecular Wire. *Phys. Rev. Lett.* **2003**, *91*, 036601.
- Stojkovic, S.; Joachim, C.; Grill, L.; Moresco, F. The Contact Conductance on a Molecular Wire. *Chem. Phys. Lett.* **2005**, *408*, 134–138.
- Manzano, C.; Soe, W. H.; Kawai, H.; Saeys, M.; Joachim, C. Origin of the Apparent (2×1) Topography of the Si(100)-c(4×2) Surface Observed in Low-Temperature STM Images. *Phys. Rev. B* **2011**, *83*, 201302(R).
- Cerda, J.; Van Hove, M. S.; Sautet, P.; Salmeron, M. Efficient Method for the Simulation of STM Images. I. Generalized Green-Function Formalism. *Phys. Rev. B* **1997**, *56*, 15885.
- Perdew, J. P.; Burke, K.; Ernzerhof, M. Generalized Gradient Approximation Made Simple. *Phys. Rev. Lett.* **1996**, *77*, 3865.
- Kresse, G.; Hafner, J. *Ab Initio* Molecular Dynamics for Liquid Metals. *Phys. Rev. B* **1993**, *47*, 558.
- Kresse, G.; Hafner, J. *Ab Initio* Molecular-Dynamics Simulation of the Liquid-Metal–Amorphous-Semiconductor Transition in Germanium. *Phys. Rev. B* **1994**, *49*, 14251.
- Kresse, G.; Furthmüller, J. Efficient Iterative Schemes for *Ab Initio* Total-Energy Calculations Using a Plane-Wave Basis Set. *Phys. Rev. B* **1996**, *54*, 11169.
- Kresse, G.; Furthmüller, J. Efficiency of *Ab-Initio* Total Energy Calculations for Metals and Semiconductors Using a Plane-Wave Basis Set. *Comput. Mater. Sci.* **1996**, *6*, 15–50.
- Heyd, J.; Scuseria, G. E.; Ernzerhof, M. Hybrid Functionals Based on a Screened Coulomb Potential. *J. Chem. Phys.* **2003**, *118*, 8207.
- Heyd, J.; Scuseria, G. E. Efficient Hybrid Density Functional Calculations in Solids: Assessment of the Heyd–Scuseria–Ernzerhof Screened Coulomb Hybrid Functional. *J. Chem. Phys.* **2004**, *121*, 1187.
- Heyd, J.; Scuseria, G. E.; Ernzerhof, M. Erratum: “Hybrid Functionals Based on a Screened Coulomb Potential” [*J. Chem. Phys.* 118, 8207 (2003)]. *J. Chem. Phys.* **2006**, *124*, 219906.